



Natural Resources
Canada

Ressources naturelles
Canada

GEOLOGICAL SURVEY OF CANADA

Archean and Paleoproterozoic cratonic rocks of Baffin Island

**M.R. St-Onge, D.J. Scott, N. Rayner, M. Sanborn-Barrie, D.R. Skipton,
B.M. Saumur, N. Wodicka, and O.M. Weller**

2020

Advance copy of a contribution to

GEOLOGICAL SURVEY OF CANADA BULLETIN 608

**Geological synthesis of Baffin Island (Nunavut) and
the Labrador–Baffin Seaway**

Edited by L.T. Dafoe and N. Bingham-Koslowski



GEOLOGICAL SURVEY OF CANADA

Archean and Paleoproterozoic cratonic rocks of Baffin Island

**M.R. St-Onge, D.J. Scott, N. Rayner, M. Sanborn-Barrie, D.R. Skipton,
B.M. Saumur, N. Wodicka, and O.M. Weller**

2020

Advance copy of a contribution to

GEOLOGICAL SURVEY OF CANADA BULLETIN 608

Geological synthesis of Baffin Island (Nunavut) and the Labrador–Baffin Seaway

Edited by L.T. Dafoe and N. Bingham-Koslowski

© Her Majesty the Queen in Right of Canada, as represented by the Minister of Natural Resources, 2020

Information contained in this publication or product may be reproduced, in part or in whole, and by any means, for personal or public non-commercial purposes, without charge or further permission, unless otherwise specified.

You are asked to:

- exercise due diligence in ensuring the accuracy of the materials reproduced;
- indicate the complete title of the materials reproduced, and the name of the author organization; and
- indicate that the reproduction is a copy of an official work that is published by Natural Resources Canada (NRCan) and that the reproduction has not been produced in affiliation with, or with the endorsement of, NRCan.

Commercial reproduction and distribution is prohibited except with written permission from NRCan. For more information, contact NRCan at nrcan.copyrightdroitdauteur.nrcan@canada.ca.

Permanent link: <https://doi.org/10.4095/321824>

This publication is available for free download through GEOSCAN (<https://geoscan.nrcan.gc.ca/>).

Recommended citation

St-Onge, M.R., Scott, D.J., Rayner, N., Sanborn-Barrie, M., Skipton, D.R., Saumur, B.M., Wodicka, N., and Weller, O.M., 2020. Archean and Paleoproterozoic cratonic rocks of Baffin Island; *advance contribution to Geological synthesis of Baffin Island (Nunavut) and the Labrador–Baffin Seaway*, (ed.) L.T. Dafoe and N. Bingham-Koslowski; Geological Survey of Canada, Bulletin 608 (in press), 29 p.
<https://doi.org/10.4095/321824>

Archean and Paleoproterozoic cratonic rocks of Baffin Island

M.R. St-Onge^{1*}, D.J. Scott², N. Rayner¹, M. Sanborn-Barrie¹, D.R. Skipton³, B.M. Saumur⁴, N. Wodicka¹, and O.M. Weller⁵

St-Onge, M.R., Scott, D.J., Rayner, N., Sanborn-Barrie, M., Skipton, D.R., Saumur, B.M., Wodicka, N., and Weller, O.M., 2020. Archean and Paleoproterozoic cratonic rocks of Baffin Island; advance contribution to Geological synthesis of Baffin Island (Nunavut) and the Labrador–Baffin Seaway, (ed.) L.T. Dafoe and N. Bingham-Koslowski; Geological Survey of Canada, Bulletin 608 (in press), 29 p. <https://doi.org/10.4095/321824>

Abstract: Archean and Paleoproterozoic cratonic rocks of Baffin Island define four stacked structural levels that are juxtaposed within the middle Paleoproterozoic Trans-Hudson Orogen. From north to south, and highest to lowest structural level, these comprise: 1) the Archean Rae Craton, unconformably overlain along its southern margin by middle Paleoproterozoic supracrustal cover (Piling Group) and stratigraphically similar units of the Hoare Bay Group on Cumberland Peninsula; 2) Archean to middle Paleoproterozoic metaplutonic units and middle Paleoproterozoic metasedimentary cover (Lake Harbour Group), collectively termed the ‘Meta Incognita microcontinent’; 3) middle Paleoproterozoic orthogneiss, interpreted as a deformed arc–magmatic terrane (Narsajuaq terrane) or alternatively as Narsajuaq-age intrusions emplaced in the Meta Incognita microcontinent; and 4) Archean orthogneiss, interpreted as the northern continuation of the lower-plate Superior Craton, and associated middle Paleoproterozoic continental-margin supracrustal cover (Povungnituk Group).

Résumé : Les roches cratoniques de l’Archéen et du Paléoprotérozoïque de l’île de Baffin définissent un empilement de quatre niveaux structuraux qui sont juxtaposés dans l’orogène trans-hudsonien du Paléoprotérozoïque moyen. Du nord au sud, et du plus haut au plus bas niveau structural, ceux-ci comprennent : 1) le craton de Rae de l’Archéen, recouvert en discordance le long de sa marge sud par des roches supracrustales de couverture du Paléoprotérozoïque moyen (Groupe de Piling) et des unités stratigraphiquement semblables du Groupe de Hoare Bay dans la péninsule Cumberland; 2) des unités métaplutoniques de l’Archéen au Paléoprotérozoïque moyen et des roches métasédimentaires de couverture du Paléoprotérozoïque moyen (Groupe de Harbour Lake), collectivement dénommées « microcontinent de Meta Incognita »; 3) des orthogneiss du Paléoprotérozoïque moyen, qui correspondraient à un terrane d’arc magmatique déformé (terrane de Narsajuaq) ou à des intrusions d’âge Narsajuaq mises en place dans le microcontinent de Meta Incognita; et 4) des orthogneiss de l’Archéen, qui constitueraient le prolongement nord du craton du lac Supérieur (plaque inférieure), et des roches supracrustales de couverture de la marge continentale associée du Paléoprotérozoïque moyen (Groupe de Povungnituk).

¹Geological Survey of Canada, 601 Booth Street, Ottawa, Ontario K1A 0E8

²Polar Knowledge Canada, 170 Laurier Avenue West, Ottawa, Ontario K1P 5V5

³Yukon Geological Survey, Government of Yukon, Box 2703, Whitehorse, Yukon Y1A 2C6

⁴Université du Québec à Montréal, 201, avenue du Président-Kennedy, Montréal, Quebec H2X 3Y7

⁵Department of Earth Sciences, University of Cambridge, Cambridge, United Kingdom

*Corresponding author (email: marc.st-onge@canada.ca)

PREVIOUS WORK

Although Martin Frobisher's second and third voyages in 1577 and 1578, directed as they were to searching for gold, had a geological connotation (Hogarth et al., 1994), geological investigation of Baffin Island properly began with fossils recovered at Silliman's Fossil Mount (Fig. 1) by C.F. Hall in 1861; this collection indicated the existence of Ordovician strata and the affinities of these strata to North American sections (Hall, 1865; Miller et al., 1954). In 1885, R. Bell of the Geological Survey of Canada (GSC) made a brief examination of the area around Amadjuak Bay on the southern coast of Baffin Island (Fig. 1; Bell, 1885) and, in 1897, he carried out a coastal reconnaissance between Big Island and Chorkbak Inlet (Fig. 1; Bell, 1901).

In 1926–1927, L.J. Weeks and M.H. Haycock built Canada's first Arctic research station and overwintered in Pangnirtung (Fig. 1). They carried out studies around the head of Cumberland Sound and west from Nettilling Fiord to Nettilling Lake (Fig. 1; Weeks, 1928a, b). In 1927, the Putnam Baffin Island Expedition explored the northern coast of Foxe Peninsula and traversed inland from Bowman Bay to Putnam Highland, documenting part of the extensive Paleozoic cover between Amadjuak Lake and Foxe Basin (Fig. 1; Putnam, 1928).

Reconnaissance geological investigations of southern Baffin Island by the GSC resumed in 1949 when Y.O. Fortier and W.L. Davison examined the coast of Meta Incognita Peninsula, and in addition made four traverses across the peninsula. Davison continued the coastal studies in 1950 and 1951, and carried out detailed mapping near Kimmirut (Fig. 1; Davison, 1959a). In 1950, he mapped the northern shore of Frobisher Bay and the eastern coast of Hall Peninsula as far north as Cape St. David (Fig. 1). The following season, he continued coastal mapping west from Kimmirut to Chorkbak Inlet (Fig. 1; Davison, 1959b), while G.C. Riley carried out geological investigations along the shores of Cumberland Sound to Cape St. David (Fig. 1; Riley, 1959). Studies of the northern shore of Hudson

Strait were continued in 1952 under the direction of Y.O. Fortier, and the shoreline was mapped between Chorkbak Inlet and the former community of Nuwata (Fig. 1), on western Foxe Peninsula.

Low-grade iron deposits discovered on southern Baffin Island during the preceding work were staked in 1956–1957 by Ultra Shawkey Mines Ltd. Interest in the economic possibilities of southern Baffin Island led the GSC to undertake more detailed work and, in 1958, R.G. Blackadar commenced mapping at a scale of 1 inch to 4 miles. He mapped the Mingo Lake and Macdonald Island map areas between 1958 and 1960 (Blackadar, 1959, 1960, 1961, 1967a, b,) and the Andrew Gordon Bay and Cory Bay map areas in 1961 and 1964 (Blackadar, 1962, 1967c).

Reconnaissance mapping of Baffin Island south of latitude 66°N was completed in 1965 during 'Operation Amadjuak', a fixed-wing- and helicopter-supported project. Bedrock mapping was carried out across eighteen 1:250 000 NTS map areas and these data, together with those derived from published and unpublished GSC maps, were compiled into three regional bedrock maps published at 1:506 880 scale by Blackadar (1967c, d, e). This was followed by a series of helicopter-borne operations in central Baffin Island (e.g. Morgan, 1983; Henderson, 1985). Bedrock mapping at 1:50 000 scale was conducted by the GSC in 1994 across a 2800 km² area centred on Ege Bay (Fig. 1), west-central Baffin Island. Mapping results, geochronological and geochemical data were presented in Bethune and Scammell (1997, 2003a, b). Subsequently, modern geoscience knowledge has been provided by field campaigns featuring helicopter-assisted foot traverses in: 1) southern Baffin Island (1995–1997; green shading in Fig. 1); 2) central Baffin Island (2000–2002; orange shading in Fig. 1); 3) southwestern Baffin Island (2006; yellow shading in Fig. 1); 4) Cumberland Peninsula (2009–2011; pale pink shading in Fig. 1); 5) Hall Peninsula (2012–2014; blue shading in Fig. 1); 6) Meta Incognita Peninsula (2014; purple shading in Fig. 1); and 7) in the Clearwater Fiord–Sylvia

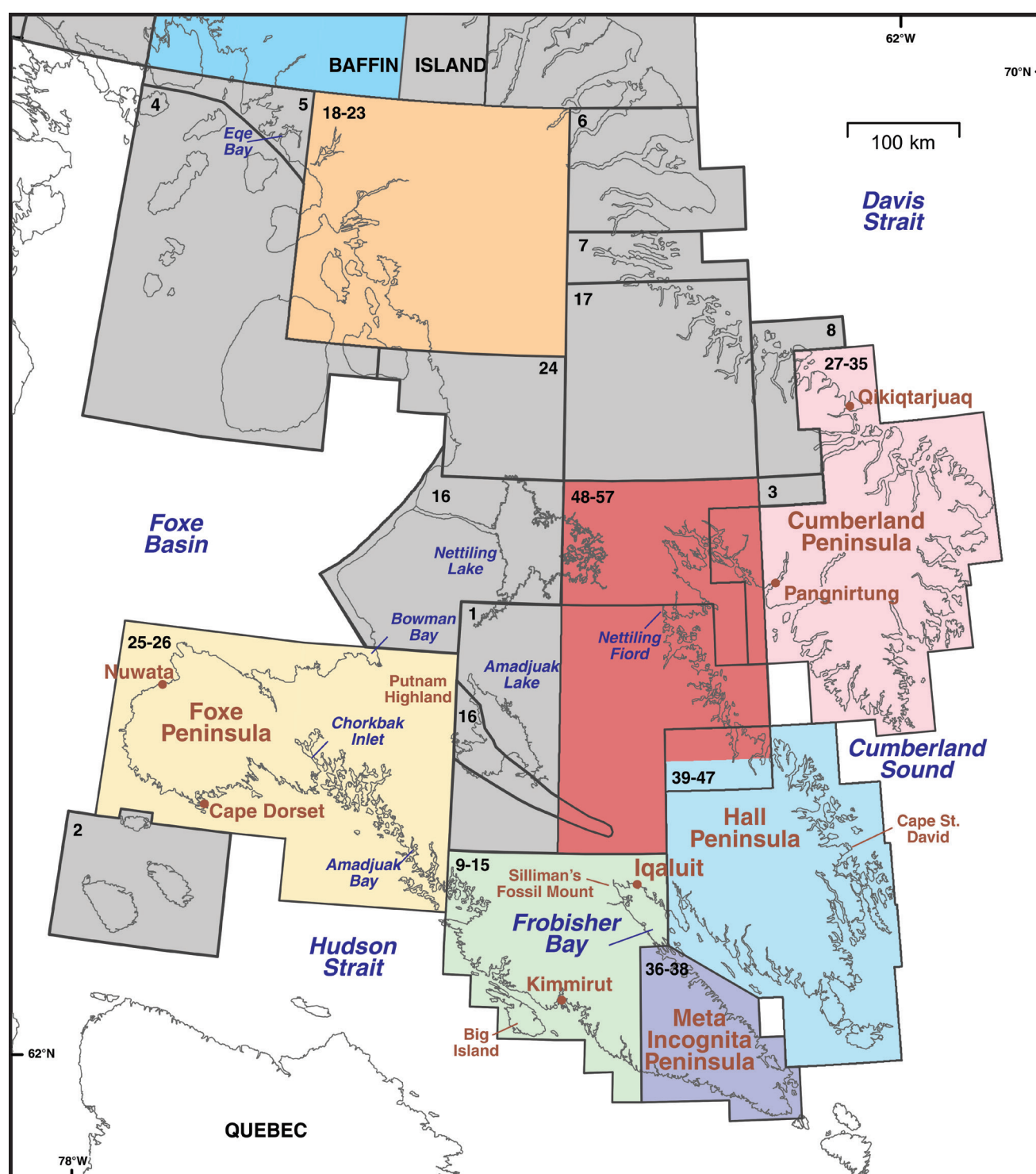


Figure 1. Summary of bedrock mapping campaigns undertaken south of latitude 70°N on Baffin Island, Nunavut. Bold numbers denote map references in chronological order, which are listed in Appendix A. Coloured shading highlights areas where field campaigns were conducted, as described in the text.

Grinnell Lake area (2015; pale red shading in Fig. 1). The latter project effectively completed the framework bedrock mapping of southern Baffin Island (Weller et al., 2015; St-Onge et al., 2016).

North of latitude 70°N, reconnaissance geological mapping was conducted by G.D. Jackson and R.G. Blackadar in 1965–1968 as part of two bedrock mapping operations on northern Baffin Island (Fig. 2; Blackadar et al., 1968a–h; Jackson and Davidson, 1975a, b; Jackson and Morgan, 1978; Jackson et al., 1979; Jackson, 1984). Mapping involved helicopter traverses with stops spaced approximately 8 km apart, supplemented by more detailed targeted work to examine the stratigraphy of supracrustal rocks, including exposures in the Mary River area (Fig. 2), where Archean greenstone belts host world-class iron deposits. In 1987, a bedrock geological map of Borden Peninsula was published (Fig. 2; Jackson and Sangster, 1987) and, in 1988, a geological map focused on the Mesoproterozoic Fury and Hecla Group was released (Fig. 2; Chandler, 1988). Jackson et al. (1975) and Jackson (2000) presented a summary of the bedrock geology of northern Baffin Island, including descriptions of lithological units and preliminary accounts of metamorphism, deformation and economic mineralization. Detailed sketch maps of the iron-bearing Mary River Group were subsequently released (Jackson, 2006).

In 2003–2005, the Canada-Nunavut Geoscience Office completed targeted bedrock mapping as a subcomponent of the 2003–2005 North Baffin project, in which surficial geology was the primary focus. Resulting 1:50 000 scale maps were published in Young et al. (2004), together with an interpreted structural–stratigraphic framework. More recently, targeted and 1:100 000 scale bedrock mapping was conducted under the Geo-mapping for Energy and Minerals program North Baffin Island Bedrock Mapping activity (2017–2018;

blue shading in Fig. 2) to bring bedrock mapping and geoscience knowledge to an equal level with that achieved on southern Baffin Island (e.g. St-Onge et al., 2015c; Weller et al., 2015).

The geological and tectonic synthesis of the Archean and Paleoproterozoic cratonic units of Baffin Island presented in this paper relies in part on original field observations and descriptions of rock formations that have been previously published by the co-authors in several field reports. Chief amongst these are the following publications, to which the reader is referred for further information: St-Onge et al. (2015b, c), Weller et al. (2015), Skipton et al. (2017), and Saumur et al. (2018).

TECTONIC FRAMEWORK

Baffin Island forms part of the northeastern (Quebec–Baffin) segment of the Trans-Hudson Orogen (THO), which is a collisional/accretionary orogenic belt that extends in a broad arcuate corridor from northeastern to south-central North America (Hoffman, 1988; Lewry and Collerson, 1990). The THO formed during the final phase of growth of the Nuna supercontinent, and *sensu lato* records closure of the Manikewan Ocean between the lower Superior and upper Churchill plates from ca. 1.92 to 1.80 Ga. In detail, the northeastern THO is a composite collision zone that comprises tectonostratigraphic assemblages accumulated on, or accreted to, the northern margin of the lower-plate Archean Superior Craton and involved a series of short-duration tectonothermal events, which encompass specific accretionary phases within the much larger orogenic system during 120 Ma of gradual ocean-basin closure (St-Onge et al., 2006, 2007, 2009; Corrigan et al., 2009; Corrigan, 2012; Weller and

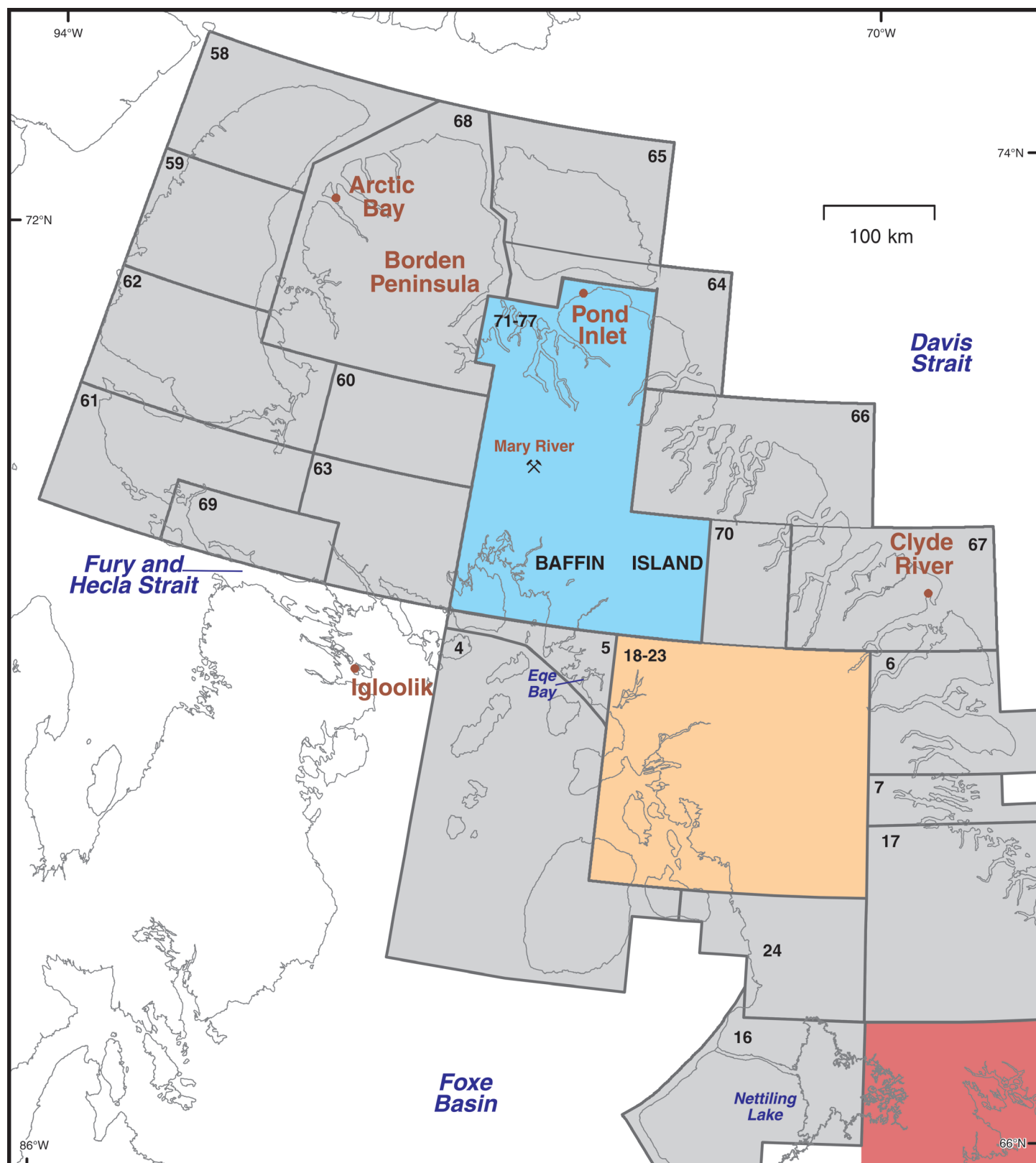


Figure 2. Summary of bedrock mapping campaigns undertaken north of latitude 70°N on Baffin Island, Nunavut. Bold numbers denote map references in chronological order, which are listed in Appendix A. Coloured shading highlights areas where field campaigns were conducted, as described in the text.

St-Onge, 2017). Four orogen-scale stacked structural levels have been identified in the eastern THO (Fig. 3). From north to south, and highest to lowest structural level, these comprise:

- Level 4 – The eastern Rae Craton (Bethune and Scammell, 2003a; Skipton et al., 2017; Saumur et al., 2018), consisting of Archean basement orthogneiss, felsic plutonic rocks and supracrustal packages, unconformably overlain along its southern margin by middle Paleoproterozoic supracrustal cover (Piling Group; Partin et al., 2014a; Wodicka et al., 2014) and stratigraphically similar units of the Hoare Bay Group on Cumberland Peninsula (Sanborn-Barrie et al., 2017). A middle Paleoproterozoic felsic plutonic suite (Qikiqtarjuaq plutonic suite; Sanborn-Barrie et al., 2011, 2013; Rayner et al., 2012) intrudes both the cratonic basement and supracrustal cover strata.
- Level 3 – Archean to middle Paleoproterozoic gneissic and meta-plutonic units and middle Paleoproterozoic metasedimentary cover units (Lake Harbour Group; Jackson and Taylor, 1972), collectively termed the ‘Meta Incognita microcontinent’ by St-Onge et al. (2000a), which represents crust rifted from the Rae Craton, or the Superior Craton, or that is exotic to both.
- Level 2 – Middle Paleoproterozoic, dominantly monzogranitic to granodioritic orthogneiss, interpreted as a deformed arc-magmatic terrane (Narsajuaq terrane; Scott, 1997; Wodicka and Scott, 1997; Thériault et al., 2001; St-Onge et al., 2009) or alternatively as Narsajuaq-age intrusions emplaced in Level 3 (Corrigan et al. 2009).
- Level 1 – Archean tonalitic to granitic orthogneiss, interpreted as the northern continuation of the lower-plate Superior Craton crystalline basement, and associated middle Paleoproterozoic continental-margin supracrustal cover (Povungnituk Group; St-Onge et al., 1996).

Levels 3 and 4 are intruded by the Qikiqtarjuaq plutonic suite (Sanborn-Barrie et al., 2011, 2013; Rayner et al., 2012), dated between ca. 1896 and 1886 Ma (Rayner, 2017), and the Cumberland batholith, which comprises various granitoid phases dated at ca. 1865 to 1845 Ma (Whalen et al., 2010; Rayner, 2015, 2017). The Cumberland batholith has been interpreted as an Andean-type batholith (St-Onge et al., 2009), or as the result of postcollisional lithospheric delamination and mantle upwelling (Whalen et al., 2010). Level 4 is unconformably overlain by the Mesoproterozoic sedimentary and volcanic units of the Borden and Fury and Hecla basins (Chandler, 1988; Jackson, 2000). All levels are cut by ca. 720 Ma basaltic dykes of the Franklin swarm, which were emplaced during plume magmatism associated with the breakup of the Rodinia Supercontinent (Heaman et al., 1992). Levels 3 and 4 are unconformably overlain by Cambro–Ordovician clastic and carbonate sedimentary strata (Blackadar, 1967e; Blackadar et al., 1968a–h), whereas Level 4 is also unconformably overlain by Cretaceous sandstone (Jackson and Davidson, 1975b; Jackson et al., 1975) and Paleocene volcanic and sedimentary strata (Clarke and Upton, 1971).

The four structural levels were progressively accreted from north to south across a series of, in part, cryptic crustal sutures during long-lived deformation associated with the THO. The oldest of these sutures, the Level 3–4 ‘Baffin suture’ (Fig. 3), is proposed to have resulted from accretion of the Meta Incognita microcontinent to the Rae Craton between 1915 ± 8 Ma (the youngest, most precise maximum age constraint for the Piling Group; Wodicka et al., 2014) and 1896 ± 8 Ma (the oldest dated phase of the Qikiqtarjuaq plutonic suite; Rayner 2017). Evidence of this suture is relatively sparse due to postaccretion magmatism engulfing the putative suture zone but includes the presence of distinct and opposite-facing, shelf-to-basin stratigraphic sequences (St-Onge et al., 2009; Weller et al., 2015). To the north of the proposed suture lies the stratigraphically south-facing Piling Group, which comprises a continental-margin sequence, characterized by basal shallow-marine

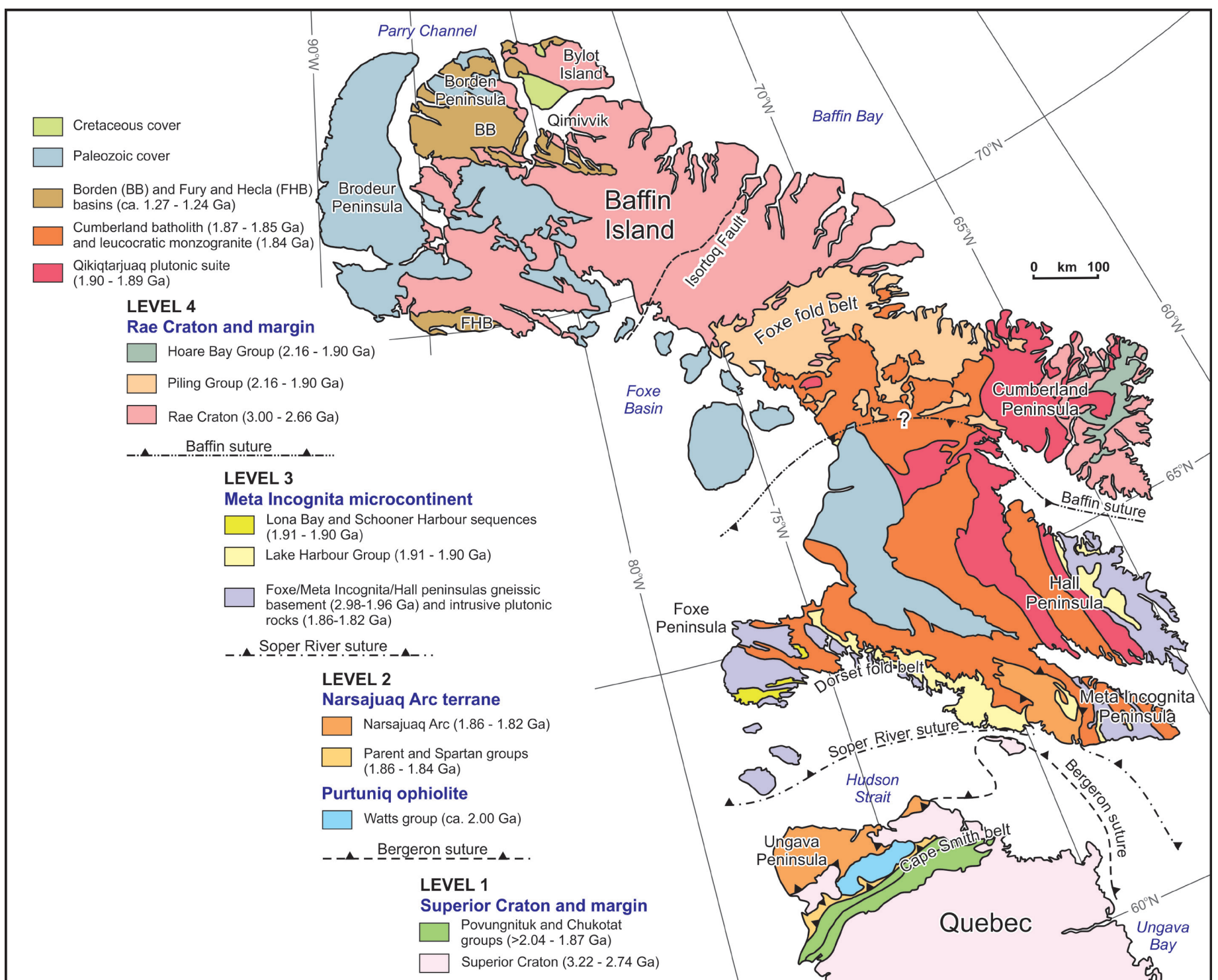


Figure 3. Simplified geological terrane map of the Quebec–Baffin segment of the Trans-Hudson Orogen (modified from St-Onge et al., 2007; Weller et al., 2015; Rayner, 2017), showing the four structural levels and three sutures that characterize the middle Paleoproterozoic assembly of Baffin Island. The map provides a regional tectonic context for the principal Archean and Paleoproterozoic tectonostratigraphic assemblages of Baffin Island.

continental-margin clastic and carbonate-platform strata, overlain by a volcano-sedimentary rift package that includes iron-formation, and capped by deep-water turbidites (Partin et al., 2014a; Wodicka et al., 2014). To the south of the proposed suture lies the Lake Harbour Group, which grades basinward to the north and comprises a clastic-carbonate continental-margin sequence (Scott et al., 1997, 2002a). Stratigraphic differences with the Piling Group include the presence of a basal orthoquartzite and the absence of iron-formation and greywacke. Further evidence for the proposed suture includes north-verging thrust imbrication of Piling Group strata in Level 4 (Corrigan et al., 2001, 2009; Scott et al., 2002b, 2003), as well as thrust imbrication of basement-cover panels in Level 3 that predate emplacement of the Cumberland batholith (St-Onge et al., 2007).

The Level 2–3 ‘Soper River suture’ (Fig. 3) records the accretion of the Narsajuaq magmatic arc to the composite Rae–Meta Incognita continental margin. Formation of the suture is bracketed between 1845 ± 2 Ma, the age of the youngest intra-oceanic phase in the arc (Dunphy and Ludden, 1998), and $1842 +5/-3$ Ma, the age of the oldest Andean-type phase of the Narsajuaq Arc (Scott, 1997). Deformation in the hanging wall of the Soper River suture is both extensive and penetrative, and manifest as a regional synmetamorphic amphibolite- to granulite-facies metamorphic foliation (St-Onge et al., 2007).

The Level 1–2 ‘Bergeron suture’ (Fig. 3) formed during terminal collision of the Superior Craton with the amalgamated mosaic of upper-plate terranes (collectively the Churchill plate or peri-Churchill collage) and is bracketed between $1820 +4/-3$ Ma, the age of the youngest dated plutonic unit in the hanging wall of the suture (Scott and Wodicka, 1998), and 1795 ± 2 Ma, the age of an undeformed dyke that crosscuts the suture (Wodicka and Scott, 1997). This event resulted in localized retrograde amphibolite-facies metamorphism of granulite-facies rocks in the upper plate of the collision on southern Baffin Island, specifically along reactivated segments of the Soper River suture and associated fluid-infiltration zones (St-Onge et al., 2000b).

ARCHEAN RAE CRATON (LEVEL 4)

On Baffin Island, the Rae Craton comprises 2901 ± 3 to 2706 ± 3 Ma granodioritic to monzogranitic orthogneiss and temporally distinct volcano-sedimentary sequences, namely the 2833 ± 3 to 2731 ± 6 Ma Meso- to Neoproterozoic Mary River Group and the younger ca. 2740 to 2725 Ma Neoproterozoic Ege Bay and Isortoq greenstone belts, all

of which are intruded by 2731 ± 3 to $2658 +16/-14$ Ma granodioritic to monzogranitic and rare tonalitic plutonic rocks (Fig. 4; Jackson et al., 1990; Scott and de Kemp, 1999; Jackson, 2000; Wodicka et al., 2002b; Bethune and Scammell, 2003a; Scott et al., 2003; Young et al., 2004, 2007; Johns and Young, 2006; Skipton et al., 2019). The Archean units of northern Baffin Island have been correlated with the Prince Albert and Repulse Bay blocks (or north Rae Domain) of the Rae Craton, the latter extending from central Nunavut to at least northern Baffin Island (Jackson and Berman, 2000; Pehrsson et al., 2011, 2013; Snyder et al., 2013; St-Onge et al., 2015a). In their type area west of Foxe Basin, the correlative Prince Albert and Repulse Bay blocks are characterized by ca. 2.97–2.60 Ga granite-greenstone belts with isotopic evidence of Eo- to Mesoarchean cratonic basement (e.g. Wodicka et al., 2011; Corrigan et al., 2013; LaFlamme et al., 2014).

On northern Baffin Island, the Archean crust of the Rae Craton is truncated by the Isortoq Fault (Jackson, 2000) and unconformably overlain by the Paleoproterozoic Piling Group (Fig. 4). Both fault and cover have been interpreted as corresponding to the northern margin of the ca. 1.92–1.80 Ma Himalayan-scale accretionary/collisional THO (St-Onge et al., 2002). The Isortoq Fault is considered to record northwest-directed thrusting of the Piling Group and underlying crystalline basement over Archean crust of northern Baffin Island at ca. 1850–1820 Ma (Jackson, 2000; Jackson and Berman, 2000; Bethune and Scammell, 2003b; Saumur et al., 2018).

Paleoproterozoic felsic plutonic rocks, ranging in age from $1897 +7/-4$ to ca. 1805 Ma and including the northernmost components of the Cumberland batholith, intrude the Piling Group and Rae Craton rocks (*see below*; Jackson et al., 1990; Henderson and Henderson, 1994; Wodicka and Scott, 1997; Scott and Wodicka, 1998; Scott, 1999; Wodicka et al., 2002b, 2014; Bethune and Scammell, 2003b; Gagné et al., 2009; Whalen et al., 2010).

Archean basement gneiss

Archean basement orthogneiss of the Rae Craton on Baffin Island (Fig. 4) mainly comprises granodiorite, tonalite, and monzogranite. Crystallization ages for units interpreted as basement to the Mary River Group (*see ‘Mary River Group’ section*), east and north of Mary River (Fig. 4), are $2851 +20/-17$ Ma for a tonalite gneiss (Jackson et al., 1990), ca. 2900 Ma for a granodiorite gneiss (Young et al., 2007; M. Young, unpub. data, 2007), and 2901 ± 3 Ma for a

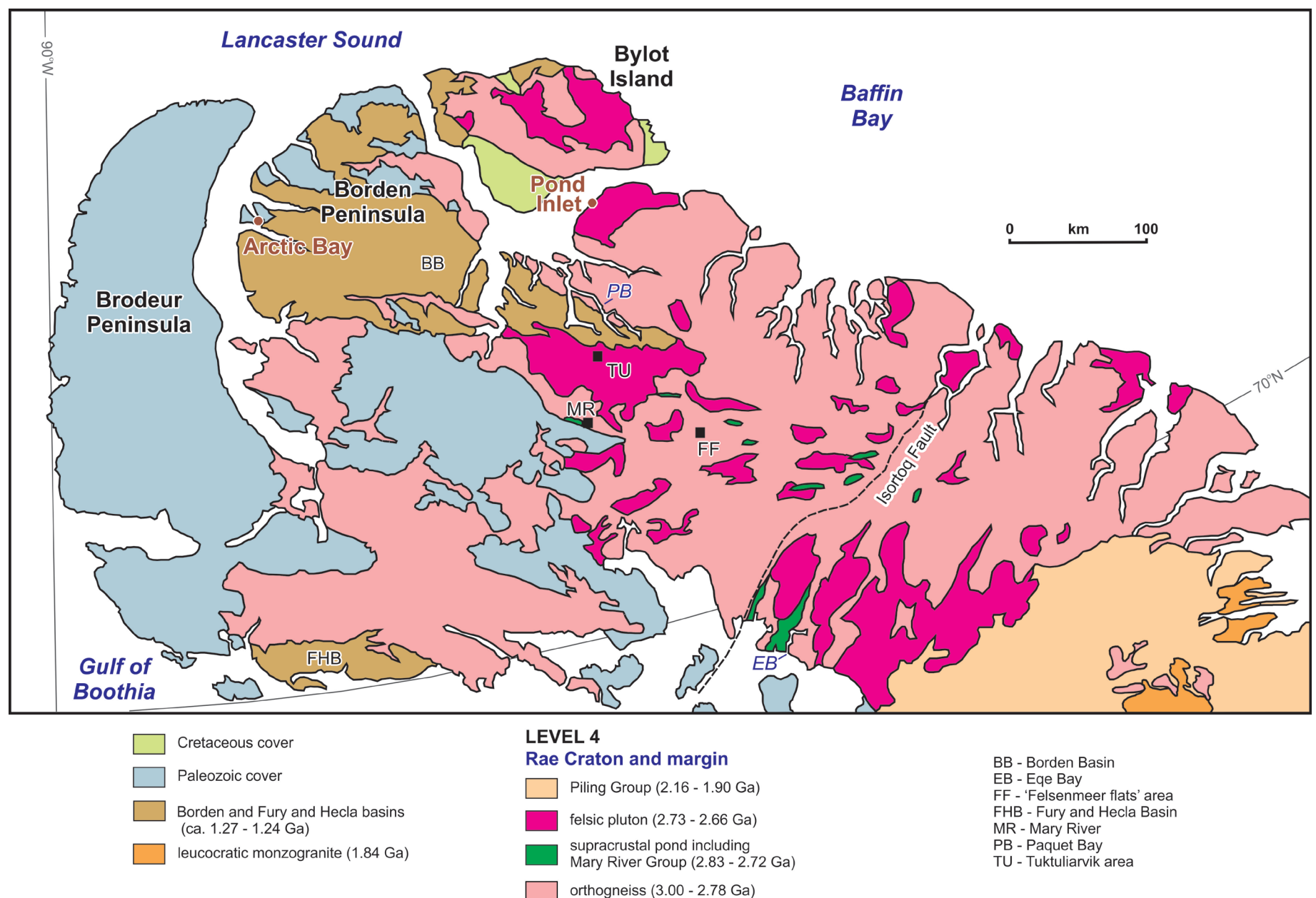


Figure 4. Geology of the Archean Rae Craton on northern Baffin Island (*after* Harrison et al., in press).

K-feldspar-phyric granodiorite (Skipton et al., 2019). These ages are within the $3000\text{--}2775 \pm 2$ Ma range of protolith ages for basement gneiss from the Ege Bay area (Fig. 4; Bethune and Scammell, 2003a) to the south.

Granodiorite–tonalite–monzogranite gneiss

Gneissic units in the Rae Craton are characteristically foliated and medium grained, with compositional banding on a 1–10 cm scale (Fig. 5a). Mafic bands contain a biotite±hornblende±magnetite assemblage, whereas felsic bands mainly consist of plagioclase–quartz±K-feldspar. The gneiss commonly contains enclaves or bands of quartz diorite, diorite, gabbro and, less commonly, hornblendite, which are oriented parallel to foliation and layering (Fig. 5a, b). The centimetre-scale gneissosity defined by alternating mafic- and felsic-rich bands is generally accompanied by decimetre- to metre-scale compositional banding resulting from the transposition of different rock types.

Mary River Group

The Mary River Group comprises mafic metavolcanic rocks with intervening strata of siliciclastic units, banded iron-formation, felsic to intermediate metavolcanic rocks and ultramafic sills/volcanic rocks. Existing U–Pb data indicate at least two temporally distinct volcanic episodes. North of the type locality at Mary River (Fig. 4), Skipton et al. (2019) documented ages of 2833 ± 3 Ma and 2829 ± 5 Ma for felsic–intermediate volcanism, whereas they reported a considerably younger crystallization age of 2731 ± 6 Ma for a dacite north of the ‘Felsenmeer flats’ area (Fig. 4). In the Ege Bay and Isortoq greenstone belts in the Ege Bay area (Fig. 4), intermediate–felsic volcanism occurred between ca. 2740 and 2725 Ma (Bethune and Scammell, 2003a).

In general, the stratigraphy of the Neoproterozoic Mary River Group comprises a lower section of dominantly mafic metavolcanic rocks with lesser psammite±quartzite, overlain by iron-formation, and an upper sequence of psammite±quartzite and felsic–intermediate metavolcanic rocks with minor mafic metavolcanic units. Ultramafic rocks form low-volume, discontinuous layers at various stratigraphic levels (Jackson, 2000; Young et al., 2004; Johns and Young, 2006; Bros and Johnston, 2017; Skipton et al., 2017; Saumur et al., 2018).

Mafic metavolcanic (and subvolcanic) rocks

Mafic metavolcanic rocks are fine- to medium-grained and contain hornblende–plagioclase±actinolite±clinopyroxene±magnetite±biotite±quartz±garnet±chlorite±epidote assemblages. The rocks are typically equigranular or characterized by hornblende, or plagioclase, that forms medium-grained crystals within a fine-grained matrix. Compositional banding is common, defined by alternating mafic and felsic layers 5–50 mm thick that may reflect primary layering. Relict volcanic textures occur locally, including fine-grained plagioclase-rich clasts or coarse-grained hornblende/clinopyroxene pods within a fine-grained mafic matrix, or layered bomb- or lens-shaped mafic clasts (Fig. 5c, d). In rare cases, mafic volcanic deposits contain thin layers of fine-grained carbonate (Fig. 5d). Fine- to medium-grained mafic rocks that lack definitive volcanic textures may represent thick flows or shallow subvolcanic intrusions.

Banded iron-formation

The Mary River Group hosts Neoproterozoic oxide- and silicate-facies banded iron-formation. Iron-formation is typically 3–10 m thick, concordant with volcano-sedimentary layering and locally forms bodies that can be more than 100 m thick and extend for tens of kilometres along strike (MacLeod, 2012). The group hosts nine high-grade iron deposits that are currently tenured to Baffinland Iron Mines Corporation, most notably the Deposit No. 1 mine at Mary River (Fig. 4). The high-grade iron ore is interpreted to have formed from banded iron-formation that underwent pervasive desilicification resulting from circulation of hot, alkaline brine (MacLeod, 2012). The deposits are described in detail in a number of studies (Jackson, 2000, 2006; Young et al., 2004; MacLeod, 2012).

The oxide-facies banded iron-formation is characterized by 0.1–3 cm scale banding of magnetite(±hematite) and chert (Fig. 5e), with local occurrences of massive magnetite beds up to 10 m thick. Silicate-facies banded iron-formation is less common and comprises alternating bands of quartz, magnetite, and cummingtonite–grunerite±garnet that are 0.1–3 cm thick (Fig. 5f). Whereas some banded iron-formations have orange and/or purple gossanous weathering, most weather dark grey, grey-blue or dark brown. Outside

the banded iron-formation, isolated ironstone layers are relatively common within mafic and ultramafic volcanic units, forming centimetre- to decimetre-scale bands of granular magnetite±hematite.

Andesite and rhyolite

Intermediate rocks are less common than mafic units in the Mary River Group. Although they contain higher proportions of plagioclase and quartz, intermediate volcanic and subvolcanic rocks have the same metamorphic mineral assemblages and similar textures as their mafic counterparts, described above.

Rhyolite is overlain by banded iron-formation and underlain by psammite in the Tuktularvik area (Fig. 4). The rhyolite is aphanitic apart from fine-grained muscovite and millimetre-scale quartz bands, which are parallel to compositional banding defined by alternating pale yellow and cream-coloured bands up to 1 cm thick.

Ultramafic rocks

Ultramafic rocks form a relatively minor component of the Mary River Group, and recent field observations (Skipton et al., 2017; Saumur et al., 2018) suggest that they are not as spatially extensive as indicated by previous studies (e.g. Davidson et al., 1979). Ultramafic rocks, which form discontinuous layers, typically comprise aligned orthopyroxene phenocrysts within a beige or light grey to black, fine-grained to aphanitic groundmass, suggesting a subvolcanic or volcanic origin (i.e. komatiite). Spinifex texture, diagnostic of quenched komatiitic flow sequences, was not observed, possibly owing to extensive recrystallization and/or deformation. In places, ultramafic rocks form medium- to coarse-grained intrusive bodies that contain clinopyroxene±orthopyroxene±hornblende±olivine.

Psammitic, quartzite, semipelite, pelite

Concordant with volcanic strata, siliciclastic sequences are mostly up to approximately 10 m thick (hundreds of metres thick at Tuktularvik; Fig. 4). Muscovite±biotite psammite is most common. Quartzite contains muscovite±biotite±garnet and is in sharp contact with (structurally) underlying monzogranite. Pelite and semipelite contain chlorite–muscovite–biotite±garnet±staurolite±magnetite, with staurolite locally forming porphyroblasts up to 7 cm long. Garnet is euhedral and typically 0.5–1 cm in size, reaching 5 cm locally.

Plutonic rocks

Quartzofeldspathic intrusions include foliated to massive quartz monzonite–granodiorite–monzogranite (±K-feldspar or plagioclase megacrysts) and aplitic to pegmatitic syenite dykes. An age of $2709 \pm 4/-3$ Ma is reported for monzogranite near Paquet Bay (Fig. 4; Jackson et al., 1990), whereas an age of 2731 ± 3 Ma is documented for a monzogranite east of Mary River (Fig. 4; Skipton et al., 2019). Further south, six calcalkaline granite–granodiorite intrusions near Ege Bay (Fig. 4) yielded similar ages ranging from ca. 2726 to 2714 Ma, and thus appear in part contemporaneous with, and to outlast, the younger phase of Mary River Group volcanism (Bethune and Scammell, 2003a).

Monzogranite–granodiorite

Medium-grained biotite±hornblende±magnetite monzogranite–granodiorite (Fig. 5g) is widespread in the Rae Craton of Baffin Island. Plutons are homogeneous and typically weakly foliated, but range from massive to strongly foliated, and can occur as L- or L>S-tectonite. Potassium-feldspar megacrysts (±1.5 cm) occur in some localities. The intrusions locally contain enclaves of diorite or gabbro, and rarely enclaves (<1 m to 10–20 m) of fine-grained, foliated, mafic volcanic rocks interpreted as Mary River Group. Weakly foliated monzogranite is observed to cut granodiorite gneiss in several localities.

Feldspar-megacrystic monzogranite to granodiorite intrusions form 1–10 km scale plutons and are characterized by euhedral, weakly compositionally zoned megacrysts (2–5 cm) of either K-feldspar or plagioclase feldspar within a medium- to coarse-grained groundmass. Mafic minerals include biotite±hornblende±magnetite. The plutons locally exhibit a weak tectonic lineation or foliation, but are typically massive due to their coarse grain size and low proportion of mafic minerals. Megacrysts are locally aligned, potentially indicative of primary magmatic flow.

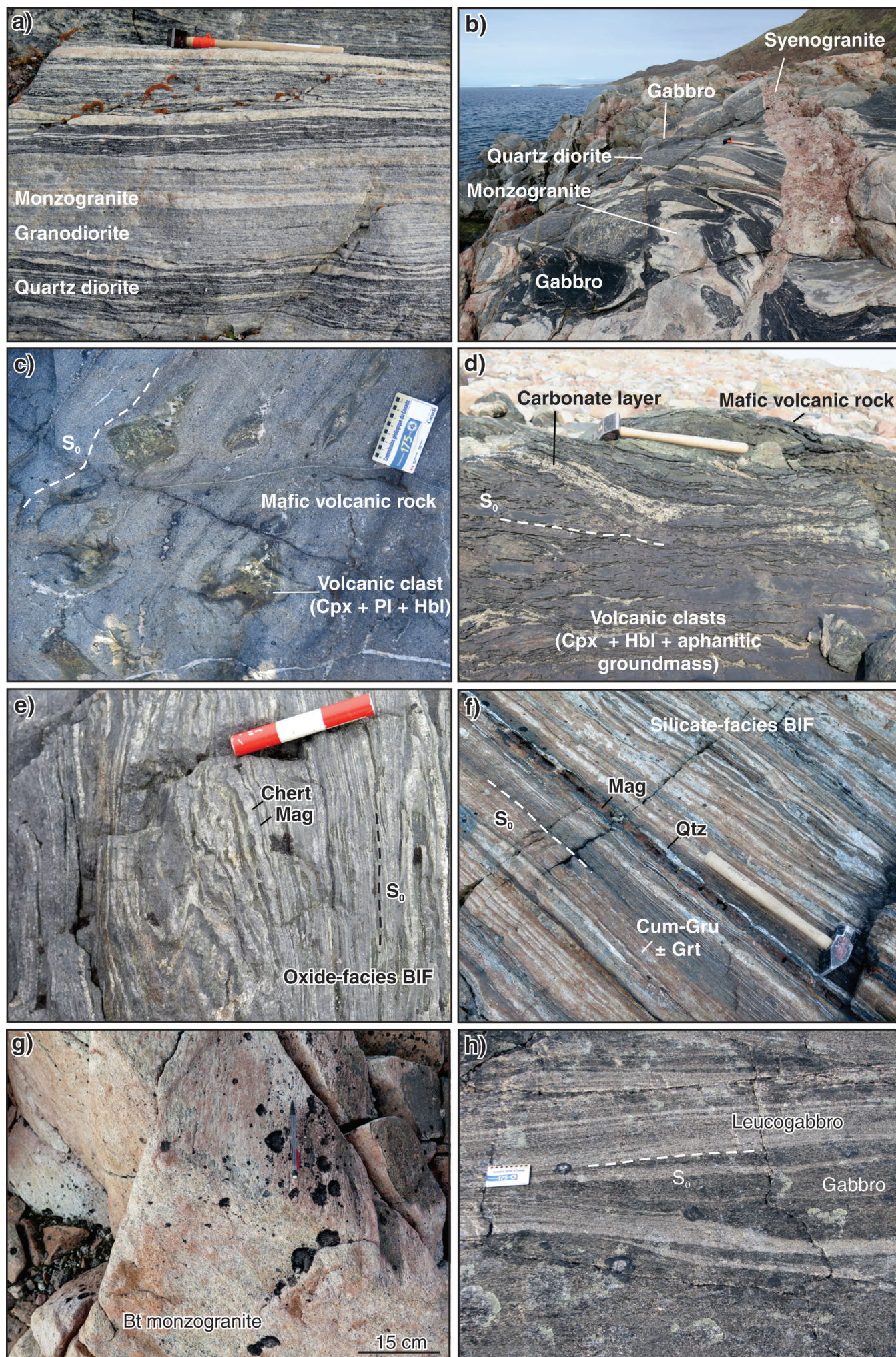


Figure 5. Rae Craton basement gneiss and Mary River Group strata, northern Baffin Island (*modified from Skipton et al., 2017*). **a)** Gneiss composed of granodiorite with bands of quartz diorite and monzogranite (hammer for scale). Photograph by D.R. Skipton. NRCan photo 2018-338. **b)** Gneiss composed of quartz diorite with monzogranite bands and gabbro enclaves/bands; folded and boudinaged gneissic bands are crosscut by a pegmatitic syenogranite dyke (hammer for scale). Photograph by D.R. Skipton. NRCan photo 2018-339. **c)** Mafic metavolcanic rock preserving volcanic layering (S_0) composed of a fine-grained matrix and pods of coarse-grained clinopyroxene (Cpx), plagioclase (Pl) and hornblende (Hbl), interpreted as volcanic clasts (scale bar = 7 cm). Photograph by D.R. Skipton. NRCan photo 2018-340. **d)** Clinopyroxene (Cpx)–hornblende (Hbl)-bearing mafic metavolcaniclastic rock with layers of fine-grained carbonate (\pm crystalline calcite) and volcanic layering (S_0) (hammer for scale). Photograph by E.R. Bros. NRCan photo 2018-341. **e)** Oxide-facies banded iron-formation near the Tuktularvik area (Fig. 4), composed of alternating layers (S_0) of magnetite (Mag) and chert (scale marker is 8 cm long). Photograph by D.R. Skipton. NRCan photo 2018-342. **f)** Silicate-facies banded iron formation in the Tuktularvik area (Fig. 4), consisting of alternating layers (S_0) of quartz (Qtz), magnetite (Mag) and cummingtonite (Cum)–grunerite (Gru) \pm garnet (Grt) (hammer for scale). Photograph by D.R. Skipton. NRCan photo 2018-343. **g)** Homogeneous biotite (Bt) monzogranite. Photograph by B.M. Saumur. NRCan photo 2018-344. **h)** Gabbro and leucogabbro layers (S_0) within a layered mafic–ultramafic intrusion (scale bar = 7 cm). Photograph by M.R. St-Onge. NRCan photo 2018-345. Mineral abbreviations after Whitney and Evans (2010).

Syenogranite

The youngest documented felsic plutonic phase comprises coarse-grained to pegmatitic, massive biotite±magnetite syenogranite dykes, 5 cm to 3 m wide. The dykes intrude the granodiorite–tonalite–monzogranite gneiss (Fig. 5b), monzogranite–granodiorite intrusions, and rarely the Mary River Group, including the banded iron-formation. Hornblende or clinopyroxene occurs locally in pegmatitic syenogranite dykes that cut hornblende-bearing plutonic units or mafic enclaves.

Diorite, gabbro, and hornblendite enclaves

Medium-grained hornblende±biotite±clinopyroxene diorite and gabbro enclaves occur within granodiorite–tonalite–monzogranite gneiss (commonly forming bands; Fig. 5a, b) and monzogranite–granodiorite intrusions; medium- to coarse-grained hornblendite enclaves are less common. Enclaves are generally foliated, less than 1 m in size, comprise less than 10% of outcrop volume and are oriented parallel to the tectonic fabrics in the host rocks.

Layered mafic–ultramafic bodies

Mafic–ultramafic intrusions comprise 100 to 500 m thick layers of gabbro/diorite with hornblende clinopyroxenite and/or websterite. Within gabbroic portions, primary decimetre-scale, rhythmic compositional layering is defined by varying proportions of plagioclase and clinopyroxene (or hornblende after clinopyroxene), producing alternating bands of leucogabbro and gabbro (Fig. 5h). Layering is irregular along strike, exhibiting truncations and layer-scale deformation that possibly reflect dynamic magmatic conditions.

PALEOPROTEROZOIC SOUTHERN MARGIN OF THE RAE CRATON (LEVEL 4)

The Paleoproterozoic Piling Group on central Baffin Island (Fig. 6) comprises shallow-water siliciclastic–carbonate strata, mafic–ultramafic volcanic rocks, and deep-water basinal strata (e.g. Morgan et al., 1976; Henderson et al., 1979; Henderson and Tippett, 1980; Tippett, 1985; Jackson, 2000; Corrigan et al., 2001; Scott et al., 2002b, 2003; St-Onge et al., 2005; Partin et al., 2014a; Wodicka et al., 2014). The shallow-water strata and volcanic rocks are generally regarded as having accumulated as a result of regional crustal

extension along the southeastern margin of the Archean Rae Craton (e.g. Rainbird et al., 2010), followed by deposition of the deep-water strata in a foreland or proto-ocean basin (Partin et al., 2014a; Wodicka et al., 2014). Subsequently, all stratigraphic units were deformed and metamorphosed during the ca. 1.92–1.80 Ga Trans-Hudson Orogeny (Corrigan et al., 2001; Scott et al., 2002b; St-Onge et al., 2006; Gagné et al., 2009). The Piling Group (Fig. 6) forms part of an extensive cover sequence on the Rae Craton, with stratigraphic correlatives extending from the western Churchill Province on mainland Nunavut (e.g. Penrhyn, Amer, Ketyet River, Chantrey, and Montresor groups; Jackson and Taylor, 1972; Taylor, 1982; Rainbird et al., 2010), across Baffin Island (Hoare Bay Group; St-Onge et al., 2009), to western Greenland (Karrat and Anap nunâ groups; Escher and Pulvertaft, 1976; Henderson and Pulvertaft, 1987; Garde and Steenfelt, 1999).

Piling Group

The Piling Group is divided into five formations (Morgan, 1983; Tippett, 1985), which comprise, in ascending stratigraphic order, the Dewar Lakes, Flint Lake, Bravo Lake, Astarte River, and Longstaff Bluff formations (Fig. 6, 7).

Dewar Lakes formation

The Dewar Lakes formation can be subdivided into three members (Scott et al., 2003), the lowest of which comprises thinly bedded, muscovite-rich quartzite, grey- to pink-weathering psammite, and feldspathic quartzite (Fig. 7a). The overlying, and by far the most widespread, middle member comprises medium to thickly bedded sillimanite±muscovite-rich quartzite (Fig. 7b) characterized by dominantly southward-directed cross-stratification. The upper member comprises thin beds of quartzite to psammite and rusty semipelite to pelite (Fig. 7c). The overall thickness of the Dewar Lakes formation varies significantly from less than 1 m to locally over 1000 m. Thickness variability may reflect primary sedimentary depocentres (Tippett, 1985; Jackson, 2000; Scott et al., 2003). Basal quartzite and rare psammite of the lower Dewar Lakes formation are in stratigraphic (locally reworked) unconformable contact with underlying Archean orthogneissic and plutonic rocks, and the formation is interpreted as a clastic sheet deposited on Rae cratonic basement. The dominance of quartz over feldspar and the presence of rock fragments throughout the formation suggest a relatively high degree of sedimentological

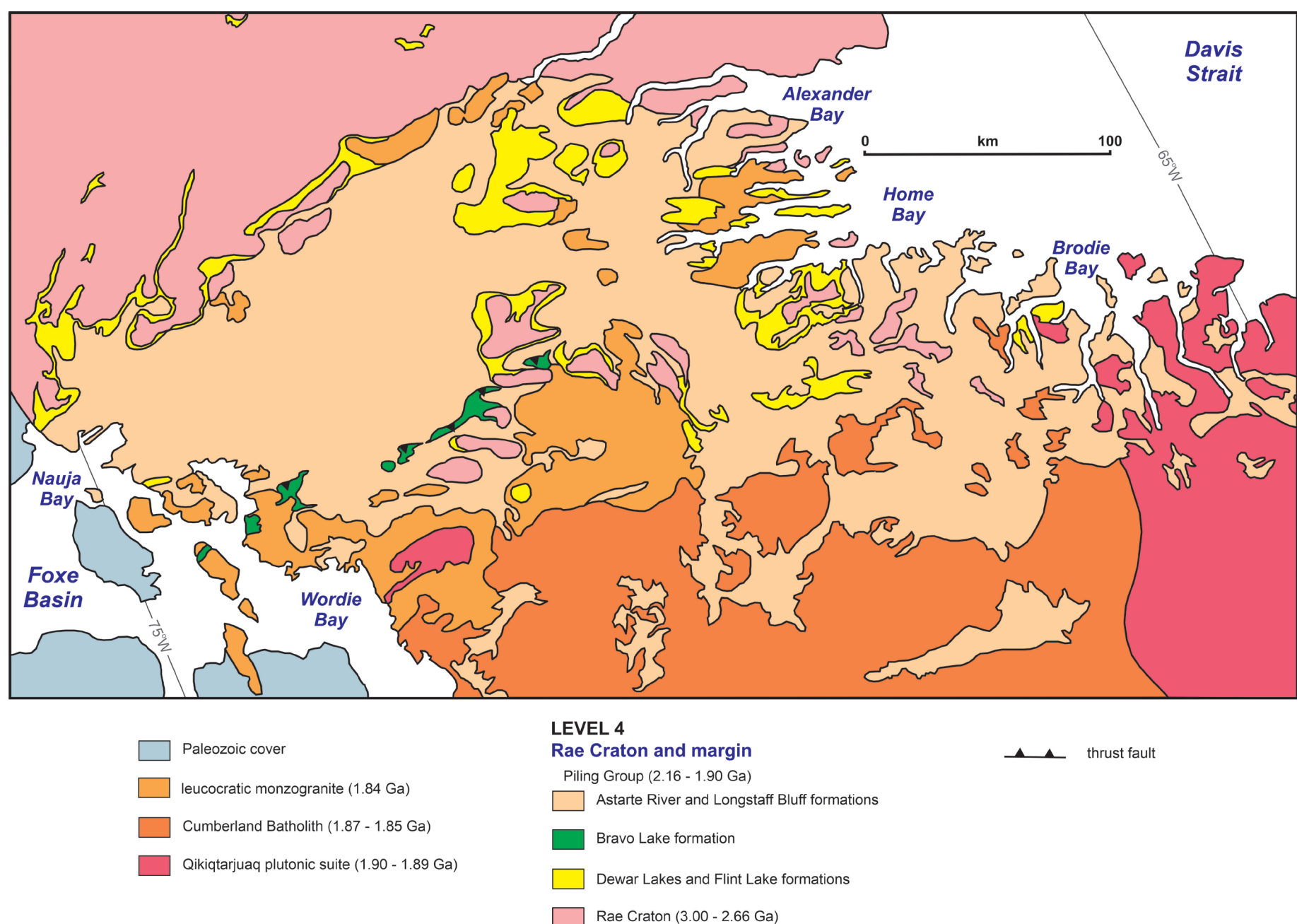


Figure 6. Geology of the Paleoproterozoic Piling Group on central Baffin Island (after Harrison et al., in press).

maturity (Tippett, 1985). Most of the Dewar Lakes formation was likely deposited in a shallow marine environment (e.g. Tippett, 1985; de Kemp et al., 2002a, b).

Flint Lake formation

White- to grey-weathering dolostone, marble, and calc-silicate strata of the Flint Lake formation (Fig. 7d) interlayered with lesser semipelite, pelite, quartzite, iron-formation, and chert, stratigraphically overlie the upper member of the Dewar Lakes formation (Morgan et al., 1976; Corrigan et al., 2001; Scott et al., 2002b; St-Onge et al., 2005). The exposed thickness of this formation varies considerably both along and across strike, from several metres to 500–1000 m (Fig. 6). The overall decrease in carbonate material toward the south led Scott et al. (2002b, 2003) to suggest that the Flint Lake formation originally formed a relatively narrow (75–100 km wide) south-facing carbonate shelf adjacent and parallel to the southeastern edge of the Rae Craton, with significant along-strike variation in primary thickness.

Bravo Lake formation

The Bravo Lake formation forms a nearly continuous, 120 km long, east-trending mafic volcanic belt in the southern part of the Piling structural basin (Fig. 6). Like the Flint Lake formation, it conformably overlies the siliciclastic rocks of the upper Dewar Lakes formation, which suggests that the lithologically distinct carbonate and volcanic sequences occupy an equivalent stratigraphic position

within the Piling Group (de Kemp et al., 2002a, b; Scott et al., 2003). Based on lithostratigraphic and structural considerations, the Bravo Lake formation, and in places the Dewar Lakes formation, are interpreted to have been tectonically juxtaposed against the younger Longstaff Bluff formation across a north- to northwest-directed thrust fault (Fig. 6; Tippett, 1985; Corrigan et al., 2001; de Kemp et al., 2002a, b; Stacey and Pattison, 2003). The Bravo Lake formation has an estimated thickness of 1.0–2.5 km and can be subdivided into two sequences (Modeland and Francis, 2003, 2004; Johns et al., 2006).

The lower sequence is dominated by pillowed, subalkaline, tholeiitic to picritic basaltic flows (Fig. 7e) and volcanoclastic rocks with iron-formation and rare intrusive mafic to ultramafic sills. The upper sequence comprises volcanoclastic rocks and mostly alkaline basaltic flows intruded by numerous ultramafic to mafic alkaline sills (Fig. 7f) and locally abundant partially sheeted dykes at its base. A succession of siliciclastic rocks 10 to 300 m thick, including quartzite, semipelite, pelite, and calcsilicate, separates the two sequences and represents a key regional stratigraphic marker. The mafic magmas range in composition from tholeiitic in the lower sequence to dominantly alkaline in the upper sequence, strikingly similar to that of modern ocean-island basalt suites (e.g. Modeland and Francis, 2004; Partin et al., 2014a). Detailed mapping suggests that the mafic–ultramafic volcanism occurred in a low-energy, shallow submarine environment (de Kemp et al., 2002a, b; Johns et al., 2006). Based on its stratigraphic setting and chemical composition, the Bravo Lake formation is interpreted to have formed in a rift setting (i.e. intracontinental rift or incipient oceanic rift; Jackson, 2000; Johns et al., 2006; Corrigan et al., 2009; Wodicka et al., 2014) or foredeep



Figure 7. Piling Group strata, central Baffin Island. **a)** Thinly bedded psammite and quartzite, lower member of the Dewar Lakes formation (hammer for scale). Photograph by M.R. St-Onge. NRCan photo 2018-350. **b)** Thick-bedded quartzite, middle member of the Dewar Lakes formation (location of hammer for scale indicated with arrow). Photograph by M.R. St-Onge. NRCan photo 2018-351. **c)** Thinly bedded psammite and quartzite of the upper member of the Dewar Lakes formation (hammer for scale). Photograph by M.R. St-Onge. NRCan photo 2018-352. **d)** Dolomitic marble (light) and calcsilicate rocks (dark) of the Flint Lake formation (nose of helicopter for scale). Photograph by M.R. St-Onge. NRCan photo 2018-353. **e)** Pillowed, subalkaline, tholeiitic to picritic basaltic flows, lower sequence of Bravo Lake formation (hammer for scale). Photograph by M.R. St-Onge. NRCan photo 2018-354. **f)** Alkaline basaltic flows intruded by ultramafic to mafic alkaline sills, upper sequence of Bravo Lake formation (hammer for scale). Photograph by M.R. St-Onge. NRCan photo 2018-355.

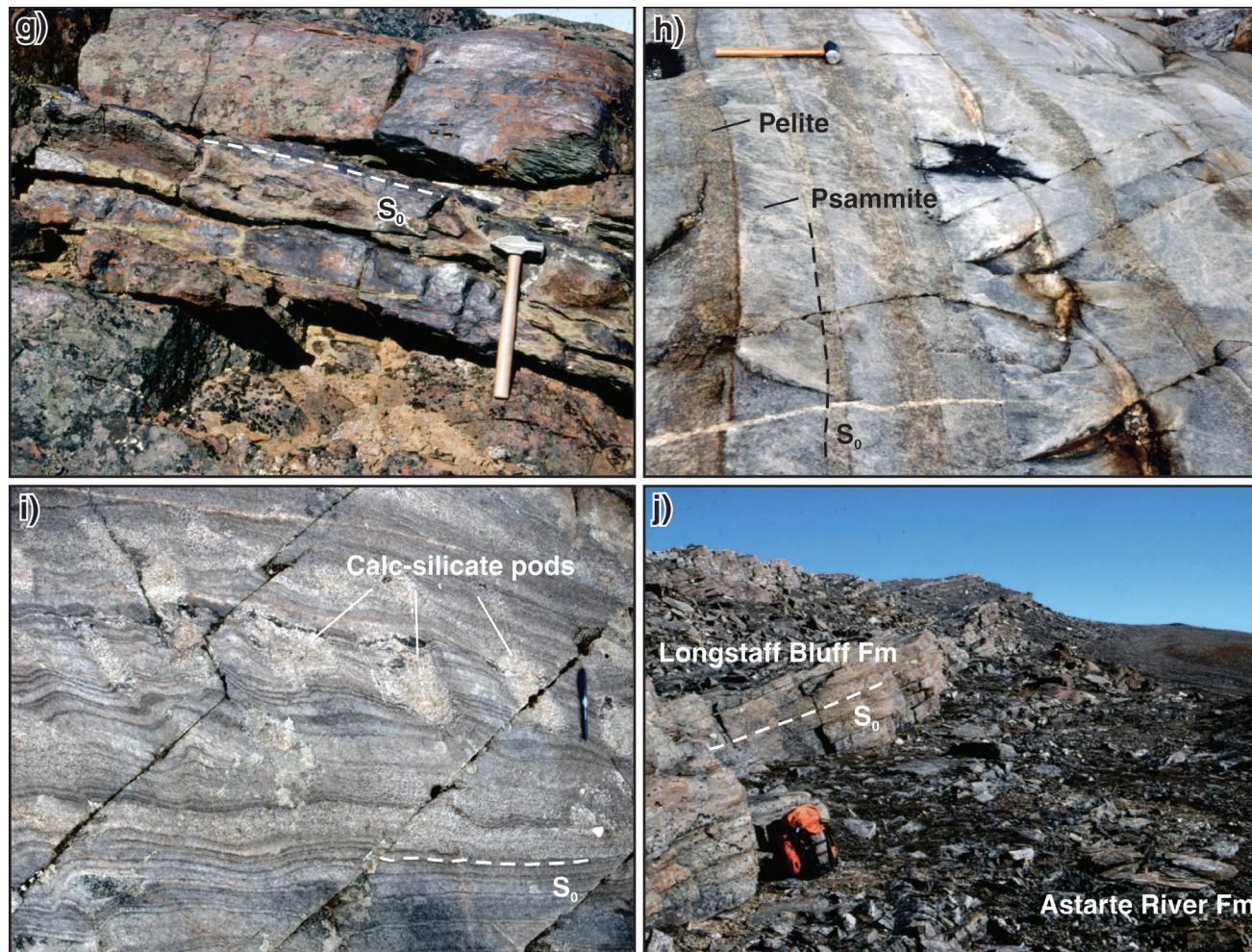


Figure 7. (cont.) **g)** Rusty, thinly bedded pelite, semipelite and ironstone of the Astarte River formation (hammer for scale). Photograph by M.R. St-Onge. NRCAN photo 2018-356. **h)** Psammite-pelite beds of the Longstaff Bluff formation displaying normally graded bedding, with stratigraphic tops to the right (hammer for scale). Photograph by M.R. St-Onge. NRCAN photo 2018-357. **i)** Calc-silicate pods in the Longstaff Bluff formation, interpreted as metamorphosed carbonate concretions (pen for scale). Photograph by M.R. St-Onge. NRCAN photo 2018-358. **j)** Ledge-forming psammite-semipelite turbidite of the Longstaff Bluff formation (Fm) on the left overlying rusty pelite of the Astarte River formation on the right (backpack for scale). Photograph by M.R. St-Onge. NRCAN photo 2018-359.

setting (Partin et al., 2014a), underlain by variably enriched mantle (Modeland and Francis, 2004). The structural trends of the sheeted dykes within the upper sequence indicate offset rifting within strike-slip pull-apart basins (Johns et al., 2006). Scattered mafic sills occur within the underlying Dewar Lakes formation and Archean basement, and the overlying Longstaff Bluff formation (Tippett, 1985; St-Onge et al., 2005). These rocks show a close geochemical correspondence with mafic-ultramafic rocks from the Bravo Lake formation, indicating a potential cogenetic relationship (Tippett, 1984, 1985; Gladstone and Francis, 2003) and suggesting that, in part, Bravo Lake magmatism continued after deposition of the Longstaff Bluff formation.

Astarte River formation

Rusty-weathering graphitic pelite, semipelite, and minor sulphide-facies iron-formation of the Astarte River formation (Fig. 7g) directly overlie carbonate rocks of the Flint Lake formation in the northwest, siliciclastic rocks of the Dewar Lakes formation in the central part of the Piling structural basin, and mafic volcanic rocks of the Bravo Lake formation in the south (Fig. 6; Scott et al., 2003). This sulphide-rich (pyrite-pyrrhotite) sequence is estimated to be over 500 m thick and marks a relatively abrupt transition from shallow-water sedimentation and volcanism to deep-water sedimentation, suggesting the onset of a tectonic process that rapidly increased rates of subsidence and led to drowning of the Flint Lake carbonate platform.

Longstaff Bluff formation

The Longstaff Bluff formation, the uppermost stratigraphic component of the Piling Group (Fig. 6), is a 3–5 km thick, monotonous succession of feldspathic psammite and greywacke, subordinate semipelite, and rare pelite interpreted as turbidite (e.g. Henderson et al., 1979; Henderson and Tippett, 1980; Tippett, 1985; Jackson, 2000; Scott et al., 2002b). These rocks are distinguished from the quartz-rich rocks of the Dewar Lakes formation by their greater mica content (notably biotite) and the dominance of plagioclase relative to K-feldspar (Tippett, 1985). Primary sedimentary features are best preserved in the dominantly low-metamorphic-grade area and type locality for the Longstaff Bluff formation northeast of Nauja Bay (Fig. 6). In this region, individual psammite beds display normally graded bedding (Fig. 7h), generally indicating an upright sequence. Other primary structures such as crossbeds, scours, and ripples are less common (Forester and Gray, 1966; Morgan et al., 1975;

Jackson, 2000; Scott et al., 2003; St-Onge et al., 2005). Paleocurrents measured from these structures in the middle and upper parts of the Longstaff Bluff formation indicate an apparent east–west sediment transport. The composition of the turbiditic rocks (e.g. euhedral feldspar crystals and crystal fragments, blue quartz, and mafic minerals) suggests derivation from, at least in part, a volcanic source area (Jackson, 2000; Corrigan et al., 2001; Scott et al., 2002b). Calc-silicate pods (Fig. 7i), interpreted as metamorphosed carbonate concretions, are ubiquitous. According to most workers, the Longstaff Bluff formation is considered to extend as migmatitic metasedimentary rocks south of the Bravo Lake formation (Fig. 6; e.g. Tippett, 1985; Henderson and Henderson, 1994; St-Onge et al. 2005).

Field relationships indicate that Longstaff Bluff turbiditic beds stratigraphically overlie both rusty pelite of the Astarte River formation (Fig. 7j) and volcanic rocks of the Bravo Lake formation. The character of the better preserved northern Longstaff Bluff formation, including the generally fine-grained nature of the turbiditic rocks, the dominance of normal-graded bedding, and the lateral continuity in bedding thicknesses, combine to suggest that the bedded strata represent distal-facies turbidite (e.g. Henderson and Tippett, 1980) deposited on the suprafan lobe portion of an outer submarine fan (Tippett, 1985). Most workers have suggested that the deep-water deposits signal a dramatic change in tectonic conditions, with the clastic detritus originating in a foreland, molasse-type basin and/or a fragmented proto-ocean basin (e.g. Jackson, 2000; Corrigan et al., 2001, 2009; Scott et al., 2003; St-Onge et al., 2005; Partin et al., 2014a; Wodicka et al., 2014). Wodicka et al. (2014) have specifically suggested a two-component source with possible input from the Snowbird tectonic zone to the west and the Bravo Lake formation more locally.

Piling Group age constraints

The U-Pb zircon and carbon-isotope chemostratigraphy data presented by Partin et al. (2014a) and Wodicka et al. (2014) provide important insights into the depositional ages of principal sedimentary units of the Piling Group and the timing of Bravo Lake formation mafic-ultramafic volcanism and sill emplacement. The youngest detrital zircon grains from samples collected in the lower, middle, and upper members of the Dewar Lakes formation have yielded highly variable, but progressively younger, maximum ages of deposition of ca. 2725 Ma, 2719 ± 22 Ma, 2312 ± 23 Ma, and 2159 ± 16 Ma, respectively (Wodicka et al., 2014). The youngest U-Pb zircon age from adjacent basement rocks (2658 +16/-14 Ma; St-Onge et al.,

2009) provides the current best maximum age for the onset of low-est Piling Group sedimentation. However, the true age of basin formation and onset of shallow-water sedimentation could be considerably younger, particularly given that the youngest detrital zircon grains in passive-margin or cratonic successions, which typically lack evidence for contemporaneous igneous activity, may be tens to hundreds of millions of years older than the time of sediment accumulation (e.g. Cawood and Nemchin, 2001; Bradley, 2008).

In the overlying Flint Lake formation, $\delta^{13}\text{C}$ values suggest formation of the carbonate platform after ca. 2.06 Ga (Partin et al., 2014a). The chemostratigraphic age constraints are consistent with the maximum age constraint of 2.16 Ga for the upper Dewar Lakes formation.

Field relationships, geochemistry, and age constraints suggest that magmatic activity related to the Bravo Lake formation occurred over a period of approximately 100 Ma. Two indirect lines of evidence indicate that tholeiitic to picritic volcanism within the lower Bravo Lake sequence may have commenced as early as ca. 1980 Ma. A 1979 ± 13 Ma anhedral zircon fragment in a trachyte dyke (Wodicka et al., 2014) could represent a xenocryst incorporated into the trachytic melt during ascent through the lower Bravo Lake formation volcanic pile. Similarly, 1980 ± 11 Ma detrital zircon grains within quartzose semipelite, taken from a channel near the base of the lower Bravo Lake formation, could be derived from erosion of adjacent lava flows or volcanoclastic rocks (Wodicka et al., 2014). Upper Bravo Lake formation magmatism is constrained at or before 1923 ± 15 Ma (Wodicka et al., 2014), the age of the upper Bravo Lake trachyte dyke with a synvolcanic origin (Johns et al., 2006). A maximum depositional age of 1940 ± 28 Ma for a lithic metawacke from the upper Bravo Lake formation (Partin et al., 2014a) is consistent with this interpretation. The youngest magmatism possibly related to the Bravo Lake formation, consisting of highly differentiated sills, occurred at $1897 +10/-5$ Ma (Wodicka et al., 2014) and 1883.3 ± 4.7 Ma (Henderson and Parrish, 1992), following deposition of the Longstaff Bluff formation.

Five Longstaff Bluff formation detrital zircon samples have yielded maximum ages of deposition of 1964 ± 9 Ma and 1931 ± 4 Ma for samples located in the high-grade area south of the Bravo Lake formation (i.e. southern Longstaff Bluff formation), and 1923 ± 7 Ma, 1915 ± 8 Ma and 1883 ± 38 Ma for samples taken north of the volcanic belt (i.e. northern Longstaff Bluff formation; Partin et al., 2014a; Wodicka et al., 2014), with the differences in ages possibly indicating diachronous deposition between the northern and southern parts of the Longstaff Bluff formation. Minimum age constraints are obtained from a $1897 +7/-4$ Ma rapakivi-textured, K-feldspar megacrystic monzogranite intrusive into the southern turbiditic strata (Fig. 6; Wodicka et al., 2014), a unit possibly correlative (Sanborn-Barrie et al., 2017) with the Qikiqtarjuaq plutonic suite of Rayner et al. (2012) and Sanborn-Barrie et al. (2013), and from in situ

ages of 1878 ± 25 Ma and 1875 ± 31 Ma for metamorphic monazite growth in northern deposits of the Longstaff Bluff formation (Gagné et al., 2009).

Hoare Bay Group

The Hoare Bay Group (Jackson, 1971, 1998) is a Paleoproterozoic supracrustal sequence exposed on central Cumberland Peninsula, eastern Baffin Island (Fig. 8). Traditionally, the group has been correlated with, and interpreted as, a deep-water equivalent of the Piling Group of central Baffin Island (Fig. 6; Jackson and Taylor, 1972; St-Onge et al., 2006). Recent bedrock mapping on Cumberland Peninsula (Sanborn-Barrie and Young, 2011; Sanborn-Barrie et al., 2013a) has further highlighted the broad lithological similarities between the Hoare Bay and Piling groups, as well as differences in the chemistry of the volcanic units; published regional syntheses (e.g. St-Onge et al., 2009) have suggested both groups may also broadly correlate with the Karrat and Anap nunâ groups of West Greenland (Hamilton, 2014).

The Hoare Bay Group is a clastic-dominated succession, the lower part of which consists of pelite, semipelite and psammite, minor orthoquartzite, marble and calc-silicate, and ultramafic–mafic volcanic and intrusive rocks. The middle part of the group, the focus of study by Keim et al. (2011) and Keim (2012), is composed of ultramafic–mafic volcanic rocks and their intrusive equivalents (Totnes Road formation) and overlain by a sequence dominated by iron-formation (Clephane Bay formation). Psammite, semipelite, and minor ultramafic–mafic volcanic and intrusive rocks comprise the upper part of the Hoare Bay Group (Hamilton, 2014).

Lower Hoare Bay Group

The lower Hoare Bay Group comprises staurolite, andalusite- and sillimanite-bearing pelite and semipelite interlayered with lesser quartzite (Fig. 9a), psammite, and siliceous marble (Hamilton, 2014). Lithological layering occurs at a millimetre- to decimetre-scale. Lenticular hornblendite bodies that locally crosscut the compositional layering in the pelitic host rocks are interpreted as feeder dykes and sills to one of three overlying ultramafic–mafic volcanic units (Mackay, 2011; Keim, 2012; Whalen et al., 2012), which locally preserve a pyroclastic texture with lapilli- and bomb-sized fragments. Massive varieties occasionally contain plagioclase-rich, millimetre-wide varioles (Hamilton, 2014).

Middle Hoare Bay Group

Stratigraphically above the uppermost pelite of the lower Hoare Bay Group, a sharp contact defines the base of the Totnes Road formation (Keim, 2012). In the type Totnes Road locality (Fig. 8), the formation comprises plagioclase-hornblende schist and gneiss,

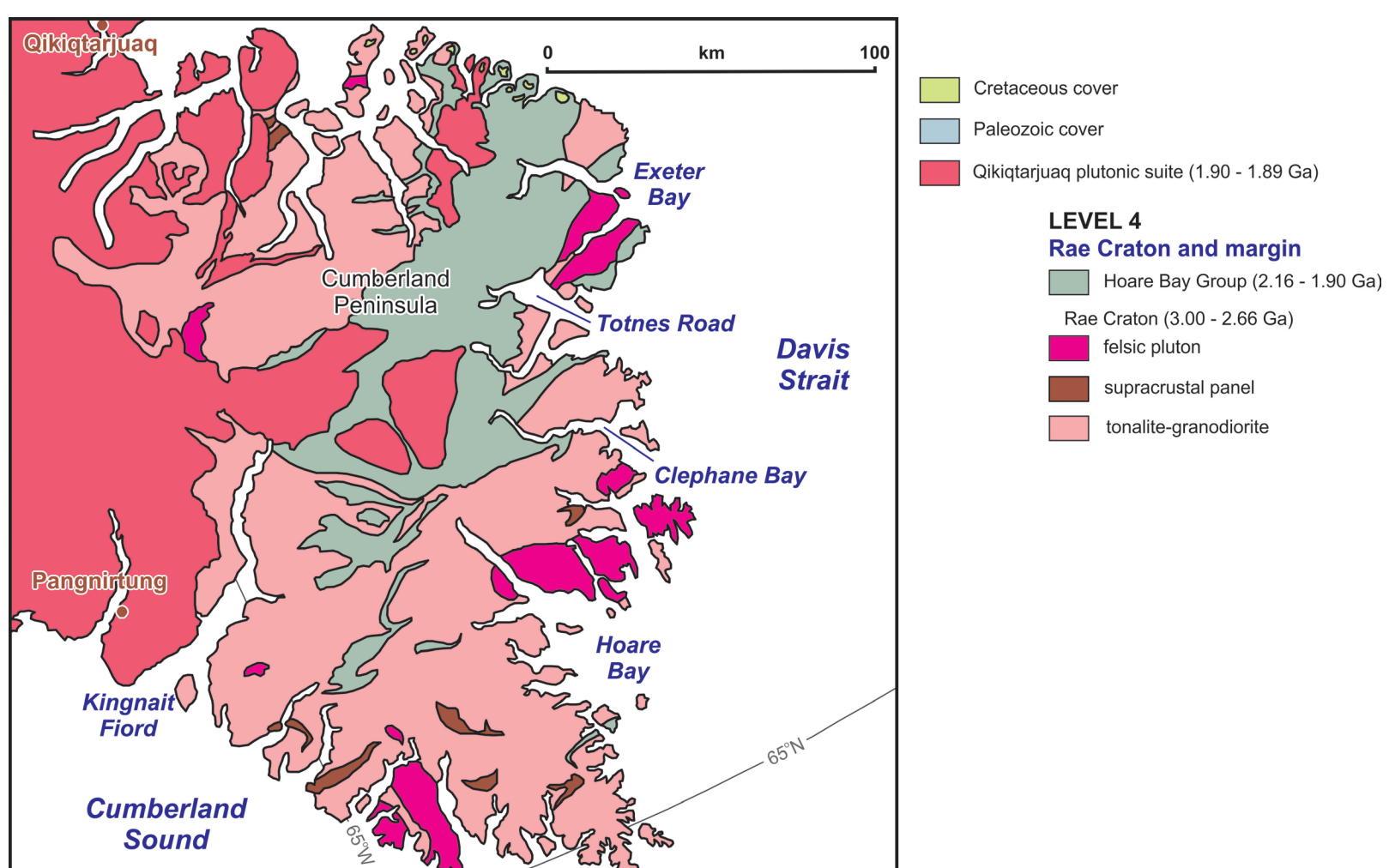


Figure 8. Geology of the Paleoproterozoic Hoare Bay Group on Cumberland Peninsula, eastern Baffin Island (after Harrison et al., in press).



Figure 9. Hoare Bay Group strata, Cumberland Peninsula, eastern Baffin Island. **a)** Orthoquartzite, lower Hoare Bay Group (geologist for scale). Photograph by M.R. St-Onge. NRCan photo 2018-360. **b)** Plagioclase-rich varioles 2–4 mm wide in tholeiitic basalt of the Totnes Road formation, middle Hoare Bay Group (pen for scale). Photograph by M.R. St-Onge. NRCan photo 2018-361. **c)** Pyroclastic unit with lapilli- and bomb-sized fragments, Totnes Road formation, middle Hoare Bay Group (pen for scale). Photograph by M.R. St-Onge. NRCan photo 2018-362. **d)** Graphite-rich shale with millimetre-scale bedding laminae and high-angle axial-planar cleavage (parallel to pen for scale), Clephane Bay formation, middle Hoare Bay Group. Photograph by M.R. St-Onge. NRCan photo 2018-363. **e)** Interbedded pelite and psammite, upper Hoare Bay Group (pen for scale). Photograph by M.R. St-Onge. NRCan photo 2018-364. **f)** Calc-silicate concretion, upper Hoare Bay Group (pen for scale). Photograph by M.R. St-Onge. NRCan photo 2018-365.

locally with clinopyroxene. Some layers are characterized by millimetre-wide, plagioclase-rich varioles (Fig. 9b), whereas others have a fragmental texture (Fig. 9c). Chemical analyses of the volcanic rocks suggest that they comprise Karasjok-type komatiite, komatiitic basalt, and tholeiitic basalt (Keim et al., 2011; Keim, 2012).

Several types of iron-formation, collectively referred to as the ‘Clephane Bay formation’ (Keim, 2012), overlie the Totnes Road formation. Silicate-facies iron-formation is represented by garnet-quartz-grunerite±magnetite layers (Storey, 2012), whereas sulphide-facies iron-formation is gossanous, recessively weathering, pyrite- and graphite-rich, and contains quartz, grunerite, and garnet in various proportions. Oxide-facies iron-formation (quartz and magnetite) can be layered on a millimetre to centimetre scale. The iron-formation is associated with graphite-rich shale and biotite-muscovite-bearing pelite (Fig. 9d; Sanborn-Barrie and Young, 2011; Sanborn-Barrie et al., 2011, 2013a; Keim et al., 2011; Keim, 2012).

Upper Hoare Bay Group

The upper Hoare Bay Group consists of a thick package of biotite±muscovite semipelite and psammite (Fig. 9e). Layering is on the centimetre- to decimetre-scale, graded bedding has been observed, and the strata are interpreted as metamorphosed wacke (Hamilton, 2014). Locally, the turbiditic beds contain elongated pods of calc-silicate that are interpreted as metamorphosed calcareous strata and concretions (Fig. 9f).

Hoare Bay Group age constraints

On eastern Baffin Island, the lowermost quartz-rich rocks of the Hoare Bay Group were initially derived from 2.99 to 2.71 Ga Archean sources (Fig. 8; Sanborn-Barrie et al., 2017), similar in age to underlying or nearby basement rocks (Rayner et al., 2012). Overlying upper Hoare Bay Group psammite–semipelitic rocks were derived from both Archean (2.80–2.69 Ga) and Paleoproterozoic (1.99–1.97 Ga) sources (Sanborn-Barrie et al., 2017).

In contrast to the middle–upper (or northern) Longstaff Bluff formation of the Piling Group, clastic rocks of the Hoare Bay Group lack detrital peaks of ca. 2.58–2.55 Ga and 1.92 Ga (Wodicka et al., 2014), with the youngest detrital zircon grains consistently establishing a maximum depositional age of 1.96 Ga (Sanborn-Barrie et al., 2017). The absence of a 1.92 Ga detrital peak in the Hoare Bay succession, may reflect diachronous deposition, with sedimentation in eastern Baffin Island predating that to the northwest. The influx of Paleoproterozoic detritus into the Hoare Bay basin after 1.96 Ga points to uplift and exhumation of an extensive belt of 1.99 to 1.97 Ga plutonic rocks potentially corresponding to either the Taltson and Thelon magmatic zones (van Breemen et al., 1987, 1992; McDonough et al., 2000) to the west, 1.99 to 1.98 Ga orthogneiss of the Prudhoe Land complex in West Greenland (Nutman et al., 2008) to the north, or both (Sanborn-Barrie et al., 2017).

Qikiqtarjuaq plutonic suite

Both the Archean basement gneiss of the southeastern Rae Craton and the overlying Paleoproterozoic cover strata of the Hoare Bay Group are cut by foliated, locally K-feldspar-phyric granodiorite±monzogranite±quartz diorite plutons that form a plutonic belt exposed between Pangnirtung and Qikiqtarjuaq (Fig. 8). This plutonic belt, which forms the spectacular peaks of the Auyuittuq National Park and was designated the ‘Qikiqtarjuaq plutonic suite’ by Sanborn-Barrie et al. (2011, 2013) and Rayner et al. (2012), seems to extend across the Baffin suture into the Meta Incognita microcontinent (Rayner, 2017; Fig. 3). Seven samples from this belt have yielded similar crystallization ages between 1896 and 1886 Ma, including:

- a biotite-hornblende-magnetite monzogranite near Pangnirtung (Fig. 8) and a biotite-hornblende-garnet granodiorite exposed 50 km northeast of Pangnirtung dated at 1894 ± 5 Ma and 1889 ± 3 Ma, respectively (Rayner et al., 2012)
- three samples of orthopyroxene-bearing monzogranite from the head, and west, of Cumberland Sound (Fig. 10) with crystallization ages between 1896 ± 8 Ma and 1887 ± 4 Ma (Rayner, 2017)
- two fine-grained biotite monzogranite samples exposed west of Nettilling Fiord (Fig. 1) with crystallization ages of 1891 ± 7 Ma and 1886 ± 5 Ma (Rayner, 2017). An orthopyroxene-bearing tonalite from further south on Hall Peninsula (Fig. 10), dated by Scott (1999) at $1890 +3/-2$ Ma, might also belong to the Qikiqtarjuaq plutonic suite. The ages for the plutonic suite are distinctly older than those for the ca. 1865–1845 Ma Cumberland batholith (Whalen et al., 2010; Rayner, 2015, 2017) described below.

ARCHEAN TO PALEOPROTEROZOIC META INCOGNITA MICROCONTINENT (LEVEL 3)

The Meta Incognita microcontinent or terrane (St-Onge et al., 2000a), which includes much of southern Baffin Island (Fig. 10), is considered to have accreted to the southern Rae Craton between 1915 ± 8 Ma (the youngest, most precise maximum age constraint for the Piling Group; Wodicka et al., 2014) and 1896 ± 8 Ma (the oldest dated phase of the Qikiqtarjuaq plutonic suite; Rayner 2017). The microcontinent comprises: 1) a clastic–carbonate-shelf succession (Lake Harbour Group) and its crystalline basement; 2) an overlying micaceous quartzite succession (Blandford Bay assemblage); 3) a western feldspathic quartzite-dominated clastic sequence (Lona Bay sequence); 4) a mafic volcanic sequence (Schooner Harbour sequence); and 5) an extensive suite of quartz diorite to monzogranitic plutons (Cumberland batholith) that intrude both the platformal strata and underlying crystalline basement. Orthogneiss samples from the stratigraphic basement to the Lake Harbour Group have yielded Archean ages between 3019 ± 5 and 2701 ± 2 Ma (Scott, 1998, 1999; Rayner, 2014, 2015; From et al., 2015), and a Paleoproterozoic age of $1950 +6/-4$ Ma (Scott and Wodicka, 1998). A 2310 ± 3 Ma granitic clast from a conglomerate with primitive mantle $\delta^{18}\text{O}$ values and positive ϵ_{Hf} values, and interpreted to have derived from the Meta Incognita microcontinent, provides additional evidence for Paleoproterozoic juvenile crust (Partin et al., 2014b). Plutons of the Cumberland batholith have yielded ages between 1865 ± 10 and 1845 ± 19 Ma (Jackson et al., 1990; Wodicka and Scott, 1997; Scott and Wodicka, 1998; Scott, 1999, Whalen et al., 2010; Rayner, 2015, 2017).

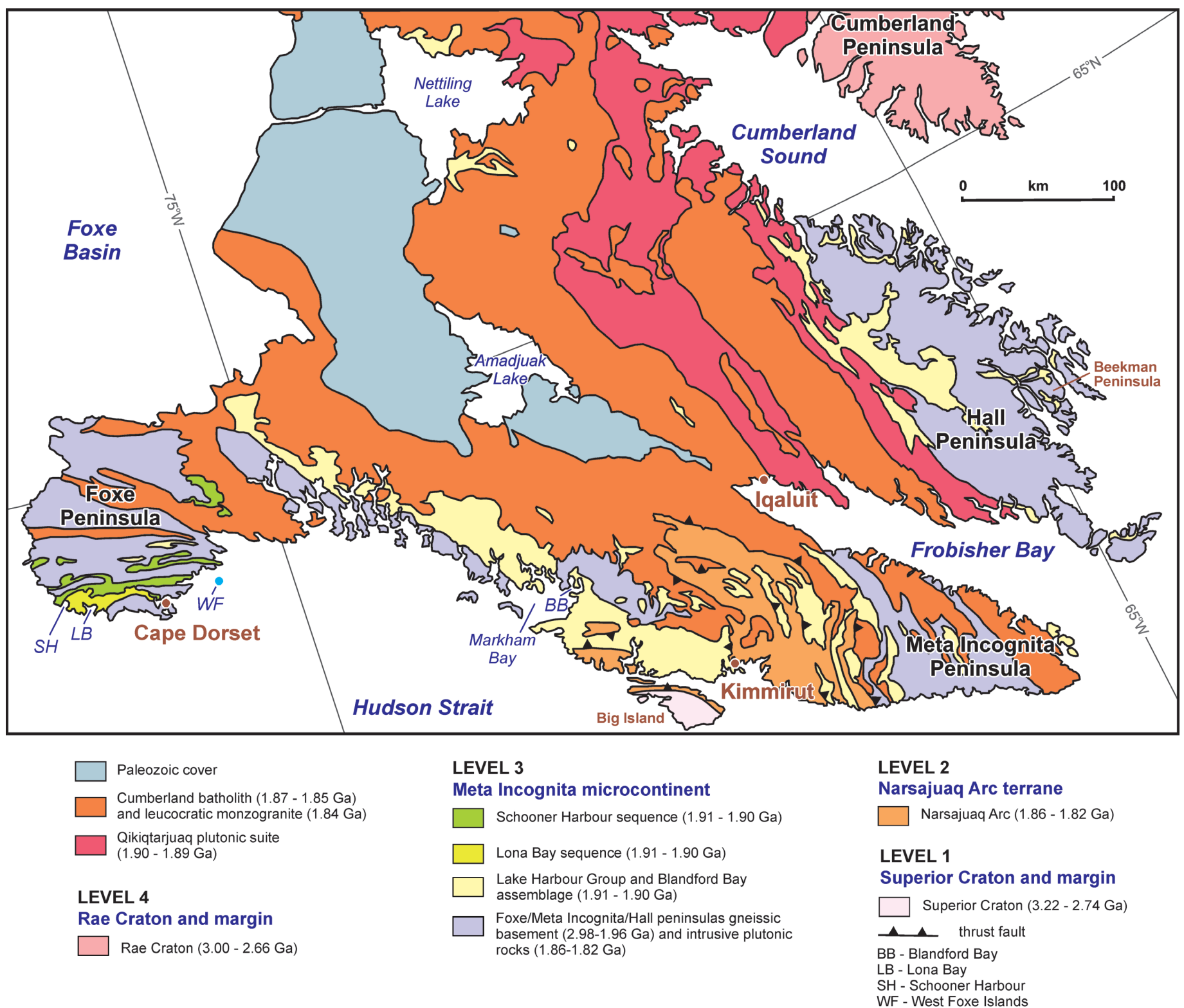


Figure 10. Geology of the Meta Incognita microcontinent, Narsajuaq Arc terrane, and the Superior Craton, southern Baffin Island (after Harrison et al., in press).

Basement orthogneiss

The basement gneiss exposed on Hall Peninsula (Fig. 10) comprises a complex assortment of polydeformed and polymetamorphosed plutonic rocks collectively termed the ‘Archean orthogneiss complex’ (From et al., 2013). The complex and similar units on Meta Incognita Peninsula and Foxe Peninsula (Fig. 10) are composed mostly of gneissic to migmatitic orthopyroxene-biotite±hornblende tonalite to porphyroclastic monzogranite with subsidiary components of well foliated to relatively massive biotite syenogranite, and boudinaged and discontinuous layers of hornblende-orthopyroxene-clinopyroxene diorite to quartz diorite (Fig. 11a; Blackadar, 1967c, d, e; Sanborn-Barrie et al., 2008; From et al., 2014; Steenkamp and St-Onge, 2014; St-Onge et al., 2015c).

Based on lithological similarities, overlying cover sequences, geochronological constraints and aeromagnetic characteristics, different cratonic correlations have been proposed for the basement gneiss of the Meta Incognita microcontinent. These include correlations with the Rae Craton of northern Baffin Island (Fig. 4) and western Greenland (Hoffman, 1988), gneiss underlying the Core Zone in northeastern Quebec (St-Onge et al., 2009), the Aasiaat domain of central western Greenland (Hollis et al., 2006a, b; Thrane and Connelly, 2006; St-Onge et al., 2009), and/or the Nain Craton of northern Labrador (Scott, 1999; Connelly, 2001; Wardle et al., 2002).

Alternatively, the basement gneiss of Meta Incognita microcontinent may represent a unique and distinct crustal component (Whalen et al., 2010).

Lake Harbour Group

Quartzite, marble, psammite and semipelite mapped on the eastern and western peninsulas of southern Baffin Island are lithologically similar to the metasedimentary strata of the contiguous Lake Harbour Group in its type locality of Kimmirut (Fig. 10; St-Onge et al., 1996, 1998; Scott et al., 1997). Two lithologically and geographically distinct sequences can be recognized. Over much of southern Baffin Island, the Lake Harbour Group is composed of quartzite, garnetiferous psammite, minor semipelite and pelite, structurally overlain by laterally continuous to boudinaged bands of pale grey to white marble and calc-silicate rocks (‘Kimmirut sequence’; Scott et al., 1997). In contrast, extensive garnetiferous psammite interlayered with pelite and/or semipelite, with less than 5% marble and calc silicate rocks (‘Markham Bay sequence’; Scott et al., 1997), is exposed on the eastern islands and bluffs of Meta Incognita Peninsula, as well as in the Markham Bay area (Fig. 10). Both sequences are cut by generally concordant sheets of mafic to ultramafic rocks (Frobisher suite; Liikane et al., 2015).

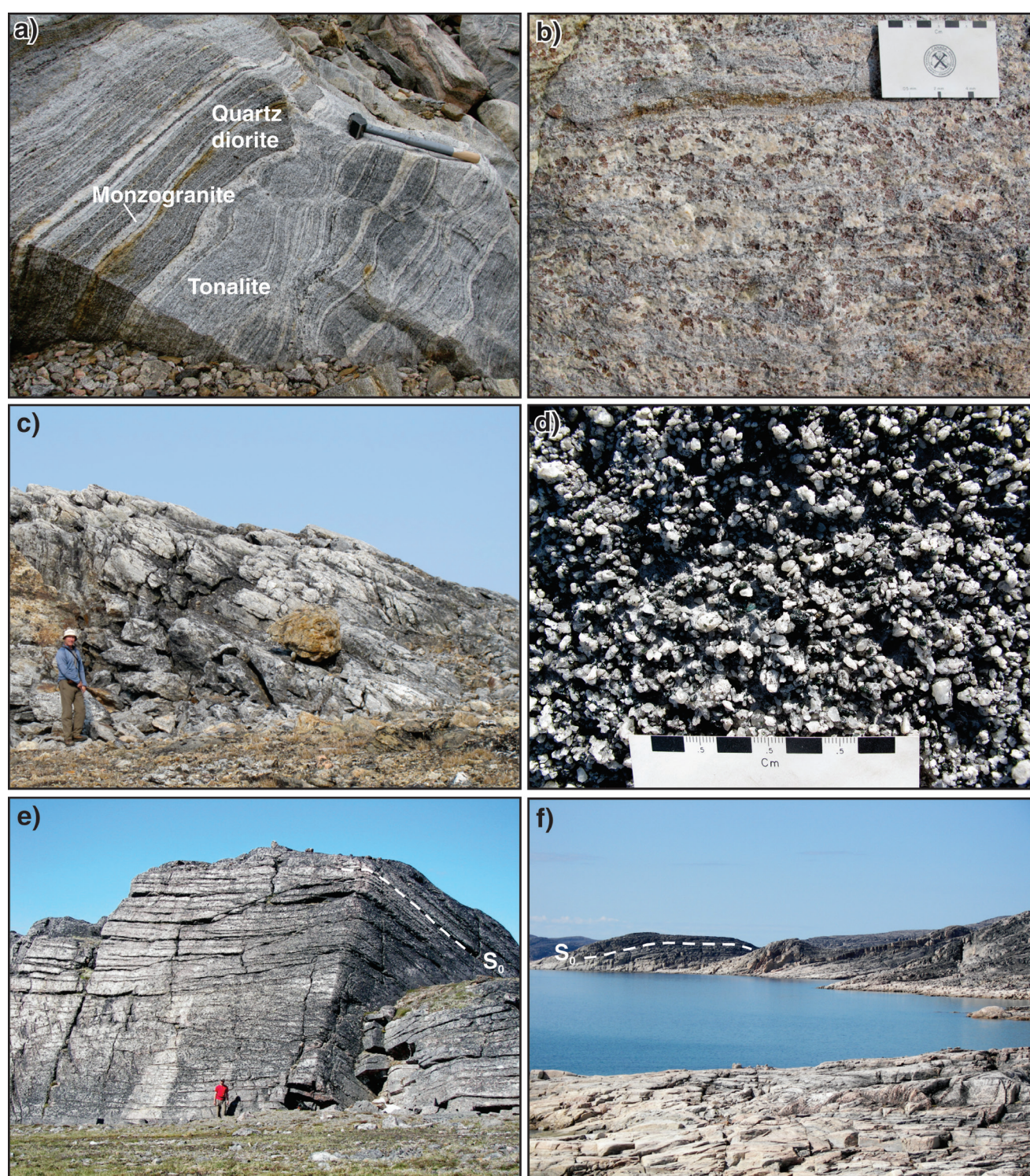


Figure 11. Hall Peninsula gneiss, Lake Harbour Group, Blandford Bay assemblage, Lona Bay sequence and Schooner Harbour sequence strata, Frobisher suite sills, southern Baffin Island (*modified in part from* St-Onge, 2015b, c). **a)** Gneissic orthopyroxene-biotite±hornblende tonalite with subsidiary components of relatively massive biotite syenogranite, and boudinaged and discontinuous layers of hornblende-orthopyroxene-clinopyroxene diorite to quartz diorite, Archean orthogneiss complex, Hall Peninsula (hammer for scale). Photograph by M.R. St-Onge. NRCan photo 2018-366. **b)** Garnet-sillimanite-biotite-leucosome psammite, Lake Harbour Group, Meta Incognita Peninsula (pen for scale). Photograph by M.R. St-Onge. NRCan photo 2018-367. **c)** Shallowly dipping, well-layered, garnet-bearing orthoquartzite, Lake Harbour Group, Meta Incognita Peninsula (geologist for scale). Photograph by D.R. Skipton. NRCan photo 2018-368. **d)** Diopside-phlogopite-spinel-apatite-quartz calcareous grit, Lake Harbour Group, Meta Incognita Peninsula. Photograph by M.R. St-Onge. NRCan photo 2018-369. **e)** Light to dark grey-weathering feldspathic quartzite, Blandford Bay assemblage, Blandford Bay (geologist for scale). Photograph by M.R. St-Onge. NRCan photo 2018-370. **f)** Cream- to buff-weathering, well-bedded, arenaceous quartzite of the Lona Bay sequence, Foxe Peninsula (width of field of view is 1 km). Photograph by M.R. St-Onge. NRCan photo 2018-371.

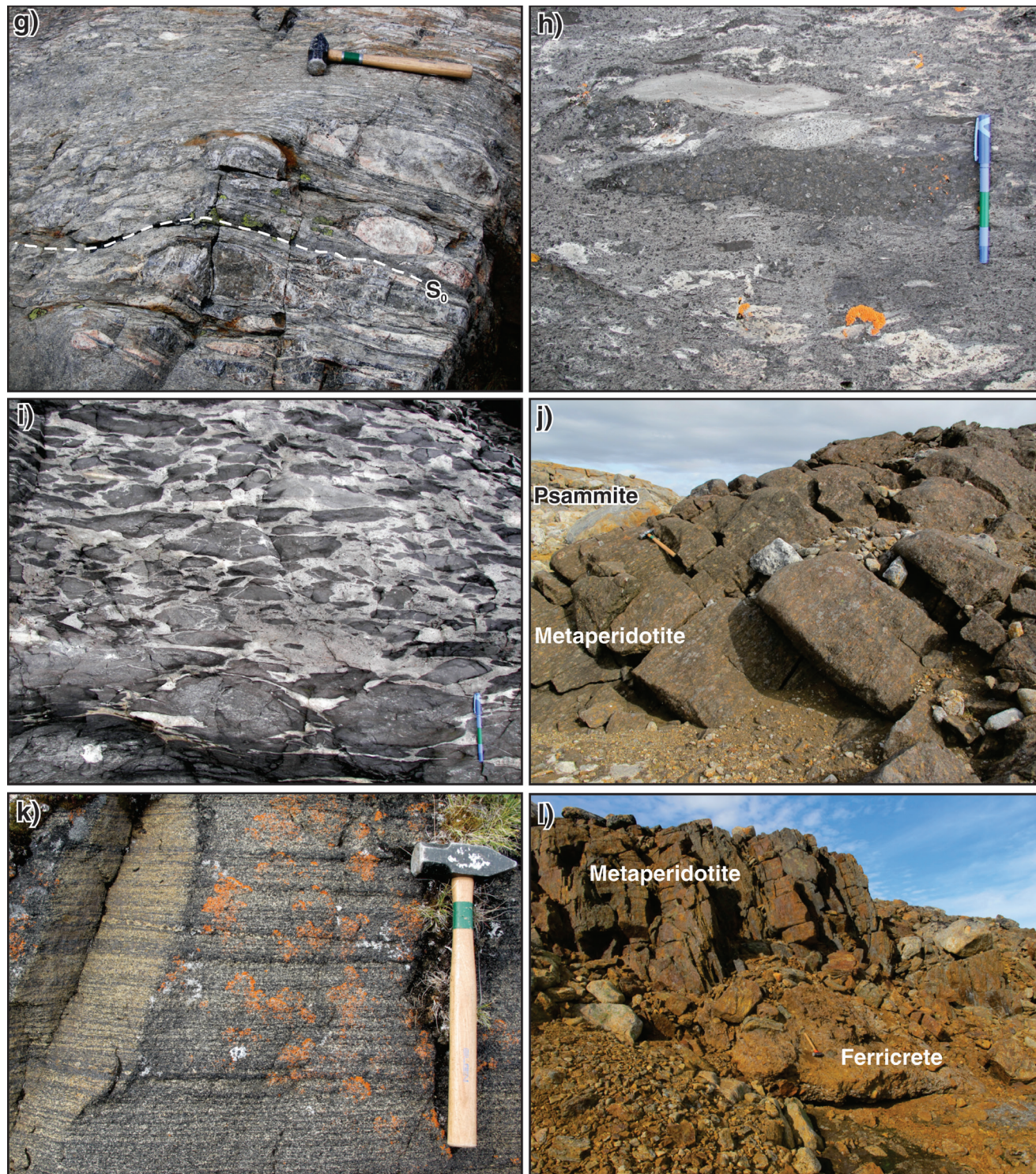


Figure 11. (cont.) **g)** Intraformational conglomeratic horizons, upper Lona Bay sequence, Foxe Peninsula (hammer for scale). Photograph by M.R. St-Onge. NRCan photo 2018-372. **h)** Primary fragmental textures in a mafic to intermediate lapilli tuff, Schooner Harbour sequence, Foxe Peninsula (pen for scale). Photograph by M.R. St-Onge. NRCan photo 2018-373. **i)** Mafic lithic fragments within an intermediate matrix in a pyroclastic layer of the Schooner Harbour sequence, Foxe Peninsula (hammer for scale). Photograph by M.R. St-Onge. NRCan photo 2018-374. **j)** Layered metaperidotite sill (Frobisher suite) emplaced in Lake Harbour Group psammite, Meta Incognita Peninsula (hammer for scale). Photograph by M.R. St-Onge. NRCan photo 2018-375. **k)** Layered metagabbro sill (Frobisher suite), Blandford Bay (hammer for scale), with rhythmic layering defined by variations in the modal amount of clinopyroxene, hornblende, and plagioclase. Photograph by M.R. St-Onge. NRCan photo 2018-376. **l)** Ferricrete below a metaperidotite sill (Frobisher suite), Meta Incognita Peninsula (hammer for scale). Photograph by M.R. St-Onge. NRCan photo 2018-377.

Psammite, quartzite, semipelite and pelite

Compositional layers within psammite range from centimetres to tens of centimetres in thickness and can be traced for up to tens of metres along strike. They are generally defined by variations in the modal abundance of quartz, plagioclase, biotite, garnet, sillimanite, cordierite and granitic melt (Fig. 11b). Garnet-sillimanite pelite typically occurs as thin layers within garnet-biotite semipelite, the latter subordinate within the psammite. Psammite and semipelite are generally rusty weathering due to trace amounts of disseminated graphite, pyrite and chalcocopyrite.

Quartzite occurs as discrete layers (Fig. 11c) several metres to several hundred metres thick. The layers compositionally range from orthoquartzite to feldspathic quartzite, commonly contain graphite±garnet±sillimanite and are strongly recrystallized. Primary sedimentary features were not observed. White leucogranite, rich in lilac garnet and sillimanite, is a ubiquitous constituent cutting the siliciclastic package, generally occurring as concordant layers or pods <0.5 m thick, but locally several tens of metres thick.

Marble and calc-silicate

Calcareous rocks are medium to coarse grained, locally with compositional layering defined by varied modal proportions of calcite, forsterite, humite, diopside, tremolite, phlogopite, spinel, apatite

and, rarely, wollastonite. Individual layers range from centimetres to metres in thickness and can be traced for tens of metres along strike. Calc-silicate rocks are commonly interlayered with siliciclastic rocks and generally associated with marble. Locally, the calcareous strata include layers of calcareous grit with abundant 1–2 mm detrital quartz grains (Fig. 11d). Thicknesses of calcareous units typically range from several decametres to about 1 km north of Kimmirut (Fig. 10). Individual marble units can be traced from 5 to 25 km along strike. No primary structures were observed in the calcareous rocks.

Blandford Bay assemblage

In the Blandford Bay area (Fig. 10), rocks of the Blandford Bay assemblage are found disconformably overlying those of the Lake Harbour Group (Scott et al., 1997).

Pelite

Rusty-weathering pelite is thinly bedded and commonly forms sections several hundreds of metres thick. Garnet, sillimanite, disseminated pyrite and minor chalcocopyrite are found throughout. Compositionally graded beds are observed locally and comprise coarser psammitic bases that pass into pelitic tops, consistent with turbidite deposits. A gradational contact separates this unit from overlying feldspathic quartzite.

Feldspathic quartzite

Light to dark grey-weathering feldspathic quartzite, typically medium- to coarse-grained, forms the dominant siliciclastic component of the Blandford Bay assemblage (Fig. 11e). Homogeneous sections up to 500 m thick are common and form prominent ridges with individual beds generally 10–20 cm thick but reaching up to 2 m in thickness. Wave-washed exposures of dominantly massive and subordinate planar-laminated quartzite on the northern shore of Blandford Bay display well-developed upright crossbedding.

Lona Bay sequence

A succession of relatively homogeneous arenaceous rocks is exposed on southwestern Foxe Peninsula, in the southern part of Baffin Island. This sequence, informally designated the ‘Lona Bay sequence’ (Fig. 10; Sanborn-Barrie et al., 2008), consists of cream-to buff-weathering quartzose rocks that are typically well bedded (Fig. 11f). In general, beds 10 to 30 cm thick are highlighted by variations in grain size, cross-stratification, and distribution of metamorphic porphyroblasts. Although locally these rocks consist of muscovite with porphyroblastic texture, their aluminous character is more typically reflected by the occurrence of white-weathering, 0.5–2 cm long knots of sillimanite±muscovite±K-feldspar±magnetite (faserkiesel texture). The Lona Bay sequence primarily forms a broad, open antiform defined by shallow, west-dipping beds exposed at Schooner Harbour in the west (Fig. 10), and shallow east-dipping beds east of Lona Bay. Toward the stratigraphic top of the exposed sequence, several conglomeratic horizons (Fig. 11g), ranging from 20 cm to 1 m in thickness, are interbedded with the arenaceous rocks. These horizons are believed to be intraformational with respect to the upper Lona Bay sequence.

On southeastern Foxe Peninsula, arenaceous rocks including muscovitic quartzite overlie semipelite and marble strata interpreted as middle to upper Lake Harbour Group. The arenaceous rocks are oriented in the same direction as the Lona Bay sequence and have been correlated with it based on composition, texture, and creamy weathering. If the correlation is correct and the contact relationships are stratigraphic rather than tectonic, it suggests that the Lona Bay sequence is younger than the Lake Harbour Group and may disconformably overlie it (Sanborn-Barrie et al., 2008).

Schooner Harbour sequence

A heterogeneous volcanic-rock-bearing supracrustal belt that structurally overlies the arenaceous strata of the Lona Bay sequence extends across southern Foxe Peninsula for approximately 100 km, from Schooner Harbour in the west, to the West Foxe Islands in the east. Kilometre-scale belts of amphibolite also occur north and northeast of this main corridor. All the above was designated the ‘Schooner Harbour sequence’ by Sanborn-Barrie et al. (2008) based on exposures of low-grade, well-preserved volcanic rock in the vicinity of Schooner Harbour (Fig. 10). Volcanic units are mainly of basaltic to andesitic composition and include lapilli tuff (Fig. 11h) and variolitic strata. Heterogeneous units characterized by epidote-rich layers and lenses are widespread throughout the Schooner Harbour sequence. Extrusive rocks of ultramafic composition are exposed along the coast near Schooner Harbour, where brilliant green-weathering rocks with a subtle fragmental texture appear to represent komatiitic lapilli stone. Inland, silver green-weathering chlorite schist interlayered with fine-grained basalt and psammite is interpreted as a highly strained and hydrated ultramafic horizon (Sanborn-Barrie et al., 2008). Rocks of andesitic composition exposed on the West Foxe Islands (Fig. 10) comprise a well bedded pyroclastic sequence that commonly shows normal grading of lithic fragments (Fig. 11i). At this locality, both matrix and fragments are commonly pyroxene-phyric. Rare, thin, cream-weathered siliceous units may represent a minor component of flow-banded rhyolite, or chert.

Low in the exposed Schooner Harbour sequence, clastic rocks associated with the volcanic units include fine-grained pelite, slate, and schist that contain medium-pressure staurolite-andalusite-garnet assemblages (Smye et al., 2009). White-weathering orthoquartzite occurs as 1 m thick horizons that alternate with amphibolite, with more psammitic units upsection. Polymictic conglomerate with flattened pebbles of granite, foliated tonalite, quartzite, and psammite is also present as discontinuous horizons generally less than 1 m thick. Beds containing clasts of variolitic basalt provide evidence of a proximal erosion event occurring during accumulation of the Schooner Harbour sequence (Sanborn-Barrie et al., 2008).

Age constraints for Meta Incognita microcontinent cover sequences

Five recent mapping campaigns on southern Baffin Island (Fig. 1) have documented that the composition, association, and context of metasedimentary rocks southwest of Cumberland Sound (Weller et al., 2015), on the adjacent Hall Peninsula (e.g. Rayner et al., 2012; Steenkamp et al., 2016), on eastern Meta Incognita Peninsula (St-Onge et al. 2015c), on western Meta Incognita Peninsula (Scott et al., 2002a), and in the Markham Bay–Cape Dorset area (Scott et al., 2002a; Sanborn-Barrie et al., 2008) are similar and can be correlated with the type Lake Harbour Group assemblage in the Kimmirut area of western Meta Incognita Peninsula (St-Onge et al., 1996; Scott et al., 1997, 2002a).

A subset of Lake Harbour Group quartzite samples from eastern Hall and Meta Incognita peninsulas (Fig. 10), interpreted as locally derived basal sedimentary rocks, preserved mostly Archean detrital ages. Significant modes have been documented at 2.92, 2.85–2.80, 2.78–2.77, 2.72, and 2.68–2.67 Ga, and minor ones at 3.30–3.20 Ga (Scott et al., 2002a; Rayner, 2014, 2015). Two samples also contain minor Paleoproterozoic detritus, one of which provides a maximum depositional age of 2010 ± 19 Ma for the basal Lake Harbour Group (Wodicka et al., 2008).

Siliciclastic and carbonate samples from stratigraphically higher levels of the Lake Harbour Group yield dominantly Paleoproterozoic detritus but tend to fall into one of two provenance-profile types. The first type is characterized by detrital zircon grains yielding distinctive age peaks at 2.60–2.50, 2.40–2.30, 2.20, 2.14–2.08, 1.97–1.95 and 1.93–1.91 Ga (Scott et al., 2002a; Rayner, 2014, 2015, 2017). Older Archean detritus generally defines subordinate peaks, except for one sample from Beekman Peninsula (Fig. 10) immediately east of Hall Peninsula, which contains significant secondary populations yielding ages between 2.95 and 2.55 Ga (Rayner, 2014). Overall, the detritus from the first provenance-profile type is inferred to be sourced from local underlying Meta Incognita microcontinent basement (Wodicka et al., 2010; Rayner, 2017). In contrast, the detritus in the second provenance-profile type is almost exclusively Paleoproterozoic in age, with dominant peaks between 2.10 and 1.87 Ga (Scott et al., 2002a, Rayner, 2014, 2015, 2017). The psammite- and quartzite-rich rocks of the second type define a belt from Cumberland Sound to the eastern tip of Meta Incognita Peninsula and share many similarities with the Tasiuyak paragneiss of northern Labrador (e.g. Scott et al., 2002a).

The maximum age of deposition of the first and second provenance-profile types in the Lake Harbour Group is very similar at 1906 ± 9 and 1907 ± 9 Ma, respectively (Rayner, 2014). The intrusive Frobisher suite, with an estimated age of ca. 1900 Ma (and possibly as old as 1922 ± 12 Ma; Liikane et al., 2015), provides a minimum age constraint for the clastic–carbonate-shelf succession.

Feldspathic quartzite of the Blandford Bay assemblage contains detritus of exclusively Archean age, in contrast to the Paleoproterozoic detritus of the stratigraphically underlying Lake Harbour Group. Scott et al. (2002a) showed a dominant mode at 2.86 Ga, and subordinate peaks at 3.64, 3.02 and 2.76 Ga. Nevertheless, as rocks of the Blandford Bay assemblage depositionally overlie those of the Lake Harbour Group, the assemblage is also constrained by a maximum age of 1906 ± 9 Ma (Scott et al., 2002a; Rayner, 2014).

Volcanic units of the Schooner Harbour sequence (Fig. 10) could not be dated successfully owing to the absence of igneous zircon, but detrital zircon populations from clastic rocks show major peaks at ca. 2.69, 2.62, 2.41, 2.31 and 2.10 Ga, and define a maximum depositional age of 2099 ± 5 Ma (Wodicka et al., 2010).

Frobisher suite

Generally concordant sheets of medium- to coarse-grained, massive to weakly foliated peridotite, pyroxenite, layered peridotite-gabbro, and homogeneous gabbro occur within the Lake Harbour Group, the Blandford Bay assemblage and the lower part of the Schooner Harbour sequence (Fig. 10; St-Onge et al., 1996, 1998, 2015b; Scott et al., 1997; Sanborn-Barrie et al., 2008; MacKay and Ansdell, 2014; Steenkamp et al., 2014). These mafic to ultramafic rocks are collectively designated the ‘Frobisher suite’ by Liikane et al. (2015). Individual units are typically 10 to 100 m thick, although some reach a few hundred metres in thickness and extend up to several kilometres along strike. They are dark green- to reddish-brown-weathering resistive units that form prominent ridges relative to adjacent supracrustal host rocks (Fig. 11j). Metagabbroic textures and compositional layering at the centimetre to metre scale defined

by variations in modal abundance of clinopyroxene, orthopyroxene, hornblende, and plagioclase are commonly preserved in the mafic bodies (Fig. 11k). The concordant nature, tabular shape, and sharp contacts of these bodies all indicate they are sills. Ultramafic bodies, either clinopyroxene-orthopyroxene±hornblende metapyroxenite or olivine-clinopyroxene-orthopyroxene metaperidotite, are common. In numerous localities, the ultramafic rocks are compositionally layered with many sills containing disseminated sulphide, some associated with a ferricrete, which consists of medium to coarse clastic sediment cemented by an iron oxy-hydroxide (Fig. 11l). A full field description of the mafic and ultramafic rocks on southern Baffin Island is provided in St-Onge et al. (2015b) and Liikane et al. (2015).

The occurrence of the ultramafic to mafic sills emplaced in the sedimentary units of the Lake Harbour Group and lower Schooner Harbour sequence suggests that the intrusive units may represent hypabyssal feeders to the mafic to ultramafic Schooner Harbour volcanic sequence (Sanborn-Barrie et al., 2008).

The layered mafic–ultramafic sills define a magmatic suite that characterizes the whole of the Meta Incognita microcontinent, as exposed on southern Baffin Island (Liikane et al., 2015). The size and distribution of the mantle-derived rocks suggest that they are the product of a major large igneous province event with a study of the petrology, geochemistry, and associated mineralization presented in Liikane (2017). A sample of Frobisher suite leucogabbro from south-central Meta Incognita Peninsula has yielded an igneous zircon crystallization age of 1922 ± 12 Ma (Liikane et al., 2015).

Cumberland batholith

The southern Rae Craton, the Piling Group cover sequence, and the crystalline and supracrustal units of Meta Incognita microcontinent are cut by plutonic rocks of the Cumberland batholith (Fig. 6, 10). The batholith is dominated by granitic phases dated between 1865 ± 10 and 1845 ± 19 Ma (Jackson et al., 1990; Wodicka and Scott, 1997; Scott and Wodicka, 1998; Scott, 1999; Whalen et al., 2010; Rayner, 2015, 2017) and has been interpreted as an Andean-type batholith (St-Onge et al., 2009), or as the result of postcollisional lithospheric delamination and mantle upwelling (Whalen et al., 2010).

Coarse-grained to pegmatitic, kilometre-scale, layered clinopyroxene-biotite-magnetite±hornblende gabbro (Fig. 12a) forms one of the older recognized plutonic suites within the batholith (Weller et al., 2015) and can include metre-scale lenses of clinopyroxene-bearing anorthosite. Quartz diorite dated

at 1865 ± 9 Ma (Rayner, 2017) occurs as fine-grained, dark-weathering, massive to foliated units (Fig. 12b) containing the assemblage biotite-clinopyroxene-orthopyroxene±hornblende.

Well-foliated biotite±orthopyroxene±magnetite±hornblende±garnet monzogranite is dominant and underlies large parts of south-central Baffin Island. These rocks are typically medium grained, tan to pink weathering and equigranular, alternating between magnetite-rich and magnetite-free domains (Weller et al., 2015). A sample of biotite monzogranite collected from the eastern end of Meta Incognita Peninsula was dated at 1865 ± 10 Ma by Rayner (2015). White-weathering, massive to foliated, fine- to medium-grained garnet-biotite±magnetite monzogranite dated at 1853 ± 8 Ma (Rayner, 2017) forms plutons and dykes that are intrusive into the biotite monzogranite, as well as the coarse-grained K-feldspar megacrystic monzogranite of the Qikiqtarjuaq plutonic suite (Fig. 12c). Garnet is present as abundant burgundy phenocrysts 2 to 30 mm across, frequently in association with biotite.

Dykes of garnet-sillimanite leucogranite (1852 ± 11 Ma; Rayner, 2017) cut the garnet-biotite monzogranite. The dykes are typically fine grained, with 1 to 5 mm lilac garnet phenocrysts and mats of sillimanite. The presence of sillimanite suggests that the leucogranite is derived from muscovite-dehydration melting of metasedimentary units (e.g. Weller et al., 2015), rather than being a highly fractionated component of the plutonic suite.

Pink- to orange-weathering, medium- to coarse-grained, massive to foliated biotite±orthopyroxene±magnetite±garnet monzogranite, with distinctive K-feldspar megacrysts (Fig. 12d), occurs throughout large parts of southern Baffin Island. Potassium-feldspar phenocrysts form augen up to 10 cm wide and locally display rapakivi textures (ovoid alkali feldspar mantled by plagioclase feldspar). Megacrystic monzogranite from Meta Incognita Peninsula was dated by Rayner (2015) at 1845 ± 19 Ma.

PALEOPROTEROZOIC NARSAJUAQ ARC TERRANE (LEVEL 2)

The Narsajuaq Arc terrane is considered to be represented by two temporally and petrologically distinct magmatic suites: an older intraoceanic suite exposed on the Ungava Peninsula of northern Quebec (Fig. 3) and a younger Andean-margin-type suite (Dunphy and Ludden, 1998), exposed both in northern Quebec and southern Baffin Island (Fig. 10). The older suite includes calc-alkaline layered

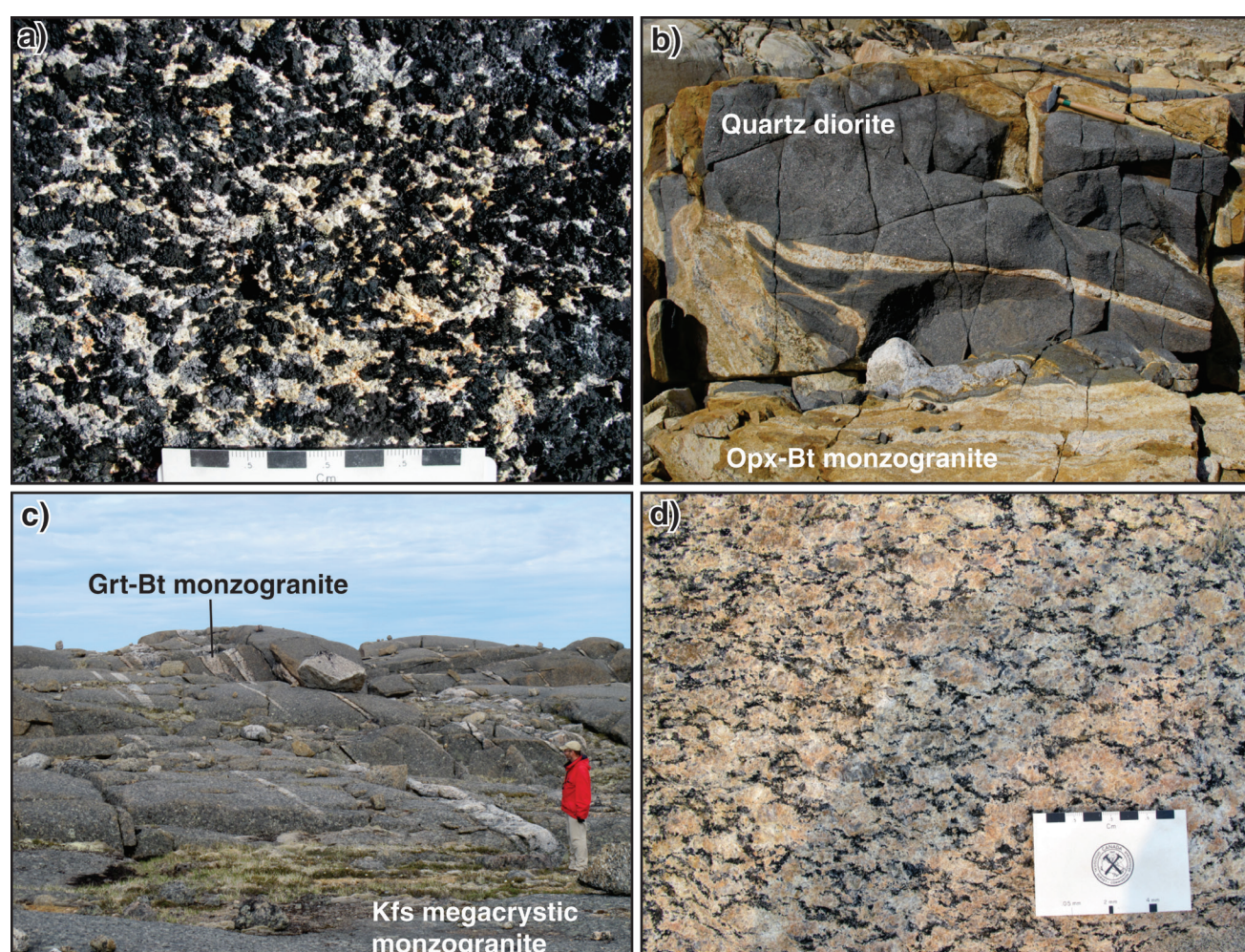


Figure 12. Plutonic suites of the Cumberland batholith, southern Baffin Island (*modified from* Weller et al., 2015). **a)** Clinopyroxene-biotite-magnetite±hornblende gabbro, Cumberland Sound region. Photograph by M.R. St-Onge. NRCAN photo 2018-378. **b)** Enclave of quartz diorite in orthopyroxene-biotite monzogranite, Meta Incognita Peninsula (hammer for scale). Photograph by M.R. St-Onge. NRCAN photo 2018-379. **c)** dykes of garnet-biotite±magnetite monzogranite emplaced in K-feldspar megacrystic monzogranite of the Qikiqtarjuaq plutonic suite, Cumberland Sound region (geologist for scale). Photograph by B.J. Dyck. NRCAN photo 2018-380. **d)** Coarse-grained, massive biotite±orthopyroxene±magnetite±garnet monzogranite, with distinctive K-feldspar megacrysts, Meta Incognita Peninsula. Photograph by M.R. St-Onge. NRCAN photo 2018-381.

diorite-tonalite gneiss (Fig. 13a), and tholeiitic to calc-alkaline basaltic andesite (Fig. 13b) to rhyolite, dated between 1863 ± 2 Ma and 1845 ± 2 Ma (St-Onge et al., 1992; Machado et al., 1993; R.R. Parrish, unpub. data, 1989). The older magmatic suite is interpreted as an island-arc assemblage built on Paleoproterozoic oceanic crust and a sliver of Archean continental crust (Thériault et al., 2001). The younger suite comprises crosscutting, foliated to massive, monzodiorite to granite plutons dated between $1842 +5/-3$ Ma and $1820 +4/-3$ Ma (Fig. 3; Machado et al., 1993; Scott, 1997; Scott and Wodicka, 1998; Rayner, 2017; R.R. Parrish, unpub. data, 1989) and interpreted as having been emplaced in a continental-margin arc setting (Dunphy and Ludden, 1998; Thériault et al., 2001).

Crosscutting field relationships (St-Onge et al., 1998) indicate that the oldest unit of the younger magmatic suite of Narsajuaq Arc on southern Baffin Island is a layered, fine- to medium-grained, grey to buff orthopyroxene-biotite±hornblende±garnet tonalitic orthogneiss with subordinate grey orthopyroxene-biotite±hornblende granodiorite layers, and pink monzogranite sheets and veins (Fig. 13c). Lenses, layers and locally discordant dykes of dark hornblende-biotite-clinopyroxene±orthopyroxene quartz diorite, up to several metres thick, commonly form an integral component of the orthogneiss. The tonalitic, granodioritic, and quartz dioritic components are cut by concordant to discordant veins of medium-grained orthopyroxene-biotite±hornblende monzogranite and by rare coarse-grained hornblende-biotite±orthopyroxene syenogranite. Grey anorthosite layers up to several tens of metres thick and over 1 km in strike length also occur.

Large areas of Narsajuaq Arc (Fig. 10) on southern Baffin Island are underlain by medium-grained, gneissic to massive orthopyroxene-biotite±hornblende monzogranite (Fig. 13d) that intrudes the layered tonalite-monzogranite gneiss described above. Coarse-grained and locally megacrystic layers can reach 100 m in thickness. A hornblende-clinopyroxene-orthopyroxene-biotite quartz diorite phase is common.

ARCHEAN SUPERIOR CRATON AND ITS PALEOPROTEROZOIC NORTHERN MARGIN (LEVEL 1)

In northern Quebec (Fig. 3), the Archean Superior Craton predominantly comprises felsic orthogneiss and biotite-hornblende±orthopyroxene plutonic units (Fig. 14a) ranging in age

between $3220 +32/-23$ Ma and 2554 ± 5 Ma (Machado et al., 1989; Mortensen and Percival, 1989; Parrish, 1989; St-Onge et al., 1992; Scott and St-Onge, 1995; Wodicka and Scott, 1997; R.R. Parrish, pers. comm., 1994). Unconformably overlying the felsic basement is a suite of parautochthonous basal clastic sedimentary strata (Fig. 14b), carbonatitic volcanoclastic rock, continental tholeiitic flood basalt (Fig. 14c) and rhyolite (Povungnituk Group, Fig. 3) associated with initial Paleoproterozoic rifting of the northern Superior Craton and yielding ages between $2038 +4/-2$ Ma and $1958.6 +3.1/-2.7$ Ma (Parrish, 1989; Machado et al., 1993; Kastek et al., 2018). In the Ungava Peninsula of northern Quebec (Fig. 3), a younger succession of predominantly Mg-rich komatiitic to tholeiitic basalt (Chukotat Group; Fig. 14d) accumulated during renewed rifting along the northern continental margin (St-Onge et al., 2000a). The Chukotat Group disconformably overlies the initial rift sedimentary and volcanic rocks and is dated between $1887 +37/-11$ Ma and 1870 ± 4 Ma (Fig. 3; Wodicka et al., 2002a; R.R. Parrish, unpub. data, 1989). The ages of the younger volcanic succession indicate that approximately 150 Ma elapsed between the onset of initial continental rifting and the subsequent renewed rifting event (St-Onge et al. 2000a).

On Big Island, just south of Baffin Island (Fig. 10), orthogneiss dated at $2875 +9/-7$ Ma (Wodicka and Scott, 1997) and associated clastic rocks containing detrital zircons ranging in age between 3.15 and 2.54 Ga, with distinct modes at 2.79, 2.73, and 2.69 Ga (Scott et al., 2002a), are correlated with the Archean Superior Craton and the Povungnituk Group clastic rift sequence, respectively (St-Onge et al., 1996; Scott et al., 2002a).

PALEOPROTEROZOIC OROGENIC BELTS AND PLATE GEOMETRIES

Within Baffin Island, the constituent Archean cratons, attendant Paleoproterozoic cover sequences, microcontinental blocks, and continental magmatic arcs, as described above, were assembled during a period of global amalgamation that occurred between ca. 1.9 and 1.8 Ga (St-Onge et al., 2009). Documentation of the geometry, age, structural evolution, magmatic context, and metamorphic framework of the intervening deformation zones and orogenic belts allows the relative upper plate versus lower plate geometry to be established in each case (Fig. 3). This in turn allows the tectonic evolution of Baffin Island during the Paleoproterozoic to be modelled as a series

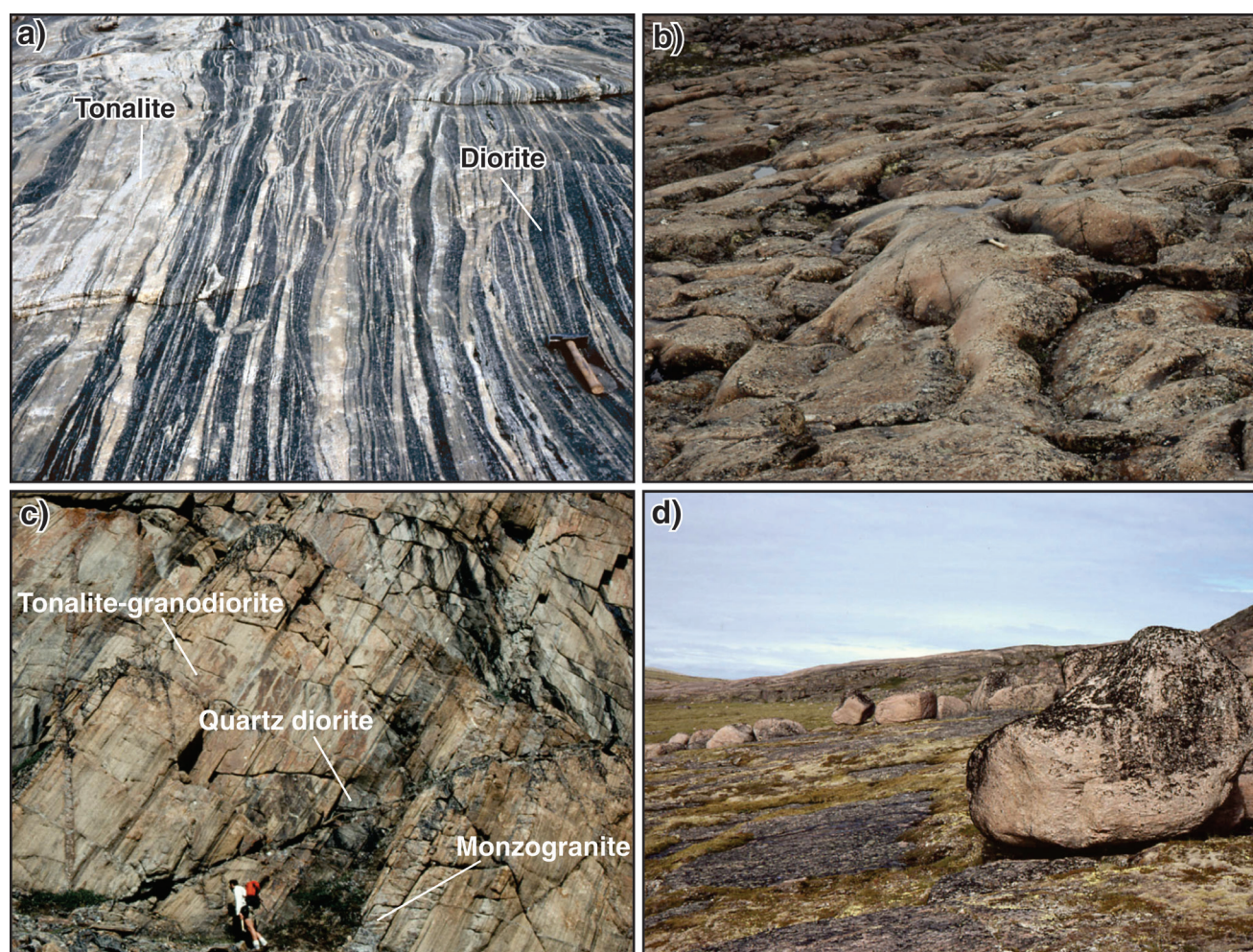


Figure 13. Magmatic components of Narsajuaq Arc terrane, northern Quebec and southern Baffin Island. **a)** Calc-alkaline layered diorite-tonalite gneiss, older suite of Narsajuaq Arc terrane, Ungava Peninsula, Quebec (hammer for scale). Photograph by M.R. St-Onge. NRCan photo 2018-382. **b)** Calc-alkaline basaltic andesite, older suite of Narsajuaq Arc terrane, Ungava Peninsula, Quebec (hammer for scale). Photograph by M.R. St-Onge. NRCan photo 2018-383. **c)** Tonalite-granodiorite gneiss with quartz diorite layers and crosscutting monzogranite dykes, younger suite of Narsajuaq Arc terrane, southern Baffin Island (geologist for scale). Photograph by M.R. St-Onge. NRCan photo 2018-384. **d)** Massive monzogranite, younger suite of Narsajuaq Arc terrane, southern Baffin Island (height of boulder on right is 2 m). Photograph by M.R. St-Onge. NRCan photo 2018-385.

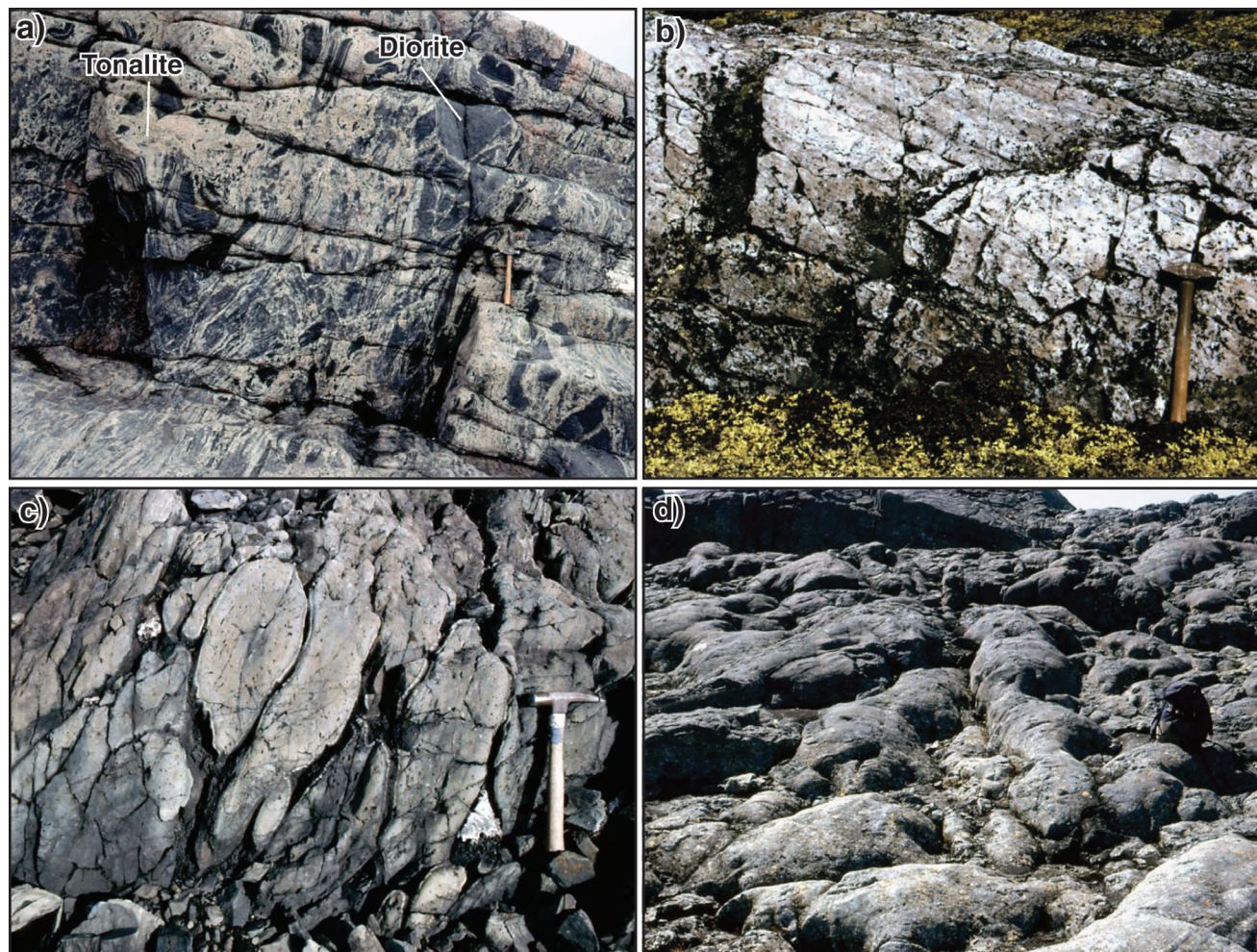


Figure 14. Superior Craton basement and cover units, northern Quebec and southern Baffin Island. **a)** Archean biotite-hornblende+orthopyroxene tonalite with abundant diorite enclaves, Superior Craton, northern Quebec (hammer for scale). Photograph by M.R. St-Onge. NRCan photo 2018-386. **b)** Shallowly-dipping, Paleoproterozoic basal quartzite, Povungnituk Group, southern Baffin Island (hammer for scale). Photograph by M.R. St-Onge. NRCan photo 2018-387. **c)** Paleoproterozoic pillowed basalt in a continental tholeiite flow, Povungnituk Group, northern Quebec (hammer for scale). Photograph by M.R. St-Onge. NRCan photo 2018-388. **d)** Lava pillows and tubes of Mg-rich komatiitic basalt, Chukotat Group, northern Quebec (backpack for scale). Photograph by M.R. St-Onge. NRCan photo 2018-389.

of cumulative accretion–collision events contributing to the southerly growth (present co-ordinates) of the Nuna Supercontinent culminating at ca. 1.8 Ga.

Qimivvik crustal shortening

Deformation along the northern margin of the Rae Craton in the Qimivvik area of northern Baffin Island (Fig. 3) is characterized by southwest-vergent crustal shortening that juxtaposed Archean crystalline basement over cover strata, potentially due to thrust faulting (Skipton et al., 2017). The peak metamorphic assemblage in pelite contains garnet, sillimanite, cordierite+K-feldspar, and foliation is defined by aligned biotite and compositional banding. Pelite hosts foliation-parallel leucogranite layers that are consistent with mica dehydration melting and peak metamorphism at upper-amphibolite- to granulite-facies conditions. Southwest-vergent folding of leucogranite layers suggests that peak metamorphism conditions were associated with pre- to synductile deformation. However, cliff exposures also reveal subvertical leucogranite dykes that stem from the leucogranite melt network within the pelitic metasedimentary rocks, and which crosscut the contact with the overlying basement orthogneiss. Preliminary in situ U-Pb ages of monazite in pelitic metasedimentary units indicate a protracted tectonometamorphic history: garnet cores contain ca. 2.5 Ga monazite inclusions, whereas matrix monazite is dominantly ca. 1.9 Ga, including foliation-parallel grains, locally with partial ca. 1.8 Ga rims (D. Skipton, pers. comm., 2018).

Foxe fold belt

Deformation along the southern margin of the Rae Craton within the Foxe fold belt of central Baffin Island (Fig. 3) is characterized by early north-verging, thin-skinned imbrication and tight intrafolial isoclinal folding of the Piling Group, followed by northeast-trending upright folding of both Paleoproterozoic cover and Archean basement, and subsequent open northwest-trending, thick-skinned crossfolding (Scott et al., 2003). Metamorphic grade increases from greenschist facies at higher structural levels to granulite facies at lower structural levels and in proximity to the plutonic units of the Qikiqtarjuaq plutonic suite (Gagné et al., 2009; Wodicka et al., 2014).

The proposed Baffin suture (St-Onge et al., 2006) separating the Archean Rae Craton and its flanking, southern Palaeoproterozoic continental-margin sedimentary and volcanic sequences (Piling and Hoare Bay groups) from accreted tectonic elements to the south (Meta Incognita microcontinent and associated Lake Harbour Group) trends east from the Foxe Basin to the head of Cumberland Sound (Fig. 3). Closing across the proposed suture is thought to postdate 1915 ± 8 Ma (the youngest, most precise maximum age constraint for the Piling Group; Wodicka et al., 2014) and predate emplacement of the 1896 ± 8 Ma to 1886 ± 5 Ma Qikiqtarjuaq plutonic suite (Rayner, 2017). Engulfment of the cryptic suture zone by younger, voluminous granitic plutons precludes any direct constraints on the polarity of the Baffin suture (St-Onge et al., 2009; Weller et al., 2015), although Corrigan et al. (2009) have presented arguments for a north-directed sense of vergence.

Dorset fold belt

Convergence between the southern margin of the Meta Incognita microcontinent and crustal domains to the south led to development of the Dorset fold belt and formation of the north-dipping Soper River suture (Fig. 3). Closing of the suture is bracketed between 1845 ± 2 Ma, the age of the youngest unit associated with the intra-oceanic phase of the accreted Narsajuaq Arc (Fig. 3; Dunphy and Ludden, 1998) and $1842 +5/-3$ Ma (Scott, 1997), the age of the oldest plutonic unit of the continental-margin arc phase of the Narsajuaq Arc (St-Onge et al., 2007).

Deformation in the Dorset fold belt includes:

- structural repetition and truncation of distinct tectonostratigraphic units yielding an overall south-southwest-verging ramp-flat fault geometry (Scott et al., 1997)
- associated tight to isoclinal folding during south- to southwest-directed deformation (Sanborn-Barrie et al., 2008)
- development of a penetrative granulite-facies compositional fabric
- formation of ribbon mylonites and transposition of crosscutting intrusive units into parallelism in the vicinity of the Soper River suture
- later, open crossfolding and localized dextral transcurrent shearing oriented northwest–southeast.

Syntectonic granulite-facies regional metamorphism associated with emplacement of the Cumberland batholith and closure of the Soper River suture is bracketed between ca. 1849 and 1835 Ma (St-Onge et al., 2007).

The south- to southwest-verging thrusting and folding documented within the Dorset fold belt and the location of the Cumberland batholith continental-margin arc rocks in the northern hanging wall of the suture suggest that the Meta Incognita microcontinent occupied an upper plate position with respect to the Narsajuaq Arc to the south (Fig. 3) during convergence across the Soper River suture.

Cape Smith belt

Within the Cape Smith belt of northern Quebec and southernmost Baffin Island (Fig. 3), parautochthonous sedimentary and volcanic strata along the northern margin of the Superior Craton are imbricated by thrust faults above a regional basal décollement (Lucas, 1989; St-Onge et al., 2001). Fault displacement was in a southerly direction, with thin-skinned imbrication and associated folding occurring in a piggyback sequence toward the southern foreland. Thrust deformation was initiated after 1870 ± 4 Ma, the age of the youngest unit within the parautochthonous Superior Craton cover sequence.

A distinct suite of late or 'out-of-sequence' thrust faults that post-date the thin-skinned structures re-imbricate the cover units of the Superior Craton (Lucas, 1989). These younger south-verging structures are thick-skinned (involving both crystalline basement and Palaeoproterozoic cover units) and are collisional in origin as they can be linked to the terrane boundary faults of the Narsajuaq Arc terrane and Purtuniqu ophiolite in northern Quebec (Fig. 3; St-Onge et al., 2001). The late faults truncate the metamorphic isograds within the Cape Smith belt and thus must postdate $1820 +4/-3$ to 1815 ± 4 Ma (Bégin, 1992). They predate the age of emplacement of postkinematic syenite plugs and syenogranite dykes at 1795 ± 2 to 1758.2 ± 1.2 Ma (St-Onge et al., 2006).

Regional, Barrovian-style, kyanite–sillimanite-grade metamorphism is associated with early thin-skinned thrusting of cover units along the northern margin of the Superior Craton (Bégin, 1992). Metamorphism is bracketed between $1820 +4/-3$ and 1815 ± 4 Ma and is interpreted as a consequence of the relaxation of isotherms in the tectonically thickened thrust belt (St-Onge and Lucas, 1991).

A south-verging tectonic boundary or crustal suture (Bergeron suture; Fig. 3) separates the northern Superior margin strata from allochthonous crustal elements to the north (St-Onge et al., 1999, 2001). Associated with, and sitting in the hanging wall of, the Bergeron suture are the crustal components of an obducted 1998 ± 2 Ma ophiolite (Watts group; Parrish, 1989; Scott et al., 1992, 1999), as well as the plutonic, volcanic, and sedimentary components of the Narsajuaq Arc (described above). Preservation of the ophiolite and the higher structural levels it represents within the Cape Smith belt is entirely a function of the late- to postcollisional, crustal-scale, orogen-parallel folding and orogen-perpendicular crossfolding that characterize the southern margin of the Trans-Hudson Orogen in northern Quebec (Lucas and Byrne, 1992). Closure of the Bergeron suture, and collision of the accreted terrane with the Superior Craton, is bracketed between $1820 +4/-3$ Ma (youngest component of the Narsajuaq Arc) and 1795 ± 2 Ma (the age of an undeformed crosscutting syenogranite pegmatite dyke) (St-Onge et al., 2006).

The architecture of the foreland thin- to thick-skinned thrust-fold belt, the geometry of the Bergeron suture, the regional Barrovian metamorphism developed within the Cape Smith belt, as well as the recent documentation of high-pressure eclogite in the crystalline basement footwall (Weller and St-Onge, 2017) corroborate the lower plate position of the Superior Craton during its collision with the accreted terranes to the north (Fig. 3).

CONCLUSIONS

Documentation of the Archean and Paleoproterozoic bedrock units and structures on Baffin Island as synthesized in this paper allows identification of an internally consistent, north-to-south sequence of accretionary and collisional tectonic events during the Paleoproterozoic (Fig. 3). These tectonic events (itemized below) first resulted in the growth of a composite upper-plate domain around the crustal nucleus represented by the Rae Craton. Initial assembly of the upper-plate (Churchill) domain was then followed by collision with the southern, lower-plate Superior Craton, which resulted in the terminal collisional phase of the Trans-Hudson Orogeny and significantly added to the landmass of the emerging Laurentian Craton.

Based on available tectonostratigraphic, structural, and geochronological data for Baffin Island, the tectonic events that characterize the accretionary–collisional growth of northeast Laurentia during the middle Paleoproterozoic are as follows (Fig. 3):

- deformation along the northern margin of the Rae Craton at ca. 1.90 Ga (Qimivvik area)
- accumulation of a stratigraphically south-facing, rift- to continental-margin sequence in a fragmented proto-ocean basin setting developed along the southern margin of the Rae Craton between ca. 2.16 and 1.91 Ga
- north–south convergence and accretion of the Meta Incognita microcontinent to the southern margin of the Rae Craton across the Baffin suture between ca. 1.91 and 1.90 Ga (Foxe fold belt)
- accretion of the Narsajuaq Arc terrane to the southern margin of the growing Churchill Domain at ca. 1.845 Ga (Dorset fold belt)
- collision of the lower plate Superior Craton with the composite upper-plate Churchill Domain between ca. 1.82 and 1.795 Ga (Cape Smith belt)

ACKNOWLEDGMENTS

The first author would like to thank the following Geological Survey of Canada and Canada Centre for Remote Sensing colleagues: D. Boerner, P. Brouillette, P. Budkewitsch, D. Corrigan, E. de Kemp, L. Dredge, A. Ford, K. Ford, S. Hanmer, J. Harris, P. Harrison, B. Harvey, D. Hodgson, O. Ijewliw, A. Jones, R. Knight, T. Little, S. Lucas, T. Lynds, A. Morin, T. Peterson, N. Rayner, M. Sanborn-Barrie, B. Saumur, D. Skipton, D. Snyder, J. Spratt, R. Thériault, V. Tschirhart, N. Wodicka; Canada-Nunavut Geoscience Office colleagues: C. Gilbert, D. James, D. Mate, H. Steenkamp, D. Scott; university colleagues: K. Ansdell (University of Saskatchewan), D. Carmichael (Queen's University), D. Francis (McGill University), R. Jamieson (Dalhousie University), H. Helmstaedt (Queen's University), S. Johnston (University of Alberta), D. Pattison (University of Calgary), D. Schneider (University of Ottawa), O. Weller (University of Cambridge), J. White (University of New Brunswick), M. Young (Dalhousie University); and university and college student field assistants: M. Allen, M. Appaqaq, F. Berniolles, E. Bros, G. Brown, J. Butler, T. Chadwick, J. Chakungal, D. Copeland, K. Dubach, B. Dyck, S. Evans, R. From, S. Gagné, J. Gladstone, C. Herd, R. Hinanik, C. Hogue, B. Hrabí, C. Huebert, H. Iyerak, S. Johns, R. Keiser, D. Liikane, C. Mackay, A. Markey, T. Milton, S. McMullen, S. Modelland, S. Noble-Nowdluk, L. Piper, J. Rae, J. Robillard, T. Rowe, J. Ruechel, I. Russell, B. Sharp, A. Simmons, A. Smye, J. Stacey, E. Turner, and C. Yakymchuk, who have all contributed greatly over the past 25 years to the understanding of the Archean and Paleoproterozoic stratigraphy, structure, and tectonic evolution of Baffin Island.

The authors gratefully acknowledge the careful reviews of this contribution by David Corrigan and Christopher Harrison.

REFERENCES

- Bégin, N.J., 1992. Contrasting mineral isograd sequences in metabasites of the Cape Smith Belt, northern Quebec, Canada: three new bathograds for mafic rocks; *Journal of Metamorphic Geology*, v. 10, p. 685–704. <https://doi.org/10.1111/j.1525-1314.1992.tb00115.x>
- Bell, R., 1885. Observations on the geology, zoology and botany of Hudson's Strait and Bay, made in 1885; Geological Survey of Canada, Annual Report v. 1, pt. DD, 32 p. <https://doi.org/10.4095/297069>
- Bell, R., 1901. Report of an exploration on the northern side of Hudson Strait; Geological Survey of Canada, Annual Report v. 11 (1898), pt. M, 46 p. <https://doi.org/10.4095/297002>
- Bethune, K.M. and Scammell, R.J., 1997. Precambrian geology, Koch Island area (part of NTS 37C), District of Franklin, Northwest Territories; Geological Survey of Canada, Open File 3391, scale 1:50 000. <https://doi.org/10.4095/208509>
- Bethune, K.M. and Scammell, R.J., 2003a. Geology, geochronology, and geochemistry of Archean rocks in the Ege Bay area, north-central Baffin Island, Canada: constraints on the depositional and tectonic history of the Mary River Group of northeastern Rae Province; *Canadian Journal of Earth Sciences*, v. 40, no. 8, p. 1137–1167. <https://doi.org/10.1139/e03-028>

- Bethune, K.M. and Scammell, R.J., 2003b. Distinguishing between Archean and Paleoproterozoic tectonism, and evolution of the Isortoq fault zone, Ege Bay area, north-central Baffin Island, Canada; *Canadian Journal of Earth Sciences*, v. 40, no. 8, p. 1111–1135. <https://doi.org/10.1139/e03-040>
- Blackadar, R.G., 1959. Cape Dorset, Baffin Island, District of Franklin, Northwest Territories; Geological Survey of Canada, Preliminary Map 11–1959, scale 1:126 720. <https://doi.org/10.4095/108525>
- Blackadar, R.G., 1960. Hobart Island, Baffin Island, District of Franklin, Northwest Territories; Geological Survey of Canada, Preliminary Map 55–1959, scale 1:253 440. <https://doi.org/10.4095/108650>
- Blackadar, R.G., 1961. Mingo Lake, Baffin Island, District of Franklin, Northwest Territories; Geological Survey of Canada, Preliminary Map 43–1960, scale 1:253 440. <https://doi.org/10.4095/108736>
- Blackadar, R.G., 1962. Geology, Andrew Gordon Bay–Cory Bay, Baffin Island, District of Franklin; Geological Survey of Canada, Preliminary Map 5–1962, scale 1:253 440. <https://doi.org/10.4095/108797>
- Blackadar, R.G., 1967a. Geology, Mingo Lake–Macdonald Island, Baffin Island, District of Franklin; Geological Survey of Canada, Map 1185A, scale 1:253 440. <https://doi.org/10.4095/107493>
- Blackadar, R.G., 1967b. Geology of Mingo Lake–Macdonald Island map area, Baffin Island, District of Franklin; Geological Survey of Canada, Memoir 345, 54 p. <https://doi.org/10.4095/100532>
- Blackadar, R.G., 1967c. Geology, Foxe Peninsula, District of Franklin; Geological Survey of Canada, Preliminary Map 16–1966, scale 1:506 880. <https://doi.org/10.4095/108489>
- Blackadar, R.G., 1967d. Geology, Cumberland Sound, District of Franklin; Geological Survey of Canada, Preliminary Map 17–1966, scale 1:506 880. <https://doi.org/10.4095/108490>
- Blackadar, R.G., 1967e. Geology, Frobisher Bay, District of Franklin; Geological Survey of Canada, Preliminary Map 18–1966, scale 1:506 880. <https://doi.org/10.4095/108491>
- Blackadar, R.G., Davison, W.L., and Trettin, H.P., 1968a. Geology, Milne Inlet, District of Franklin; Geological Survey of Canada, Map 1235A, scale 1:253 440. <https://doi.org/10.4095/107494>
- Blackadar, R.G., Davison, W.L., and Trettin, H.P., 1968b. Geology, Navy Board Inlet, District of Franklin; Geological Survey of Canada, Map 1236A, scale 1:253 440. <https://doi.org/10.4095/107498>
- Blackadar, R.G., Davison, W.L., and Trettin, H.P., 1968c. Geology, Arctic Bay–Cape Clarence, District of Franklin; Geological Survey of Canada, Map 1237A, scale 1:253 440. <https://doi.org/10.4095/107330>
- Blackadar, R.G., Davison, W.L., and Trettin, H.P., 1968d. Geology, Moffet Inlet–Fitzgerald Bay, District of Franklin; Geological Survey of Canada, Map 1238A, scale 1:253 440. <https://doi.org/10.4095/107497>
- Blackadar, R.G., Davison, W.L., and Trettin, H.P., 1968e. Geology, Phillips Creek, District of Franklin; Geological Survey of Canada, Map 1239A, scale 1:253 440. <https://doi.org/10.4095/107510>
- Blackadar, R.G., Davison, W.L., and Trettin, H.P., 1968f. Geology, Agu Bay–Easter Cape, District of Franklin; Geological Survey of Canada, Map 1240A, scale 1:253 440. <https://doi.org/10.4095/107336>
- Blackadar, R.G., Davison, W.L., and Trettin, H.P., 1968g. Geology, Berlinguet Inlet–Bourassa Bay, District of Franklin; Geological Survey of Canada, Map 1241A, scale 1:253 440. <https://doi.org/10.4095/107412>
- Blackadar, R.G., Davison, W.L., and Trettin, H.P., 1968h. Geology, Erichsen Lake area, District of Franklin; Geological Survey of Canada, Map 1242A, scale 1:253 440. <https://doi.org/10.4095/108947>
- Bradley, D.C., 2008. Passive margins through earth history; *Earth-Science Reviews*, v. 91, p. 1–26. <https://doi.org/10.1016/j.earscirev.2008.08.001>
- Bros, E.R. and Johnston, S.T., 2017. Field observations of the Mary River Group south of Tay Sound, northern Baffin Island, Nunavut: stratigraphy and structure of supracrustal sequences and surrounding plutonic suites; *in* Summary of activities 2017, Canada-Nunavut Geoscience Office, p. 69–79.
- Cawood, P.A. and Nemchin, A.A., 2001. Paleogeographic development of the east Laurentian margin: constraints from U-Pb dating of detrital zircons in the Newfoundland Appalachians; *Geological Society of America Bulletin*, v. 113, p. 1234–1246. [https://doi.org/10.1130/00167606\(2001\)113](https://doi.org/10.1130/00167606(2001)113)
- Chandler, F.W., 1988. Geology of the late Precambrian Fury and Hecla Group, northwest Baffin Island, District of Franklin; Geological Survey of Canada, Bulletin 370, 30 p. <https://doi.org/10.4095/126938>
- Clarke, D.B. and Upton, B.G.J., 1971. Tertiary basalts of Baffin Island: field relations and tectonic setting; *Canadian Journal of Earth Sciences*, v. 8, p. 248–258. <https://doi.org/10.1139/e71-025>
- Connelly, J.N., 2001. Constraining the timing of metamorphism: U-Pb and Sm-Nd ages from a transect across the northern Torngat Orogen, Labrador, Canada; *The Journal of Geology*, v. 109, p. 57–77. <https://doi.org/10.1086/317965>
- Corrigan, D., 2012. Paleoproterozoic crustal evolution and tectonic processes: insights from the LITHOPROBE program in the Trans-Hudson Orogen, Canada; *in* Tectonic Styles in Canada: the LITHOPROBE perspective, (ed.) J.A. Percival, F.A. Cook, and R.M. Clowes; Geological Association of Canada, Special Paper 49, p. 237–284.
- Corrigan, D., Scott, D.J., and St-Onge, M.R., 2001. Geology of the northern margin of the Trans-Hudson Orogen (Foxe Fold Belt), central Baffin Island, Nunavut; Geological Survey of Canada, Current Research 2001-C23, 27 p. <https://doi.org/10.4095/212249>
- Corrigan, D., Pehrsson, S., Wodicka, N., and de Kemp, E., 2009. The Palaeoproterozoic Trans-Hudson Orogen: a prototype of modern accretionary processes; *Ancient orogens and modern analogues*, (ed.) J.B. Murphy, J.D. Keppie, and A.J. Hynes; Geological Society, Special Publication 327, p. 457–479. <https://doi.org/10.1144/SP327.19>
- Corrigan, D., Nadeau, L., Brouillette, P., Wodicka, N., Houllé, M.G., Tremblay, T., Machado, G., and Keating, P., 2013. Overview of the GEM Multiple Metals-Melville Peninsula project, central Melville Peninsula, Nunavut; Geological Survey of Canada, Current Research 2013–19, 21 p. <https://doi.org/10.4095/292862>
- Davidson, A., Jackson, G.D., and Morgan, W.C., 1979. Geology, Icebound Lake, District of Franklin; Geological Survey of Canada, Map 1451A, scale 1:250 000. <https://doi.org/10.4095/109161>
- Davison, W.L., 1959a. Lake Harbour, Baffin Island, District of Franklin, Northwest Territories; Geological Survey of Canada, Preliminary Map 29–1958, scale 1: 63 360. <https://doi.org/10.4095/108520>
- Davison, W.L., 1959b. Foxe Peninsula, eastern part, Baffin Island, District of Franklin, Northwest Territories; Geological Survey of Canada, Preliminary Map 4–1959, scale 1:253 440. <https://doi.org/10.4095/108511>
- de Kemp, E.A., Sherwin, T., Ryder, I., Davies, A., and Snyder, D., 2002a. Detailed stratigraphic, structural, and three-dimensional mapping of the basal surface of the Paleoproterozoic Bravo Lake Formation, Nadluardjuk Lake area, Central Baffin Island, Nunavut, Canada; Geological Survey of Canada, Current Research 2002-C18, 10 p. <https://doi.org/10.4095/213195>
- de Kemp, E.A., Sherwin, T., Ryder, I., Davies, A., and Snyder, D., 2002b. Paleoproterozoic geology, Nadluardjuk Lake area, central Baffin Island, Nunavut; Geological Survey of Canada, Open File 4168, scale 1:15 000. <https://doi.org/10.4095/213475>
- Dunphy, J.M. and Ludden, J.N., 1998. Petrological and geochemical characteristics of a Paleoproterozoic magmatic arc (Narsajuaq Terrane, Ungava Orogen, Canada) and comparisons to Superior Province granitoids; *Precambrian Research*, v. 91, p. 109–142. [https://doi.org/10.1016/S0301-9268\(98\)00041-2](https://doi.org/10.1016/S0301-9268(98)00041-2)
- Escher, A. and Pulvertaft, T.C.R., 1976. Rinkian mobile belt of West Greenland; *in* Geology of Greenland, (ed.) A. Escher and W.S. Watt; Grønlands geologiske Undersøgelse, Copenhagen, p. 104–119.
- Forester, W. and Gray, N., 1966. Geological studies on Baffin Island; *in* Field report, north-central Baffin Island, (ed.) O.H. Løken; Department of Energy, Mines and Resources, Geographical Branch, p. 93–96.

- From, R.E., Camacho, A.L., and St-Onge, M.R., 2013. Preliminary observations on the nature and origin of the eastern orthogneiss complex of southern Hall Peninsula, Baffin Island, Nunavut; *in* Summary of activities 2012, Canada-Nunavut Geoscience Office, p. 43–54.
- From, R.E., St-Onge, M.R., and Camacho, A.L., 2014. Preliminary characterization of the Archean orthogneiss complex of Hall Peninsula, Baffin Island, Nunavut; *in* Summary of activities 2013, Canada-Nunavut Geoscience Office, p. 53–62.
- From, R.E., Rayner, N.M., and Camacho, A., 2015. Archean magmatism and metamorphism of eastern Hall Peninsula, southern Baffin Island, Nunavut; *in* Summary of activities 2015, Canada-Nunavut Geoscience Office, p. 73–88.
- Gagné, S., Jamieson, R.A., MacKay, R., Wodicka, N., and Corrigan, D., 2009. Texture, composition, and age variations in monazite from the lower amphibolite to the granulite facies, Longstaff Bluff Formation, Baffin Island, Canada: *Canadian Mineralogist*, v. 47, p. 847–869. <https://doi.org/10.3749/canmin.47.4.847>
- Garde, A.A. and Steenfelt, A., 1999. Precambrian geology of Nuussuaq and the area north-east of Disko Bugt, West Greenland; *in* Precambrian geology of the Disko Bugt region, West Greenland, (ed.) F. Kalsbeek; Geology of Greenland Survey, Bulletin 181, p. 6–40.
- Gladstone, J. and Francis, D., 2003. The origin of basaltic intrusions within the Longstaff Bluff formation, central Baffin Island, Nunavut; Joint Central Baffin/Committee Bay Workshop; Geological Association of Canada (Geological Survey of Canada), Program with Abstracts, v. 1, p. 22.
- Hall, C.F., 1865. Arctic researches, and life among the Esquimaux: being the narrative of an expedition in search of Sir John Franklin, in the years 1860, 1861, and 1862; Harper & Brothers, New York, New York, 595 p.
- Hamilton, B.M., 2014. A detailed description of the Hoare Bay group and Paleoproterozoic plutonic rocks near Mischief Glacier and Clephane Bay, Cumberland Peninsula, Baffin Island, Nunavut; Geological Survey of Canada, Current Research 2014–3, 23 p. <https://doi.org/10.4095/293891>
- Harrison, J.C., St-Onge, M.R., Paul, D., and Brodaric, B., in press. Geology of Canada (north of 60); Geological Survey of Canada, Canadian Geoscience Map 293, scale 1:3 000 000.
- Heaman, L.M., LeCheminant, A.N., and Rainbird, R.H., 1992. Nature and timing of Franklin igneous events, Canada: implications for a Late Proterozoic mantle plume and the break-up of Laurentia; *Earth and Planetary Science Letters*, v. 109, p. 117–131. [https://doi.org/10.1016/0012-821X\(92\)90078-A](https://doi.org/10.1016/0012-821X(92)90078-A)
- Henderson, J.R., 1985. Geology, McBeth Fiord–Cape Henry Kater, District of Franklin; Geological Survey of Canada, Map 1605A, scale 1:250 000. <https://doi.org/10.4095/120467>
- Henderson, J.R. and Parrish, R.R., 1992. Geochronology and structural geology of the Early Proterozoic Foxe–Rinkian Orogen, Baffin Island, NWT; Geological Survey of Canada, Current Activities Forum 1992, Program with Abstracts, p. 12.
- Henderson, G. and Pulvertaft, T.C.R., 1987. The lithostratigraphy and structure of a Lower Proterozoic dome and nappe complex, Geological map of Greenland, scale 1:100 000, Marmorilik 71–V.2 Syd, Nûgâtsiaq 71 V.2 Nord, and Pangnertôq 72 V.2 Syd; Grønlands Geologiske Undersøgelse, descriptive text, 72 p.
- Henderson, J.R. and Tippett, C.R., 1980. Foxe Fold Belt in eastern Baffin Island, District of Franklin; *in* Current research, Part A; Geological Survey of Canada, Paper 80–1A, p. 147–152. <https://doi.org/10.4095/106195>
- Henderson, J.R., Henderson, M.N., Groot, J., Heijke, P., Falardeau, F., Perreault, S., and Derome, I., 1994. Geology, Dewar Lakes area, central Baffin Island, District of Franklin, Northwest Territories (parts of 27 B and 37 A); Geological Survey of Canada, Open File 2924, scale 1:100 000. <https://doi.org/10.4095/194767>
- Henderson, J.R., Shaw, D., Mazurski, M., Henderson, M., Green, R., and Brisbin, D., 1979. Geology of part of Foxe Fold Belt, central Baffin Island, District of Franklin; *in* Current research, Part A; Geological Survey of Canada, Paper 79–1A, p. 95–99. <https://doi.org/10.4095/104833>
- Hoffman, P.F., 1988. United Plates of America, the birth of a craton: Early Proterozoic assembly and growth of Laurentia; *Annual Review of Earth and Planetary Sciences*, v. 16, p. 543–603. <https://doi.org/10.1146/annurev.ea.16.050188.002551>
- Hogarth, D.D., Boreham, P.W., and Mitchell, J.G., 1994. Martin Frobisher’s northwest venture, 1576–1581: mines, minerals & metallurgy; Canadian Museum of Civilization, Mercury Series, Directorate paper no. 7, 181 p.
- Hollis, J.A., Frei, D., Van Gool, J.A.M., Garde, A.A., and Persson, M., 2006a. Using zircon geochronology to resolve the Archean geology of southern West Greenland; Geological Survey of Denmark and Greenland, Bulletin no. 10, p. 49–52.
- Hollis, J.A., Keiding, M., Stensgaard, B.M., Van Gool, J.A.M., and Garde, A.A., 2006b. Evolution of Neoproterozoic supracrustal belts at the northern margin of the North Atlantic Craton, West Greenland; *in* Precambrian crustal evolution and Cretaceous–Palaeogene faulting in West Greenland, (ed.) A.A. Garde and F. Kalsbeek; Geological Survey of Denmark and Greenland, Bulletin no. 11, p. 9–31.
- Jackson, G.D., 1971. Operation Penny Highlands, south-central Baffin Island; *in* Report of activities, Part A; Geological Survey of Canada, Paper 71–1A, p. 138–140. <https://doi.org/10.4095/105595>
- Jackson, G.D., 1984. Geology, Clyde River, District of Franklin; Geological Survey of Canada, Map 1582A, scale 1:250 000. <https://doi.org/10.4095/119788>
- Jackson, G.D., 1998. Geology, Okoa Bay–Padloping Island area, District of Franklin, Northwest Territories; Geological Survey of Canada, Open File 3532, scale 1:250 000. <https://doi.org/10.4095/209911>
- Jackson, G.D., 2000. Geology of the Clyde–Cockburn Land map area, north-central Baffin Island, Nunavut; Geological Survey of Canada, Memoir 440, 316 p. <https://doi.org/10.4095/211268>
- Jackson, G.D., 2006. Field data, NTS 37G/5 and G/6, northern Baffin Island, Nunavut, Canada; Geological Survey of Canada, Open File 5317, scale 1:50 000. <https://doi.org/10.4095/222169>
- Jackson, G.D. and Berman, R.G., 2000. Precambrian metamorphic and tectonic evolution of northern Baffin Island, Nunavut, Canada; *Canadian Mineralogist*, v. 38, p. 399–421. <https://doi.org/10.2113/gscanmin.38.2.399>
- Jackson, G.D. and Davidson, A., 1975a. Geology, Pond Inlet and Nova Zembla Island, District of Franklin; Geological Survey of Canada, Map 1396A, scale 1:250 000. <https://doi.org/10.4095/109005>
- Jackson, G.D. and Davidson, A., 1975b. Geology, Bylot Island, District of Franklin; Geological Survey of Canada, Map 1397A, scale 1:250 000. <https://doi.org/10.4095/109007>
- Jackson, G.D. and Morgan, W.C., 1978. Geology, Conn Lake, District of Franklin; Geological Survey of Canada, Map 1458A, scale 1:250 000. <https://doi.org/10.4095/109162>
- Jackson, G.D. and Sangster, D.F., 1987. Geology and resource potential of a proposed national park, Bylot Island and north-western Baffin Island, Northwest Territories; Geological Survey of Canada, Paper 87–17, 31 p. <https://doi.org/10.4095/122369>
- Jackson, G.D. and Taylor, F.C., 1972. Correlation of major Aphebian rock units in the northeastern Canadian Shield; *Canadian Journal of Earth Sciences*, v. 9, p. 1650–1669. <https://doi.org/10.1139/e72-146>
- Jackson, G.D., Davidson, A., and Morgan, W.C., 1975. Geology of the Pond Inlet map-area, Baffin Island, District of Franklin (38A, 38B, part of 48A); Geological Survey of Canada, Paper 74–25, 33 p. <https://doi.org/10.4095/102498>
- Jackson, G.D., Morgan, W.C., and Davidson, A., 1979. Geology, Buchan Gulf–Scott Inlet, District of Franklin; Geological Survey of Canada, Map 1449A, scale 1:250 000. <https://doi.org/10.4095/109159>
- Jackson, G.D., Hunt, P.A., Loveridge, W.D., and Parrish, R.R., 1990. Reconnaissance geochronology of Baffin Island, N.W.T.; *in* Radiogenic age and isotopic studies: report 3; Geological Survey of Canada, Paper 89–2, p. 123–148. <https://doi.org/10.4095/129079>

- Johns, S.M. and Young, M.D., 2006. Bedrock geology and economic potential of the Archean Mary River group, northern Baffin Island, Nunavut; Geological Survey of Canada, Current Research 2006-C5, 13 p. <https://doi.org/10.4095/222954>
- Johns, S.M., Helmstaedt, H.H., and Kyser, T.K., 2006. Paleoproterozoic submarine intrabasinal rifting, Baffin Island, Nunavut, Canada: volcanic structure and geochemistry of the Bravo Lake Formation; Canadian Journal of Earth Sciences, v. 43, p. 593–616. <https://doi.org/10.1139/e06-009>
- Kastek, N., Ernst, R.E., Cousens, B.L., Kamo, S.L., Bleeker, W., Söderlund, U., Baragar, W.R.A., and Sylvester, P., 2018. U-Pb geochronology and geochemistry of the Povungnituk Group of the Cape Smith Belt: part of a craton-scale circa 2.0 Ga Minto–Povungnituk Large Igneous Province, northern Superior Craton; Lithos, v. 320–321, p. 315–331. <https://doi.org/10.1016/j.lithos.2018.09.026>
- Keim, R.D., 2012. Stratigraphy, petrology and geochemistry of the North Touak–Cape Dyer volcanic belt, and implications for the tectonic setting of the Paleoproterozoic Hoare Bay Group, eastern Baffin Island; M.Sc. thesis, University of Saskatchewan, Saskatoon, Saskatchewan, 124 p.
- Keim, R.D., Sanborn-Barrie, M., Ansdell, K., and Young, M.D., 2011. Totnes Road metavolcanic rocks: a fragmental Ti-enriched komatiitic volcanic suite on Cumberland Peninsula, Baffin Island, Nunavut; Geological Survey of Canada, Current Research 2011–13, 18 p. <https://doi.org/10.4095/289072>
- LaFlamme, C., McFarlane, C.R.M., and Corrigan, D., 2014. U–Pb, Lu–Hf and REE in zircon from 3.2 to 2.6 Ga Archean gneisses of the Repulse Bay block, Melville Peninsula, Nunavut; Precambrian Research, v. 252, p. 223–239. <https://doi.org/10.1016/j.precamres.2014.07.012>
- Lewry, J.F. and Collerson, K.D., 1990. The Trans-Hudson Orogen; extent, subdivision, and problems; in The Early Proterozoic Trans-Hudson Orogen of North America, (ed.) J.F. Lewry and M.R. Stauffer; Geological Association of Canada, Special Paper 37, p. 1–14.
- Liikane, D.A., 2017. Geochemical, isotopic, and mineralogical characterization of the Frobisher suite mafic–ultramafic sills, southern Baffin Island, Nunavut, with implications for mineral potential; M.Sc. thesis, Carleton University, Ottawa, Ontario, 437 p.
- Liikane, D.A., St-Onge, M.R., Kjarsgaard, B.A., Rayner, N.M., Ernst, R.E., and Kastek, N., 2015. Frobisher suite mafic, ultramafic and layered mafic–ultramafic sills, southern Baffin Island, Nunavut; in Summary of activities 2015, Canada-Nunavut Geoscience Office, p. 21–32.
- Lucas, S.B., 1989. Structural evolution of the Cape Smith thrust belt and the role of out-of-sequence faulting in the thickening of mountain belts; Tectonics, v. 8, p. 655–676. <https://doi.org/10.1029/TC008i004p00655>
- Lucas, S.B. and Byrne, T., 1992. Footwall involvement during arc–continent collision, Ungava Orogen, northern Canada; Journal of the Geological Society, v. 149, p. 237–248. <https://doi.org/10.1144/gsjgs.149.2.0237>
- Machado, N., Goulet, N., and Gariépy, C., 1989. U–Pb geochronology of reactivated Archean basement and of Hudsonian metamorphism in the northern Labrador Trough; Canadian Journal of Earth Sciences, v. 26, p. 1–15. <https://doi.org/10.1139/e89-001>
- Machado, N., David, J., Scott, D.J., Lamothe, D., Philippe, S., and Gariépy, C., 1993. U–Pb geochronology of the western Cape Smith Belt, Canada: new insights on the age of initial rifting and arc magmatism; Precambrian Research, v. 63, p. 211–223. [https://doi.org/10.1016/0301-9268\(93\)90034-Y](https://doi.org/10.1016/0301-9268(93)90034-Y)
- Mackay, C., 2011. Petrographic and geochemical study of the origin of “spotted” dykes and their relationship to the North Touak–Cape Dyer volcanic belt: Cumberland Peninsula, Baffin Island; B.Sc. thesis, University of Saskatchewan, Saskatoon, Saskatchewan, 29 p.
- MacKay, C.B. and Ansdell, K.M., 2014. Geochemical study of mafic and ultramafic rocks from southern Hall Peninsula, Baffin Island, Nunavut; in Summary of activities 2013, Canada-Nunavut Geoscience Office, p. 85–92.
- MacLeod, M.E., 2012. Metallogenic setting of high-grade iron ores, Mary River District, north Baffin Island, Nunavut; M.Sc. thesis, University of Western Ontario, London, Ontario, 285 p.
- McDonough, M.R., McNicoll, V.J., Schetselaar, E.M., and Grover, T.W., 2000. Geochronological and kinematic constraints on crustal shortening and escape in a two-sided oblique-slip collisional and magmatic orogen, Paleoproterozoic Taltson magmatic zone, northeastern Alberta; Canadian Journal of Earth Sciences, v. 37, p. 1549–1573. <https://doi.org/10.1139/e00-089>
- Miller, A.K., Youngquist, W., and Collinson, C., 1954. Ordovician cephalopod fauna of Baffin Island; Geological Society of America, Memoir 62, 234 p.
- Modeland, S.J. and Francis, D., 2003. Paleoproterozoic alkaline magmatism of the Bravo Lake formation on central Baffin Island; Geological Association of Canada–Mineralogical Association of Canada–Society of Economic Geologists, Joint Annual Meeting, Vancouver, May 25–28, 2003, Abstracts, v. 28, p. 115.
- Modeland, S.J. and Francis, D., 2004. Implications of high field-strength element anomalies in Paleoproterozoic mafic alkaline magmas of central Baffin Island; Eos, Transactions American Geophysical Union, 28–31 May 2004, Montreal, Joint Assembly Supplement, v. 85, no. 17, Abstract V14A-03.
- Morgan, W.C., 1983. Geology, Lake Gillian, District of Franklin; Geological Survey of Canada, Map 1560A, scale 1:250 000. <https://doi.org/10.4095/127057>
- Morgan, W.C., Bourne, J., Herd, R.K., Pickett, J.W., and Tippett, C.R., 1975. Geology of the Foxe Fold Belt, Baffin Island, District of Franklin; in Current research, Part A; Geological Survey of Canada, Paper 75–1A, p. 343–347. <https://doi.org/10.4095/104561>
- Morgan, W.C., Okulitch, A.V., and Thompson, P.H., 1976. Stratigraphy, structure and metamorphism of the west half of the Foxe Fold Belt, Baffin Island; in Current research, Part B; Geological Survey of Canada, Paper 76–1B, p. 387–391. <https://doi.org/10.4095/104230>
- Mortensen, J.K. and Percival, J.A., 1989. Reconnaissance U–Pb zircon and monazite geochronology of the Lac Clairambault area, Ashuanipi complex, Quebec; in Radiogenic age and isotopic studies: report 1; Geological Survey of Canada, Paper 87–2, p. 135–142. <https://doi.org/10.4095/122758>
- Nutman, A.P., Dawes, P.R., Kalsbeek, F., and Hamilton, M.A., 2008. Palaeoproterozoic and Archaean gneiss complexes in northern Greenland: Palaeoproterozoic terrane assembly in the High Arctic; Precambrian Research, v. 161, p. 419–451. <https://doi.org/10.1016/j.precamres.2007.09.006>
- Parrish, R.R., 1989. U–Pb geochronology of the Cape Smith Belt and Sugluk block, northern Quebec; Geoscience Canada, v. 16, p. 126–130.
- Partin, C.A., Bekker, A., Corrigan, D., Modeland, S.J., Francis, D., and Davis, D.W., 2014a. Revised age and correlation of the Paleoproterozoic Penrhyn and Piling groups of Arctic Canada; Geological Association of Canada–Mineralogical Association of Canada Joint Annual Meeting, Fredericton, May 21–23, 2014, Abstracts, v. 37, p. 213–214.
- Partin, C.A., Bekker, A., Sylvester, P.J., Wodicka, N., Stern, R.A., Chacko, T., and Heaman, L., 2014b. Filling in the juvenile magmatic gap: evidence for uninterrupted Paleoproterozoic plate tectonics; Earth and Planetary Science Letters, v. 388, p. 123–133. <https://doi.org/10.1016/j.epsl.2013.11.041>
- Pehrsson, S., Jefferson, C., Corrigan, D., Sanborn-Barrie, M., Berman, R., and Peterson, T., 2011. Unravelling the mineral potential of the Churchill province; Prospectors and Developers Association of Canada, Annual Convention, Toronto, Ontario, March 4–7, 2011, CD-ROM (abstract).
- Pehrsson, S.J., Berman, R.G., Eglinton, B., and Rainbird, R., 2013. Two Neoproterozoic supercontinents revisited: the case for a Rae family of cratons; Precambrian Research, v. 232, p. 27–43. <https://doi.org/10.1016/j.precamres.2013.02.005>
- Putnam, G.P., 1928. The Putnam Baffin Island Expedition; Geographical Review, v. 18, no. 1, p. 1–40. <https://doi.org/10.2307/208761>
- Rainbird, R.H., Davis, W.J., Pehrsson, S.J., Wodicka, N., Rayner, N., and Skulski, T., 2010. Early Paleoproterozoic supracrustal assemblages of the Rae domain, Nunavut, Canada: intracratonic basin development during supercontinent break-up and assembly; Precambrian Research, v. 181, p. 167–186. <https://doi.org/10.1016/j.precamres.2010.06.005>

- Rayner, N.M., 2014. New U-Pb geochronological results from Hall Peninsula, Baffin Island, Nunavut; *in* Summary of activities 2013, Canada-Nunavut Geoscience Office, p. 39–52.
- Rayner, N.M., 2015. New (2013–2014) U-Pb geochronological results from northern Hall Peninsula, southern Baffin Island, Nunavut; *in* Summary of activities 2014, Canada-Nunavut Geoscience Office, p. 31–44.
- Rayner, N.M., 2017. U-Pb zircon geochronology constraints on timing of plutonism and sedimentary provenance from the Clearwater Fiord–Sylvia Grinnell Lake area, southern Baffin Island, Nunavut; Geological Survey of Canada, Open File 8204, 32 p. <https://doi.org/10.4095/299720>
- Rayner, N.M., Sanborn-Barrie, M., Young, M.D., and Whalen, J.B., 2012. U-Pb ages of Archean basement and Paleoproterozoic plutonic rocks, southern Cumberland Peninsula, eastern Baffin Island, Nunavut; Geological Survey of Canada, Current Research 2012–8, 28 p. <https://doi.org/10.4095/291401>
- Riley, G.C., 1959. Cumberland Sound, Baffin Island, District of Franklin, Northwest Territories; Geological Survey of Canada, Map 1061A, scale 1:506 880. <https://doi.org/10.4095/107415>
- Sanborn-Barrie, M. and Young, M., 2011. Bulk compositional data for sulfidic and gossanous rocks from Cumberland Peninsula, Baffin Island, Nunavut; Geological Survey of Canada, Open File 6916, 11 p. <https://doi.org/10.4095/288710>
- Sanborn-Barrie, M. and Young, M., 2013. Geology, Qikiqtarjuaq, Nunavut; Geological Survey of Canada, Canadian Geoscience Map 39 (preliminary edition), scale 1:100 000. <https://doi.org/10.4095/292016>
- Sanborn-Barrie, M., St-Onge, M.R., Young, M.D., and James, D.T., 2008. Bedrock geology of southwestern Baffin Island, Nunavut: expanding the tectonostratigraphic framework with relevance to mineral resources; Geological Survey of Canada, Paper 2008–6, 16 p. <https://doi.org/10.4095/225179>
- Sanborn-Barrie, M., Young, M., Whalen, J., James, D., and St-Onge, M.R., 2011. Geology Touak Fiord, Nunavut; Geological Survey of Canada, Canadian Geoscience Map 3 (second preliminary edition), scale 1:100 000. <https://doi.org/10.4095/288931>
- Sanborn-Barrie, M., Young, M., Keim, R., and Hamilton, B., 2013. Geology, Sunneshine Fiord, Baffin Island, Nunavut; Geological Survey of Canada, Canadian Geoscience Map 6, (preliminary edition), scale 1:100 000. <https://doi.org/10.4095/288931>
- Sanborn-Barrie, M., Thrane, K., Wodicka, N., and Rayner, N., 2017. The Laurentia–West Greenland connection at 1.9 Ga: new insights from the Rinkian fold belt; *Gondwana Research*, v. 51, p. 289–309. <https://doi.org/10.1016/j.gr.2017.07.002>
- Saumur, B.M., Skipton, D.R., St-Onge, M.R., Bros, E.R., Acosta-Gongora, P., Kelly, C.J., Morin, A., O’Brien, M.E., Johnston, S.T., and Weller, O.M., 2018. Precambrian geology of the surroundings of Steensby Inlet and western Barnes Ice Cap (parts of NTS 37E, 37F, 37G), Baffin Island, Nunavut; *in* Summary of activities 2018; Canada-Nunavut Geoscience Office, p. 29–46.
- Scott, D.J., 1997. Geology, U-Pb, and Pb-Pb geochronology of the Lake Harbour area, southern Baffin Island: implications for the Paleoproterozoic tectonic evolution of northeastern Laurentia; *Canadian Journal of Earth Sciences*, v. 34, p. 140–155. <https://doi.org/10.1139/e17-012>
- Scott, D.J., 1998. U-Pb ages of Archean crust in the southeast arm of the Rae Province, southeastern Ungava Bay, Quebec; *in* Radiogenic age and isotopic studies: report 11; Geological Survey of Canada, Current Research 1998-F, p. 41–45. <https://doi.org/10.4095/210054>
- Scott, D.J., 1999. U-Pb geochronology of the eastern Hall Peninsula, southern Baffin Island, Canada: a northern link between the Archean of West Greenland and the Paleoproterozoic Torngat Orogen of northern Labrador; *Precambrian Research*, v. 93, p. 5–26. [https://doi.org/10.1016/S0301-9268\(98\)00095-3](https://doi.org/10.1016/S0301-9268(98)00095-3)
- Scott, D.J. and de Kemp, E.A., 1999. An overview of the bedrock geology of northern Baffin Island and the northern Melville Peninsula, Northwest Territories (Nunavut); *in* North Baffin Partnership Project: summary of investigations, (ed.) D.G. Richardson; Geological Survey of Canada, Open File 3637, p. 5–21. <https://doi.org/10.4095/210287>
- Scott, D.J. and St-Onge, M.R., 1995. Constraints on Pb closure temperature in titanite based on rocks from the Ungava orogen, Canada: implications for U-Pb geochronology and P-T-t path determinations; *Geology*, v. 23, p. 1123–1126. [https://doi.org/10.1130/0091-7613\(1995\)023%3c1123:COPCTI%3e2.3.CO%3b2](https://doi.org/10.1130/0091-7613(1995)023%3c1123:COPCTI%3e2.3.CO%3b2)
- Scott, D.J. and Wodicka, N.A., 1998. A second report on the U-Pb geochronology of southern Baffin Island, Northwest Territories; *in* Radiogenic age and isotopic studies: report 11; Geological Survey of Canada, Current Research 1998-F, p. 47–57. <https://doi.org/10.4095/210055>
- Scott, D.J., Helmstaedt, H., and Bickle, M.J., 1992. Purtunig ophiolite, Cape Smith belt, northern Quebec, Canada: a reconstructed section of Early Proterozoic oceanic crust; *Geology*, v. 20, p. 173–176. [https://doi.org/10.1130/0091-7613\(1992\)020%3c0173:POCSBN%3e2.3.CO%3b2](https://doi.org/10.1130/0091-7613(1992)020%3c0173:POCSBN%3e2.3.CO%3b2)
- Scott, D.J., St-Onge, M.R., Wodicka, N., and Hanmer, S., 1997. Geology of the Markham Bay–Crooks Inlet area, southern Baffin Island, Northwest Territories; *in* Current research 1997-C; Geological Survey of Canada, p. 157–166. <https://doi.org/10.4095/208641>
- Scott, D.J., St-Onge, M.R., Lucas, S.B., and Helmstaedt, H., 1999. The 2.00 Ga Purtunig ophiolite, Cape Smith Belt, Canada: MORB-like crust intruded by OIB-like magmatism; *Ophioliti*, v. 24, p. 199–215.
- Scott, D.J., Stern, R.A., St-Onge, M.R., and McMullen, S.M., 2002a. U-Pb geochronology of detrital zircons in metasedimentary rocks from southern Baffin Island: implications for the Paleoproterozoic tectonic evolution of northeastern Laurentia; *Canadian Journal of Earth Sciences*, v. 39, no. 5, p. 611–623. <https://doi.org/10.1139/e01-093>
- Scott, D.J., St-Onge, M.R., and Corrigan, D., 2002b. Geology of the Paleoproterozoic Piling Group and underlying Archean gneiss, central Baffin Island, Nunavut; Geological Survey of Canada, Current Research 2002-C17, 10 p. <https://doi.org/10.4095/213194>
- Scott, D.J., St-Onge, M.R., and Corrigan, D., 2003. Geology of the Archean Rae Craton and Mary River Group and the Paleoproterozoic Piling Group, central Baffin Island, Nunavut; Geological Survey of Canada, Current Research 2003-C26, 12 p. <https://doi.org/10.4095/214208>
- Skipton, D.R., Saumur, B.M., St-Onge, M.R., Wodicka, N., Bros, E.R., Morin, A., Brouillette, P., Weller, O.M., and Johnston, S.T., 2017. Precambrian bedrock geology of the Pond Inlet–Mary River area, northern Baffin Island, Nunavut; *in* Summary of activities 2017, Canada-Nunavut Geoscience Office, p. 49–67.
- Skipton, D.R., Wodicka, N., McNicoll, V., Saumur, B.M., St-Onge, M.R., and Young, M.D., 2019. U-Pb zircon geochronology of Archean greenstone belts (Mary River Group) and surrounding Archean to Paleoproterozoic rocks, northern Baffin Island, Nunavut; Geological Survey of Canada, Open File 8585, 43 p. <https://doi.org/10.4095/314938>
- Smye, A.J., St-Onge, M.R., and Waters, D.J., 2009. Contrasting metamorphic pressure-temperature histories within the Trans-Hudson Orogen’s hinterland, southwest Baffin Island, Nunavut; Geological Survey of Canada, Current Research 2009–6, 21 p. <https://doi.org/10.4095/247603>
- Snyder, D.B., Berman, R.G., Kendall, J.-M., and Sanborn-Barrie, M., 2013. Seismic anisotropy and mantle structure of the Rae craton, central Canada, from joint interpretation of SKS splitting and receiver functions; *Precambrian Research*, v. 232, p. 189–208. <https://doi.org/10.1016/j.precamres.2012.03.003>
- St-Onge, M.R. and Lucas, S.B., 1991. Evolution of regional metamorphism in the Cape Smith Trust Belt (northern Quebec, Canada): interaction of tectonic and thermal processes; *Journal of Metamorphic Geology*, v. 9, p. 515–534. <https://doi.org/10.1111/j.1525-1314.1991.tb00545.x>
- St-Onge, M.R., Lucas, S.B., and Parrish, R.R., 1992. Terrane accretion in the internal zone of the Ungava Orogen, northern Quebec, Part 1: tectonostratigraphic assemblages and their tectonic implications; *Canadian Journal of Earth Sciences*, v. 29, p. 746–764. <https://doi.org/10.1139/e92-064>
- St-Onge, M.R., Hanmer, S., and Scott, D.J., 1996. Geology of the Meta Incognita Peninsula, south Baffin Island, Northwest Territories: tectonostratigraphic units and regional correlations; *in* Current research 1996-C; Geological Survey of Canada, p. 63–72. <https://doi.org/10.4095/207444>

- St-Onge, M.R., Scott, D.J., Wodicka, N., and Lucas, S.B., 1998. Geology of the McKellar Bay–Wight Inlet–Frobisher Bay area, southern Baffin Island, Northwest Territories; *in* Current research 1998-C; Geological Survey of Canada, p. 43–53. <https://doi.org/10.4095/209512>
- St-Onge, M.R., Lucas, S.B., Scott, D.J., and Wodicka, N., 1999. Upper and lower plate juxtaposition, deformation and metamorphism during crustal convergence, Trans-Hudson Orogen (Quebec–Baffin segment), Canada; *Precambrian Research*, v. 93, p. 27–49. [https://doi.org/10.1016/S0301-9268\(98\)00096-5](https://doi.org/10.1016/S0301-9268(98)00096-5)
- St-Onge, M.R., Scott, D.J., and Lucas, S.B., 2000a. Early partitioning of Quebec: microcontinent formation in the Paleoproterozoic; *Geology*, v. 28, p. 323–326. [https://doi.org/10.1130/0091-7613\(2000\)28%3c323:EPOQMF%3e2.0.CO%3b2](https://doi.org/10.1130/0091-7613(2000)28%3c323:EPOQMF%3e2.0.CO%3b2)
- St-Onge, M.R., Wodicka, N., and Lucas, S.B., 2000b. Granulite- and amphibolite-facies metamorphism in a convergent-plate-margin setting: synthesis of the Quebec–Baffin segment of the Trans-Hudson Orogen; *Canadian Mineralogist*, v. 38, p. 379–398. <https://doi.org/10.2113/gscanmin.38.2.379>
- St-Onge, M.R., Scott, D.J., and Wodicka, N., 2001. Terrane boundaries within Trans-Hudson Orogen (Quebec–Baffin segment), Canada: changing structural and metamorphic character from foreland to hinterland; *Precambrian Research*, v. 107, p. 75–91. [https://doi.org/10.1016/S0301-9268\(00\)00155-8](https://doi.org/10.1016/S0301-9268(00)00155-8)
- St-Onge, M.R., Scott, D.J., and Wodicka, N., 2002. Review of crustal architecture and evolution in the Ungava Peninsula–Baffin Island area: connection to the LITHOPROBE ECSOOT transect; *Canadian Journal of Earth Sciences*, v. 39, p. 589–610. <https://doi.org/10.1139/e02-022>
- St-Onge, M.R., Scott, D.J., Corrigan, D., and Wodicka, N., 2005. Geology, central Baffin Island, Nunavut; Geological Survey of Canada, Maps 2077A to 2082A, scale 1:100 000. <https://doi.org/10.4095/221054> and <https://doi.org/10.4095/221091> to <https://doi.org/10.4095/221095>
- St-Onge, M.R., Searle, M.P., and Wodicka, N., 2006. Trans-Hudson Orogen of North America and Himalaya–Karakoram–Tibetan Orogen of Asia: structural and thermal characteristics of the lower and upper plates; *Tectonics*, v. 25, TC4006, 22 p. <https://doi.org/10.1029/2005TC001907>
- St-Onge, M.R., Wodicka, N., and Ijewliw, O., 2007. Polymetamorphic evolution of the Trans-Hudson Orogen, Baffin Island, Canada: integration of petrological, structural and geochronological data; *Journal of Petrology*, v. 48, p. 271–302. <https://doi.org/10.1093/petrology/egl060>
- St-Onge, M.R., Van Gool, J.A.M., Garde, A.A., and Scott, D.J., 2009. Correlation of Archaean and Palaeoproterozoic units between northeastern Canada and western Greenland: constraining the pre-collisional upper plate accretionary history of the Trans-Hudson orogen; *in* Earth accretionary systems in space and time, (ed.) P.A. Cawood and A. Kroner; Geological Society of London, Special Publications, v. 318, p. 193–235. <https://doi.org/10.1144/SP318.7>
- St-Onge, M.R., Harrison, J.C., Paul, D., Tella, S., Brent, T.A., Jauer, C.D., and Maclean, B.C., 2015a. Tectonic map of Arctic Canada; Geological Survey of Canada, Canadian Geoscience Map 187 (preliminary edition), scale 1:4 000 000. <https://doi.org/10.4095/295945>
- St-Onge, M.R., Rayner, N.M., Liikane, D., and Chadwick, T., 2015b. Mafic, ultramafic and layered mafic–ultramafic sills, Meta Incognita Peninsula, southern Baffin Island, Nunavut; *in* Summary of activities 2014, Canada-Nunavut Geoscience Office, p. 11–16.
- St-Onge, M.R., Rayner, N.M., Steenkamp, H.M., and Skipton, D.R., 2015c. Bedrock mapping of eastern Meta Incognita Peninsula, southern Baffin Island, Nunavut; *in* Summary of activities 2014, Canada-Nunavut Geoscience Office, p. 105–118.
- St-Onge, M.R., Weller, O.M., and Rayner, N.M., 2016. 2016 report of activities for completing the regional bedrock mapping of the southern half of Baffin Island: GEM 2 Baffin Project; Geological Survey of Canada, Open File 8118, 11 p. <https://doi.org/10.4095/299195>
- Stacey, J.R. and Pattison, D.R.M., 2003. Stratigraphy, structure, and petrology of a representative klippe of the Bravo Lake Formation, Piling Group, central Baffin Island, Nunavut; Geological Survey of Canada, Current Research 2003-C13, 11 p. <https://doi.org/10.4095/214195>
- Steenkamp, H.M. and St-Onge, M.R., 2014. Overview of the 2013 regional bedrock mapping program on northern Hall Peninsula, Baffin Island, Nunavut; *in* Summary of activities 2013, Canada-Nunavut Geoscience Office, p. 27–38.
- Steenkamp, H.M., Bros, E.R., and St-Onge, M.R., 2014. Altered ultramafic and layered mafic–ultramafic intrusions: new economic and carving stone potential on northern Hall Peninsula, Baffin Island, Nunavut; *in* Summary of activities 2013, Canada-Nunavut Geoscience Office, p. 11–20.
- Steenkamp, H.M., Gilbert, C., St-Onge, M.R., 2016. Geology, Beekman Peninsula (south), Baffin Island, Nunavut, NTS 25P (south) and 15-M (part); Geological Survey of Canada, Canadian Geoscience Map 267 (preliminary edition); Canada-Nunavut Geoscience Office, Open File 2016-04, scale 1:100 000. <https://doi.org/10.4095/297351>
- Storey, E., 2012. Characterization of silicate-facies meta-iron formation from Cumberland Peninsula, Baffin Island, Canada; B.Sc. thesis, University of Calgary, Calgary, Alberta, 109 p.
- Taylor, F.C., 1982. Precambrian geology of the Canadian North borderlands; *in* Geology of the North Atlantic Borderlands, (ed.) J.W. Kerr, A.J. Fergusson, and L.C. Machan; Canadian Society of Petroleum Geologists, Memoir no. 7, p. 11–30.
- Thériault, R.J., St-Onge, M.R., and Scott, D.J., 2001. Nd isotopic and geochemical signature of the Paleoproterozoic Trans-Hudson Orogen, southern Baffin Island, Canada: implications for the evolution of eastern Laurentia; *Precambrian Research*, v. 108, p. 113–138. [https://doi.org/10.1016/S0301-9268\(00\)00159-5](https://doi.org/10.1016/S0301-9268(00)00159-5)
- Thrane, K. and Connelly, J.N., 2006. Zircon geochronology from the Kangaatsiaq–Qasigiannuit region, the northern part of the 1.9–1.8 Ga Nagssugtoqidian orogen, West Greenland; Geological Survey of Denmark and Greenland, Bulletin no. 11, p. 87–99.
- Tippett, C.R., 1984. Supplementary data concerning “Geology of a transect through the southern margin of the Foxe Fold Belt, central Baffin Island, District of Franklin”; Geological Survey of Canada, Open File 1111, 84 p. <https://doi.org/10.4095/129946>
- Tippett, C.R., 1985. Geology of a transect through the southern margin of the Foxe Fold Belt, central Baffin Island, District of Franklin; Geological Survey of Canada, Open File 1110, 77 p. <https://doi.org/10.4095/129953>
- van Breemen, O., Henderson, J.B., Loveridge, W.D., and Thompson, P.H., 1987. U–Pb zircon and monazite geochronology and zircon morphology of granulites and a granite from the Thelon tectonic zone, Healey Lake and Artillery Lake map areas, N.W.T.; *in* Current research, Part A; Geological Survey of Canada, Paper 87-1A, p. 783–801. <https://doi.org/10.4095/122484>
- van Breemen, O., Bostock, H.H., and Loveridge, W.D., 1992. Geochronology of granites along the margin of the northern Taltson magmatic zone and western Rae Province, Northwest Territories; *in* Radiogenic age and isotopic studies: report 5; Geological Survey of Canada, Current Research 91-2, p. 17–24. <https://doi.org/10.4095/132907>
- Wardle, R.J., James, D.T., Scott, D.J., and Hall, J., 2002. The southeastern Churchill Province: synthesis of a Palaeoproterozoic transpressional orogeny; *Canadian Journal of Earth Sciences*, v. 39, p. 639–663. <https://doi.org/10.1139/e02-004>
- Weeks, L.J., 1928a. Head of Cumberland Sound and route to Nettilling Lake, Baffin Island; Geological Survey of Canada, Map 219A, scale 1:506 880. <https://doi.org/10.4095/107406>
- Weeks, L.J., 1928b. Cumberland Sound area, Baffin Island; Geological Survey of Canada, Summary Report 1927, pt. C, p. 83–95. <https://doi.org/10.4095/297953>
- Weller, O.M. and St-Onge, M.R., 2017. Record of modern-style plate tectonics in the Palaeoproterozoic Trans-Hudson orogen; *Nature Geoscience*, v. 10, p. 305–311. <https://doi.org/10.1038/ngeo2904>
- Weller, O.M., Dyck, B.J., St-Onge, M.R., Rayner, N.M., and Tschirhart, V., 2015. Completing the bedrock mapping of southern Baffin Island, Nunavut: plutonic suites and regional stratigraphy; *in* Summary of activities 2015, Canada-Nunavut Geoscience Office, p. 33–48.

- Whalen, J.B., Wodicka, N., Taylor, B.E., and Jackson, G.D., 2010. Cumberland batholith, Trans-Hudson Orogen, Canada: petrogenesis and implications for Paleoproterozoic crustal and orogenic processes; *Lithos*, v. 117, p. 99–118. <https://doi.org/10.1016/j.lithos.2010.02.008>
- Whalen, J.B., Sanborn-Barrie, M., and Young, M., 2012. Geochemical data from Archean and Paleoproterozoic plutonic and volcanic rocks of Cumberland Peninsula, eastern Baffin Island, Nunavut; Geological Survey of Canada, Open File 6933, 15 p. <https://doi.org/10.4095/291453>
- Whitney, D.L., and Evans, B.W., 2010. Abbreviations for names of rock-forming minerals; *The American Mineralogist*, v. 95, p. 185–187. <https://doi.org/10.2138/am.2010.3371>
- Wodicka, N. and Scott, D.J., 1997. A preliminary report on the U-Pb geochronology of the Meta Incognita Peninsula, southern Baffin Island, Northwest Territories; *in* Current research 1997-C; Geological Survey of Canada, p. 167–178. <https://doi.org/10.4095/208642>
- Wodicka, N., Madore, L., Larbi, Y., and Vicker, P., 2002a. Géochronologie U-Pb de filons-couches mafiques de la Ceinture de Cape Smith et de la Fosse du Labrador; *in* 23^e Séminaire d'information sur la recherche géologique, Ministère des Ressources naturelles du Québec, Programme et résumés, DV 2002–10, p. 48.
- Wodicka, N., St-Onge, M.R., Scott, D.J., and Corrigan, D., 2002b. Preliminary report on the U-Pb geochronology of the northern margin of the Trans-Hudson Orogen, central Baffin Island; *in* Radiogenic age and isotopic studies: report 15 (ed.) R.A. Stern; Geological Survey of Canada, Current Research 2002-F7, 12 p. <https://doi.org/10.4095/213623>
- Wodicka, N., St-Onge, M.R., and Whalen, J.B., 2008. Characteristics of two opposing continental margin successions in northeast Laurentia; *Geochimica et Cosmochimica Acta*, Goldschmidt Conference Abstracts 2008, v. 72, A1030.
- Wodicka, N., Whalen, J.B., St-Onge, M.R., and Corrigan, D., 2010. Meta Incognita microcontinent revisited: insights from U-Pb geochronology and Nd isotopes; Geological Association of Canada-Mineralogical Association of Canada, GeoCanada 2010 Conference, Calgary, May 10–14, 2010, Abstracts, v. 35.
- Wodicka, N., Corrigan, D., Nadeau, L., and Erdmann, S., 2011. New U-Pb geochronological results from Melville Peninsula: unraveling the Archean and Early Paleoproterozoic magmatic history of the north-central Rae craton; Geological Association of Canada-Mineralogical Association of Canada Annual Meeting, Ottawa, May 25–27, 2011, Abstracts, v. 34, p. 236.
- Wodicka, N., St-Onge, M.R., Corrigan, D., Scott, D.J., and Whalen, J.B., 2014. Did a proto-ocean basin form along the southeastern Rae cratonic margin? Evidence from U-Pb geochronology, geochemistry (Sm-Nd and whole-rock), and stratigraphy of the Paleoproterozoic Piling Group, northern Canada; *Geological Society of America Bulletin*, v. 126, p. 1625–1653. <https://doi.org/10.1130/B31028.1>
- Young, M.D., Sandeman, H., Berniolles, F., and Gertzbein, P.M., 2004. A preliminary stratigraphic and structural geology framework of the Archean Mary River Group, northern Baffin Island, Nunavut; Geological Survey of Canada, Current Research 2004-C1, 14 p. <https://doi.org/10.4095/215376>
- Young, M., Sandeman, H., Creaser, R., and James, D., 2007. Mesozoic to Neoproterozoic crustal growth and recycling on northern Baffin Island and correlation of Rae Province rocks across mainland Nunavut and Greenland; Geological Association of Canada-Mineralogical Association of Canada, Yellowknife, May 23–25, 2007, Program with Abstracts, v. 32, p. 89.

**APPENDIX A – MAP REFERENCES IN
FIGURES 1 AND 2**

1. Blackadar, R.G., 1967. Geology, Cumberland Sound, District of Franklin; Geological Survey of Canada, Preliminary Map 17-1966, scale 1:506 880. <https://doi.org/10.4095/108490>
2. Blackadar, R.G., 1970. Nottingham, Salisbury, and Mill Islands, District of Franklin; Geological Survey of Canada, Map 1205A, scale 1:250 000. <https://doi.org/10.4095/109212>
3. Jackson, G.D., 1971. Operation Penny Highlands, south-central Baffin Island; in Report of activities, Part A; Geological Survey of Canada, Paper 71-1 A, p. 138–140. <https://doi.org/10.4095/105595>
4. Trettin, H.P., 1975. Geology, Lower Paleozoic geology, central and eastern parts of Foxe Basin and Baird Peninsula, Baffin Island; Geological Survey of Canada, Map 1406A, scale 1:500 000. <https://doi.org/10.4095/109081>
5. Morgan, W.C., 1982. Geology, Koch Island, District of Franklin; Geological Survey of Canada, Map 1535A, scale 1:250 000. <https://doi.org/10.4095/127056>
6. Henderson, J.R., 1985a. Geology, McBeth Fiord–Cape Henry Kater, District of Franklin; Geological Survey of Canada, Map 1605A, scale 1:250 000. <https://doi.org/10.4095/120467>
7. Henderson, J.R., 1985b. Geology, Ekalugad Fiord–Home Bay, District of Franklin; Geological Survey of Canada, Map 1606A, scale 1:250 000. <https://doi.org/10.4095/120468>
8. Jackson, G.D., 1998. Geology, Okoa Bay Padloping Island area, District of Franklin, Northwest Territories; Geological Survey of Canada, Open File 3532, scale 1:250 000. <https://doi.org/10.4095/209911>
9. St-Onge, M.R., Scott, D.J., and Wodicka, N., 1999a. Geology, Frobisher Bay, Nunavut; Geological Survey of Canada, Map 1979A, scale 1:100 000. <https://doi.org/10.4095/210833>
10. St-Onge, M.R., Scott, D.J., and Wodicka, N., 1999b. Geology, Hidden Bay, Nunavut; Geological Survey of Canada, Map 1980A, scale 1:100 000. <https://doi.org/10.4095/210835>
11. St-Onge, M.R., Scott, D.J., and Wodicka, N., 1999c. Geology, McKellar Bay, Nunavut; Geological Survey of Canada, Map 1981A, scale 1:100 000. <https://doi.org/10.4095/210836>
12. St-Onge, M.R., Scott, D.J., and Wodicka, N., 1999d. Geology, Wright Inlet, Nunavut; Geological Survey of Canada, Map 1982A, scale 1:100 000. <https://doi.org/10.4095/210840>
13. St-Onge, M.R., Scott, D.J., and Wodicka, N., 1999e. Geology, Blandford Bay, Nunavut; Geological Survey of Canada, Map 1983A, scale 1:100 000. <https://doi.org/10.4095/210837>
14. St-Onge, M.R., Scott, D.J., and Wodicka, N., 1999f. Geology, Crooks Inlet, Nunavut; Geological Survey of Canada, Map 1984A, scale 1:100 000. <https://doi.org/10.4095/210838>
15. St-Onge, M.R., Scott, D.J., and Wodicka, N., 1999g. Geology, White Strait, Nunavut; Geological Survey of Canada, Map 1985A, scale 1:100 000. <https://doi.org/10.4095/210839>
16. Sanford, B.V. and Grant, A.C., 2000. Geological framework of the Ordovician system in the southeast Arctic platform, Nunavut; in *Geology and paleontology of the southeast Arctic Platform and southern Baffin Island, Nunavut*, (ed.) A.D. McCracken and T.E. Bolton; Geological Survey of Canada, Bulletin 557, p. 13–38. <https://doi.org/10.4095/211845>
17. Jackson, G.D., 2002. Geology, Isurtuq River–Nedlukseak Fiord, Nunavut; Geological Survey of Canada, Open File 4259, scale 1:250 000. <https://doi.org/10.4095/213304>
18. St-Onge, M.R., Scott, D.J., Corrigan, D., and Wodicka, N., 2005a. Geology, Ikpik Bay, Baffin Island, Nunavut; Geological Survey of Canada, Map 2077A, scale 1:100 000. <https://doi.org/10.4095/221054>
19. St-Onge, M.R., Scott, D.J., Corrigan, D., and Wodicka, N., 2005b. Geology, Flyway Lake, Baffin Island, Nunavut; Geological Survey of Canada, Map 2078A, scale 1:100 000. <https://doi.org/10.4095/221091>
20. St-Onge, M.R., Scott, D.J., Corrigan, D., and Wodicka, N., 2005c. Geology, Clyde River, Baffin Island, Nunavut; Geological Survey of Canada, Map 2079A, scale 1:100 000. <https://doi.org/10.4095/221092>
21. St-Onge, M.R., Scott, D.J., Corrigan, D., and Wodicka, N., 2005d. Geology, Piling Bay, Baffin Island, Nunavut; Geological Survey of Canada, Map 2080A, scale 1:100 000. <https://doi.org/10.4095/221093>
22. St-Onge, M.R., Scott, D.J., Corrigan, D., and Wodicka, N., 2005e. Geology, Straits Bay, Baffin Island, Nunavut; Geological Survey of Canada, Map 2081A, scale 1:100 000. <https://doi.org/10.4095/221094>
23. St-Onge, M.R., Scott, D.J., Corrigan, D., and Wodicka, N., 2005f. Geology, Dewar Lakes, Baffin Island, Nunavut; Geological Survey of Canada, Map 2082A, scale 1:100 000. <https://doi.org/10.4095/221095>
24. Jackson, G.D., 2006. Geology, Hantzsch River area, Baffin Island, Nunavut; Geological Survey of Canada, Open File 4202, scale 1:250 000. <https://doi.org/10.4095/221809>
25. St-Onge, M.R., Sanborn-Barrie, M., and Young, M., 2007a. Geology, Mingo Lake, Baffin Island, Nunavut; Geological Survey of Canada, Open File 5433, scale 1:250 000. <https://doi.org/10.4095/224163>
26. St-Onge, M.R., Sanborn-Barrie, M., and Young, M., 2007b. Geology, Foxe Peninsula, Baffin Island, Nunavut; Geological Survey of Canada, Open File 5434, scale 1:250 000. <https://doi.org/10.4095/224222>
27. Sanborn-Barrie, M., Young, M., Whalen, J., and James, D., 2011a. Geology, Ujuktuk Fiord, Nunavut; Geological Survey of Canada, Canadian Geoscience Map 1, (second preliminary edition), scale 1:100 000. <https://doi.org/10.4095/289237>
28. Sanborn-Barrie, M., Young, M., and Whalen, J., 2011b. Geology, Kingnait Fiord, Nunavut; Geological Survey of Canada, Canadian Geoscience Map 2, (second preliminary edition), scale 1:100 000. <https://doi.org/10.4095/289238>
29. Sanborn-Barrie, M., Young, M., Whalen, J., James, D., and St-Onge, M.R., 2011c. Geology, Touak Fiord, Nunavut; Geological Survey of Canada, Canadian Geoscience Map 3 (second preliminary edition), scale 1:100 000. <https://doi.org/10.4095/289239>
30. Sanborn-Barrie, M. and Young, M., 2013a. Geology, Circle Lake, Nunavut; Geological Survey of Canada, Canadian Geoscience Map 5 (preliminary edition), scale 1:100 000. <https://doi.org/10.4095/288929>
31. Sanborn-Barrie, M., Young, M., Keim, R., and Hamilton, B.M., 2013b. Geology, Sunneshine Fiord, Baffin Island, Nunavut; Geological Survey of Canada, Canadian Geoscience Map 6 (preliminary edition), scale 1:100 000. <https://doi.org/10.4095/288931>
32. Sanborn-Barrie, M. and Young, M., 2013c. Geology, Padle Fiord, Baffin Island, Nunavut; Geological Survey of Canada, Canadian Geoscience Map 37 (preliminary edition), scale 1:100 000. <https://doi.org/10.4095/292014>
33. Sanborn-Barrie, M. and Young, M., 2013d. Geology, Durban Harbour, Baffin Island, Nunavut; Geological Survey of Canada, Canadian Geoscience Map 38 (preliminary edition), scale 1:100 000. <https://doi.org/10.4095/292015>
34. Sanborn-Barrie, M. and Young, M., 2013e. Geology, Qikiqtarjuaq, Baffin Island, Nunavut; Geological Survey of Canada, Canadian Geoscience Map 39 (preliminary edition), scale 1:100 000. <https://doi.org/10.4095/292016>
35. Jackson, G.D. and Sanborn-Barrie, M., 2014. Geology, Pangnirtung Fiord, Baffin Island, Nunavut; Geological Survey of Canada, Canadian Geoscience Map 4 (preliminary edition), scale 1:100 000. <https://doi.org/10.4095/288928>
36. St-Onge, M.R., Rayner, N.M., Steenkamp, H.M., and Gilbert, C., 2015a. Geology, Terra Nivea, Baffin Island, Nunavut; Geological Survey of Canada, Canadian Geoscience Map 215E (preliminary); Canada-Nunavut Geoscience Office, Open File Map 2015-02E, scale 1:100 000. <https://doi.org/10.4095/296104>
37. St-Onge, M.R., Rayner, N.M., Steenkamp, H.M., and Gilbert, C., 2015b. Geology, Pritzler Harbour, Baffin Island, Nunavut; Geological Survey of Canada, Canadian Geoscience Map 216E (preliminary edition); Canada-Nunavut Geoscience Office, Open File Map 2015-03E, scale 1:100 000. <https://doi.org/10.4095/296109>

38. St-Onge, M.R., Rayner, N.M., Steenkamp, H.M., and Gilbert, C., 2015c. Geology, Grinnell Glacier, Baffin Island, Nunavut; Geological Survey of Canada, Canadian Geoscience Map 217E (preliminary edition); Canada-Nunavut Geoscience Office, Open File Map 2015-04E, scale 1:100 000. <https://doi.org/10.4095/296111>
39. Steenkamp, H.M., Gilbert, C., and St-Onge, M.R., 2016a. Geology, Loks Land, Baffin Island, Nunavut, NTS 25I (part); Geological Survey of Canada, Canadian Geoscience Map 264 (preliminary edition); Canada-Nunavut Geoscience Office, Open File Map 2016-01, scale 1:100 000. <https://doi.org/10.4095/297344>
40. Steenkamp, H.M., Gilbert, C., and St-Onge, M.R., 2016b. Geology, Ward Inlet (south), Baffin Island, Nunavut, NTS 25O (south) and 25-J (part); Geological Survey of Canada, Canadian Geoscience Map 266 (preliminary edition); Canada-Nunavut Geoscience Office, Open File Map 2016-02, scale 1:100 000. <https://doi.org/10.4095/297349>
41. Steenkamp, H.M., Gilbert, C., and St-Onge, M.R., 2016c. Geology, Ward Inlet (north), Baffin Island, Nunavut, NTS 25O (north); Geological Survey of Canada, Canadian Geoscience Map 265 (preliminary edition); Canada-Nunavut Geoscience Office, Open File Map 2016-03, scale 1:100 000. <https://doi.org/10.4095/297348>
42. Steenkamp, H.M., Gilbert, C., St-Onge, M.R., 2016d. Geology, Beekman Peninsula (south), Baffin Island, Nunavut, NTS 25P (south) and 15M (part); Geological Survey of Canada, Canadian Geoscience Map 267 (preliminary edition); Canada-Nunavut Geoscience Office, Open File Map 2016-04, scale 1:100 000. <https://doi.org/10.4095/297351>
43. Steenkamp, H.M., Gilbert, C., and St-Onge, M.R., 2016e. Geology, Beekman Peninsula (north), Baffin Island, Nunavut, NTS 25P (north) and 15M (part); Geological Survey of Canada, Canadian Geoscience Map 268 (preliminary edition); Canada-Nunavut Geoscience Office, Open File Map 2016-05, scale 1:100 000. <https://doi.org/10.4095/297352>
44. Steenkamp, H.M., Gilbert, C., and St-Onge, M.R., 2016f. Geology, Leybourne Islands (south), Baffin Island, Nunavut, NTS 26A (south); Geological Survey of Canada, Canadian Geoscience Map 269 (preliminary edition); Canada-Nunavut Geoscience Office, Open File Map 2016-06, scale 1:100 000. <https://doi.org/10.4095/297353>
45. Steenkamp, H.M., Gilbert, C., and St-Onge, M.R., 2016g. Geology, Leybourne Islands (north), Baffin Island, Nunavut, NTS 26A (north); Geological Survey of Canada, Canadian Geoscience Map 271 (preliminary edition); Canada-Nunavut Geoscience Office, Open File Map 2016-07, scale 1:100 000. <https://doi.org/10.4095/297355>
46. Steenkamp, H.M., Gilbert, C., and St-Onge, M.R., 2016h. Geology, Chidliak Bay (south), Baffin Island, Nunavut, NTS 26B (south); Geological Survey of Canada, Canadian Geoscience Map 272 (preliminary edition); Canada-Nunavut Geoscience Office, Open File Map 2016-08, scale 1:100 000. <https://doi.org/10.4095/297357>
47. Steenkamp, H.M., Gilbert, C., and St-Onge, M.R., 2016i. Geology, Chidliak Bay (north), Baffin Island, NTS 26B (north); Geological Survey of Canada, Canadian Geoscience Map 270 (preliminary edition); Canada-Nunavut Geoscience Office, Open File Map 2016-09, scale 1:100 000. <https://doi.org/10.4095/297354>
48. St-Onge, M.R., Weller, O.M., Dyck, B.J., Rayner, N.M., Chadwick T., and Liikane, D., 2016a. Geology, Sylvia Grinnell Lake (north), Baffin Island, Nunavut; Geological Survey of Canada, Canadian Geoscience Map 253E (preliminary edition); Canada-Nunavut Geoscience Office, Open File Map 2016-10E, scale 1:100 000. <https://doi.org/10.4095/297592>
49. St-Onge, M.R., Weller, O.M., Dyck, B.J., Rayner, N.M., Chadwick T., and Liikane, D., 2016b. Geology, Sylvia Grinnell Lake (south), Baffin Island, Nunavut; Geological Survey of Canada, Canadian Geoscience Map 254E (preliminary edition); Canada-Nunavut Geoscience Office, Open File Map 2016-11E, scale 1:100 000. <https://doi.org/10.4095/297593>
50. St-Onge, M.R., Weller, O.M., Dyck, B.J., Rayner, N.M., Chadwick T., and Liikane, D., 2016c. Geology, Amittok Lake (north), Baffin Island, Nunavut; Geological Survey of Canada, Canadian Geoscience Map 255E (preliminary edition); Canada-Nunavut Geoscience Office, Open File Map 2016-12E, scale 1:100 000. <https://doi.org/10.4095/297790>
51. St-Onge, M.R., Weller, O.M., Dyck, B.J., Rayner, N.M., Chadwick T., and Liikane, D., 2016d. Geology, Amittok Lake (south), Baffin Island, Nunavut; Geological Survey of Canada, Canadian Geoscience Map 256E (preliminary edition); Canada-Nunavut Geoscience Office, Open File Map 2016-13E, scale 1:100 000. <https://doi.org/10.4095/297791>
52. St-Onge, M.R., Weller, O.M., Dyck, B.J., Rayner, N.M., Chadwick T., and Liikane, D., 2016e. Geology, Clearwater Fiord (north), Baffin Island, Nunavut; Geological Survey of Canada, Canadian Geoscience Map 257E (preliminary edition); Canada-Nunavut Geoscience Office, Open File Map 2016-14E, scale 1:100 000. <https://doi.org/10.4095/297792>
53. St-Onge, M.R., Weller, O.M., Dyck, B.J., Rayner, N.M., Chadwick T., and Liikane, D., 2016f. Geology, Clearwater Fiord (south), Baffin Island, Nunavut; Geological Survey of Canada, Canadian Geoscience Map 258E (preliminary edition); Canada-Nunavut Geoscience Office, Open File Map 2016-15E, scale 1:100 000. <https://doi.org/10.4095/297793>
54. St-Onge, M.R., Weller, O.M., Dyck, B.J., Rayner, N.M., Chadwick T., and Liikane, D., 2016g. Geology, McKeand River (north), Baffin Island, Nunavut; Geological Survey of Canada, Canadian Geoscience Map 259E (preliminary edition); Canada-Nunavut Geoscience Office, Open File Map 2016-16E, scale 1:100 000. <https://doi.org/10.4095/297594>
55. St-Onge, M.R., Weller, O.M., Dyck, B.J., Rayner, N.M., Chadwick T., and Liikane, D., 2016h. Geology, McKeand River (south), Baffin Island, Nunavut; Geological Survey of Canada, Canadian Geoscience Map 260E (preliminary edition); Canada-Nunavut Geoscience Office, Open File Map 2016-17E, scale 1:100 000. <https://doi.org/10.4095/297595>
56. St-Onge, M.R., Weller, O.M., Dyck, B.J., Rayner, N.M., Chadwick T., and Liikane, D., 2016i. Geology, Irvine Inlet (north), Baffin Island, Nunavut; Geological Survey of Canada, Canadian Geoscience Map 261E (preliminary edition); Canada-Nunavut Geoscience Office, Open File Map 2016-18E, scale 1:100 000. <https://doi.org/10.4095/297794>
57. St-Onge, M.R., Weller, O.M., Dyck, B.J., Rayner, N.M., Chadwick T., and Liikane, D., 2016j. Geology, Irvine Inlet (south), Baffin Island, Nunavut; Geological Survey of Canada, Canadian Geoscience Map 262E (preliminary edition); Canada-Nunavut Geoscience Office, Open File Map 2016-19E, scale 1:100 000. <https://doi.org/10.4095/297795>
58. Blackadar, R.G., Davison, W.L., and Trettin, H.P., 1968a. Geology, Arctic Bay–Cape Clarence, District of Franklin; Geological Survey of Canada, Map 1237A, scale 1:253 440. <https://doi.org/10.4095/107330>
59. Blackadar, R.G., Davison, W.L., and Trettin, H.P., 1968b. Geology, Moffet Inlet–Fitzgerald Bay, District of Franklin; Geological Survey of Canada, Map 1238A, scale 1:253 440. <https://doi.org/10.4095/107497>
60. Blackadar, R.G., Davison, W.L., and Trettin, H.P., 1968c. Geology, Phillips Creek, District of Franklin; Geological Survey of Canada, Map 1239A, scale 1:253 440. <https://doi.org/10.4095/107510>
61. Blackadar, R.G., Davison, W.L., and Trettin, H.P., 1968d. Geology, Agu Bay–Easter Cape, District of Franklin; Geological Survey of Canada, Map 1240A, scale 1:253 440. <https://doi.org/10.4095/107336>
62. Blackadar, R.G., Davison, W.L., and Trettin, H.P., 1968e. Geology, Berlinguet Inlet–Bourassa Bay, District of Franklin; Geological Survey of Canada, Map 1241A, scale 1:253 440. <https://doi.org/10.4095/107412>
63. Blackadar, R.G., Davison, W.L., and Trettin, H.P., 1968f. Geology, Erichsen Lake, District of Franklin; Geological Survey of Canada, Map 1242A, scale 1:253 440. <https://doi.org/10.4095/108947>
64. Jackson, G.D. and Davidson, A., 1975a. Geology, Pond Inlet and Nova Zembla Island, District of Franklin; Geological Survey of Canada, Map 1396A, scale 1:250 000. <https://doi.org/10.4095/109005>
65. Jackson, G.D. and Davidson, A., 1975b. Geology, Bylot Island, District of Franklin; Geological Survey of Canada, Map 1397A, scale 1:250 000. <https://doi.org/10.4095/109007>

66. Jackson, G.D., Morgan, W.C., and Davidson, A., 1979. Geology, Buchan Gulf–Scott Island, District of Franklin; Geological Survey of Canada, Map 1449A, scale 1:250 000. <https://doi.org/10.4095/109159>
67. Jackson, G.D., 1984. Geology, Clyde River, District of Franklin; Geological Survey of Canada, Map 1582A, scale 1:250 000. <https://doi.org/10.4095/119788>
68. Jackson, G.D. and Sangster, D.F., 1987. Geology and resource potential of a proposed national park, Bylot Island and northwest Baffin Island, Northwest Territories; Geological Survey of Canada, Paper 87-17, 31 p. <https://doi.org/10.4095/122369>
69. Chandler, F.W., 1988. Geology of the late Precambrian Fury and Hecla Group, northwest Baffin Island, District of Franklin; Geological Survey of Canada, Bulletin 370, p. <https://doi.org/10.4095/126938>
70. Jackson, G.D. and Morgan, W.C., 1979. Geology, Conn Lake, District of Franklin; Geological Survey of Canada, Map 1458A, scale 1:250 000. <https://doi.org/10.4095/109162>
71. Skipton, D.R., Saumur, B.M., St-Onge, M.R., Wodicka, N., Bros, E.R., Currie, L.D., Weller, O.M., and Haggart, J.W., 2018. Bedrock geology, Pond Inlet, Nunavut, part of NTS 38-B; Geological Survey of Canada, Canadian Geoscience Map 347, scale 1:100 000. <https://doi.org/10.4095/306578>
72. Saumur, B.M., Skipton, D.R., St-Onge, M.R., Wodicka, N., Bros, E.R., and Weller, O.M., 2018. Bedrock geology, Mumiksa–Milne Inlet, Nunavut, parts of NTS 38-B and 48-A; Geological Survey of Canada, Canadian Geoscience Map 348, scale 1:100 000. <https://doi.org/10.4095/306579>
73. Saumur, B.M., Skipton, D.R., St-Onge, M.R., Jackson, G.D., Wodicka, N., Bros, E.R., and Weller, O.M., in press. Geology, Angijurjuk–Mary River (37G west), Nunavut; Geological Survey of Canada, Canadian Geoscience Map 403, scale 1:100 000.
74. Skipton, D.R., Saumur, B.M., St-Onge, M.R., Bros, E.R., and Weller, O.M., in press. Geology, Ravn River (37G east), Nunavut; Geological Survey of Canada, Canadian Geoscience Map 405, scale 1:100 000.
75. Saumur, B.M., Skipton, D.R., Zhang, S., St-Onge, M.R., Bros, E.R., Acosta-Gongora, P., Kelly, C.J., O'Brien, M.E., Weller, O.M., and Johnston, S.T., in press. Geology, Nina Bang Lake (37F west), Nunavut; Geological Survey of Canada, Canadian Geoscience Map 404, scale 1:100 000.
76. Skipton, D.R., Saumur, B.M., St-Onge, M.R., Bros, E.R., Acosta-Gongora, P., Kelly, C.J., O'Brien, M.E., Johnston, S.T., and Weller, O.M., in press. Geology, Rowley River–Isortoq River (37F east), Nunavut; Geological Survey of Canada, Canadian Geoscience Map 406, scale 1:100 000.
77. Skipton, D.R., Saumur, B.M., St-Onge, M.R., Bros, E.R., Acosta-Gongora, P., Kelly, C.J., O'Brien, M.E., Weller, O.M., and Johnston, S.T., in press. Geology, Barnes Ice Cap Northwest (37E west), Nunavut; Geological Survey of Canada, Canadian Geoscience Map 402, scale 1:100 000.